STUDIES ON LIFE ASPECTS OF FILAMENT WOUND COMPOSITES FOR AEROSPACE APPLICATION

A dissertation work submitted in partial fulfilment of the requirements for the award of the degree of

DOCTOR OF PHILOSOPHY

in

MECHANICAL ENGINEERING

By

LOKESH SRIVASTAVA
(Roll No. 716021)

Under the supervision of

Dr. LANKA KRISHNANAND
Professor (HAG)

Co-Supervisor

Dr. N. KISHORE NATH
(Scientist-G, ASL, DRDO, Hyderabad)

DEPARTMENT OF MECHANICAL ENGINEERING
NATIONAL INSTITUTE OF TECHNOLOGY
WARANGAL – 506004 (TS), INDIA.
MAY 2023

DEPARTMENT OF MECHANICAL ENGINEERING
NATIONAL INSTITUTE OF TECHNOLOGY
WARANGAL – 506004, INDIA

CERTIFICATE

This is to certify that the work presented in the thesis entitled **"STUDIES ON LIFE ASPECTS OF FILAMENT WOUND COMPOSITES FOR AEROSPACE APPLICATION"** which is being submitted by **Mr. Lokesh Srivastava (Roll No. 716021)**, is a bonafide work submitted to National Institute of Technology, Warangal in partial fulfilment of the requirement for the award of the degree of **Doctor of Philosophy** in **Mechanical Engineering**.

To the best of our knowledge, the work incorporated in the thesis has not been submitted to any other university or institute for the award of any other degree or diploma.

Prof. L. Krishnanand
Thesis Supervisor
Professor (HAG)
Department of Mechanical Engineering
National Institute of Technology
Warangal, India – 506004

Dr. N. Kishore Nath
Thesis Co-Supervisor
Scientist -G
Advanced Systems Laboratory
Defence R & D Organisation
Hyderabad, India - 500058

Prof. V. Suresh Babu
Chairman, DSC
Professor and Head
Department of Mechanical Engineering
National Institute of Technology
Warangal, India – 506004.

Approval Sheet

This Thesis entitled **STUDIES ON LIFE ASPECTS OF FILAMENT WOUND COMPOSITES FOR AEROSPACE APPLICATION** by **Lokesh Srivastava** is approved for the degree of Doctor of Philosophy

Examiners

(Dr. Sumantra Mandal)

Supervisor

(Dr. Lanka Krishnanand)

Co-Supervisor

(Dr. N. Kishore Nath)

Chairman

(Dr. V. Suresh Babu)

Date:

Place:

Declaration

This is to certify that the work presented in the thesis entitled "Studies on Life Aspects of Filament Wound Composites for Aerospace Application" is a bonafide work done by me under the supervision of Dr. L. Krishnanand, Professor (HAG), Mechanical Engineering Department and co-supervision of Dr. N. Kishore Nath, Scientist-G, Advanced Systems Laboratory, DRDO, Hyderabad and is not submitted elsewhere for the award of any degree.

I declare that this written submission represents my ideas in my own words and where other's ideas or words have been included, I have adequately cited the references. I also declare that I have adhered to all academic honesty and integrity principles and have not misrepresented, fabricated, or falsified any idea/data/fact/source in my submission. I understand that any violation of the above will be a cause for disciplinary action by the Institute and can also evoke penal action from the sources which have thus not been properly cited or from whom proper permission has not been taken when needed.

……..

(Signature)

Lokesh Srivastava

(Name of the student)

716021

(Roll Number)

Date:

……..

DEDICATED

TO

MY FAMILY,

TEACHERS

&

THE ALMIGHTY

Acknowledgement

First of all, I would like to express my deepest gratitude and profound indebtedness to Dr. L. Krishnanand, Professor of Mechanical Engineering Department, National Institute of Technology, Warangal and Dr. N. Kishore Nath, Scientist 'G' of Advanced Systems Laboratory, Hyderabad for allowing me to carry out doctoral work under their guidance. This work is a reflection of their thoughts, encouragement, guidance and permanent impulse at all stages of my work.

I sincerely thank Prof. N. V. Ramana Rao, Director, National Institute of Technology Warangal, India, for providing the necessary facilities and encouragement throughout my work. I am thankful to Prof. V. Suresh Babu, Head, Department of Mechanical Engineering, NIT Warangal, Prof. N. Selvaraj and other faculty members for their encouragement and continuous support.

I want to express my sincere indebtedness to the Departmental Scrutiny Committee members, Prof. A. Neelakanteswara Rao, Prof. R. N. Rao, Department of Mechanical Engineering, and Prof. N. Narasaiah, Department of Metallurgical and Materials Engineering for their adeptness and formative discussions during this research work.

I am grateful to Dr. M.R.M Babu, Distinguished Scientist & Director, Advanced Systems Laboratory, Hyderabad for his constant support and motivation.

I am thankful to Dr. Manoj Kumar Buragohain, Scientist 'G', Advanced Systems Laboratory, Hyderabad for his encouragement and support extended during the period. I am grateful to Dr. G. Rama Rao, Dr. S. K. Sahoo, Shri. CH Ugender, and Shri Y. Gangadhar Sinha, Scientist 'F', Advanced Systems Laboratory, Hyderabad for their continuous support.

I would like to express my special thanks to Dr. R. Srinivasan, Shri. D. Laxman and Shri. P. Sunil Kumar, Advanced Systems Laboratory for providing invaluable guidance as well as theoretical & experimental support and useful discussions.

I wish to thank especially Dr. Ch Sri Chaitanya, Shri. Mohan Kumar and other research scholars who had always been kind to me and supported me during this period. I am very much grateful to Shri. Amit Gupta, Scientist-E and Shri Pushpam Dayal, JRF for the help concerning the computer-related problems and during test specimen manufacturing.

I wish to thank Head, HRDG and members of the Internal screening committee, Advanced Systems Laboratory for their motivation and support.

At the end, I want to say the biggest thanks in this world to those who gave me the strength to survive, the power to move on, and the reason to love: my mother late Smt. Kalawati

Lal and my father Shri. Shambhu Dayal Lal. I am also deeply thankful to my sister Smt. Anju Srivastava and Smt. Annoo Saxena, mother-in-law Smt. Dolly Kishor, Father-in-law Shri. Kishore Kumar Sharan and other family members for their strong determination and continuous inspiration throughout this work.

Lastly to my wife Naveli Aradhana, my son Advik and my daughter Avika Adritanaya, perhaps the words are not sufficient to express my thanks. Thus, I only say thank you to all of them for everything. I would also like to acknowledge the support given by all the persons who have directly or indirectly supported me.

Lokesh Srivastava

Contents

List of Figures

List of Tables

List of Abbreviations and Symbols

AE	:	Acoustic Emission
AET	:	Acoustic Emission Testing
ASTM	:	American Society for Testing and Materials
AT	:	Acceptance Testing
BMI	:	Bismaleimide
BS	:	British Standard
CC	:	Cubic centimetre
CDT	:	Cylinder to Dome Transition
C/E	:	Carbon Epoxy
CHNS-O	:	Carbon, Hydrogen, Nitrogen, Sulphur & Oxygen Analyser
cm	:	Centimetres
CMC	:	Ceramic Matrix Composite
COPV	:	Composite Overwrapped Pressure Vessel
cP	:	Centipoise
CPV	:	Composite Pressure Vessel
CRMC	:	Composite Rocket Motor Casing
CVD	:	Chemical Vapour Deposition
CTE	:	Coefficient of Thermal Expansion
°C		Degree Celsius
dB	:	Decibels
DGEBA	:	Bisphenol A Diglycidyl Ether
DMA	:	Dynamic Mechanical Analysis
DSC	:	Differential Scanning Calorimeter
EPDM	:	Ethylene Propylene Diene Monomer
FE	:	Fore End
FEA	:	Finite Element Analysis
FoS	:	Factor of Safety
FMEA	:	Failure Mode and Effect Analysis
FMECA	:	Failure Mode Effect and Criticality Analysis
FR	:	Felicity Ratio
FRP	:	Fibre Reinforced Plastic

FV	:	Flight Vibration
FW	:	Filament Winding
G/E	:	Glass Epoxy
GFRP	:	Glass Fibre Reinforced Polymer or Plastics
gm	:	Gram (unit of weight)
HT	:	High Temperature
IE	:	Igniter End
ILSS	:	Inter Laminar Shear Strength
ISAT	:	Intensified Accelerated Trials
JSG	:	Joint Service Guidelines
JSS	:	Joint Service Specification
K	:	Kelvin
KHz	:	Kilohertz
km	:	Kilometres
L	:	Length
LINAC	:	Linear Accelerator
LPS	:	Liquid Propulsion System
LT	:	Low Temperature
LV	:	Launch Vehicle
LVDT	:	Linear Variable Differential Transformer
MEOP	:	Maximum Expected Operating Pressure
MHz	:	Megahertz
MIL-STD	:	Military Standard
mm	:	Millimetres
MMC	:	Metal Matrix Composite
MoS	:	Margin of Safety
msec	:	Milliseconds
NDE	:	Non-Destructive Evaluation
NDT	:	Non-Destructive Testing
NE	:	Nozzle End
NEI	:	Nozzle End Insulation
NI	:	Nozzle Insert

OB	:	Ordnance Board
PAN	:	Poly Acrylo Nitrile
PMC	:	Polymer Matrix Composite
PoP	:	Plaster of Paris
PPT	:	Proof Pressure Testing
PSD	:	Power Spectral Density
QC	:	Quality Control
QT	:	Qualification Testing
RH	:	Relative Humidity
RMC	:	Rocket Motor Casing
RPN	:	Risk Priority Number
RT	:	Radiographic Testing
RTM	:	Resin Transfer Moulding
SHM	:	Structural Health Monitoring
SRB	:	Solid Rocket Booster
SRBP	:	Synthetic Resin Bonded Paper
SRM	:	Solid Rocket Motor
SPS	:	Solid Propulsion System
T_g	:	Glass Transition Temperature
TMA	:	Thermo Mechanical Analysis
TPS	:	Thermal Protection System
TV	:	Transport Vibration
UD	:	Uni-Direction
UT	:	Ultrasonic Testing
UTM	:	Universal Testing Machine
UV	:	Ultraviolet
VARTM	:	Vacuum Assisted Resin Transfer Moulding
V_f	:	Fibre Volume Fraction
µs	:	Micro strains
ø	:	Diameter

ABSTRACT

The missile systems and Launch Vehicles (LV) predominantly use composite materials due to high range and enhanced payload requirements. The airframe, motor casing and various other subsystems of missile and Launch vehicles are designed with composite materials. Presently, Composite Rocket Motor Casing (CRMC) is realised with Carbon-Epoxy (C/E) and Glass Epoxy (G/E) composite. The CRMC is a high-end application product and is optimally designed with a marginal Factor of Safety (FoS) and calls for a high order of reliability. The structural performance of CRMC depends on its structural integrity against the designed load envelope. However, the unavoidable, unfavourable variations in the processing and subsequent life cycle stages such as transportation, handling, storage, service, and environmental conditions may degrade the structural integrity and performance. Also, long-duration storage results in ageing and degradation which can cause premature failure. Therefore, the effect of service and environmental conditions on the structural integrity/performance as well as on the useful life of CRMC to be investigated.

In this present study, the complete research work is formulated in three phases, in the first phase studies are carried out at the specimen level and in the second and third phases, studies are performed on flight-worthy hardware. In the first phase, to conduct the systematic experimental study, C/E and G/E composite specimens are synthesised using Filament Winding (FW) method. The specimens are tested for various physical and mechanical properties to understand the behaviour and performance of starting raw materials. In addition, C/E samples are exposed to the maximum expected service temperature and the corresponding strength degradation is evaluated.

The second phase performs studies on a flight worth C/E CRMC. At first, as a systematic risk assessment framework, Failure Mode Effect Analysis (FMEA) studies are performed on typical CRMC to study all potential failure modes and their severities. The outcome is instrumental in finalising the measurement and inspection plan. CRMC once realised, is pressure tested to demonstrate its ability to sustain the designed Maximum Expected Operating Pressure (MEOP). During Proof Pressure Test (PPT), Acoustic Emission (AE), strain and dilation are measured to study the real-time dynamic behaviour under pressure loads. The structural integrity of the composite case is tested through Ultrasonic (UT) and Radiographic Testing (RT). To evaluate the periodic performance, the realised composite case is stored at ambient and PPT shall be carried out again after 5 years. The PPT strain, dilation and (Non-Destructive Testing) NDT are carried out similarly to the first-time pressure test. The

test results are compared, and no noticeable changes are observed. In addition, to validate the life period of 10 years, a CRMC with 10 years of service life (manufactured using the same material system and manufacturing process) is identified and PPT tested as per the established test plan. The strain, dilation and NDT results are compared. With the above periodic performance evaluation, a health assessment is made to validate the post-deployment service life of C/E CRMC for a period of 10 years.

In the third phase, the performance of the G/E composite case is experimentally evaluated in an integrated way through ground static firing. The static test resembles actual operational conditions expected during flight; accordingly, the present study is carried out on a sub-system level resembling the actual flight hardware configuration. A specific performance evaluation test matrix is formulated considering the various dynamic and thermal conditions as expected during the operational service life of a Solid Rocket Motor (SRM) with a G/E composite case. The articles are subjected to those planned tests, followed by ground static firing. The pressure versus time is plotted for all test cases. The ballistic parameters result of the virgin (without subjecting it to any test) SRM is considered as a reference for comparative studies with the rest of all other test results. The experimental test results are analysed and reveal that various dynamic environmental conditions like random and transport vibration, acceleration, and shock environments do not affect the structural performance of composite cases. As a part of accelerated ageing studies, SRM with the composite case is also subjected to Intensified Standard Alternating Trials (ISAT) according to Joint Service Guide (JSG). Post accelerated exposures, the SRM with composite cases are periodically withdrawn and static tested to validate a service life of 10 years. In addition to accelerated trials, the performance of the composite case is also compared with the performances of 10 years old naturally aged composite case. The test results demonstrate and confirm the successful performance of the G/E composite case corresponding to a service life of 10 years.

CHAPTER 1

INTRODUCTION

1.1. General

Launch Vehicle (LV) is a rocket designed to carry a payload from Earth's surface through outer space, either to another surface point or into space. Sub-orbital LV include long-range ballistic missiles, sounding rockets, and various crewed systems designed for space application. These systems are mostly configured in two to four rocket stages to provide a sufficient incremental change in velocity. LV and long-range missile systems consist of various propulsion stages designed to meet mission requirements. These stages are jettisoned one after another once the propellant is burned out, to meet the designed mission profile. LV and Missile systems use different types of rocket fuel including the Solid Propulsion System (SPS), Liquid Propulsion System (LPS), and cryogenic fuels fed rocket engines. The propulsion system provides thrust to the vehicle to lift its weight and gain momentum against the gravitational pull [1]. The long-range missile systems are deployed and kept in storage, subjected to handling and operational trials until they are used. Since these systems are principally strategic and mostly intended for one-time use during service life, their safe life post-deployment is always a matter of concern. Strategic weapon systems remain dormant for a long time after deployment before being required to perform their mission reliably [2,3].

The safety and reliability of missile sub-systems during their intended life are of primary concern in missile performance due to the high cost and risk involved. The development of missile systems always demands improved mission performance. The missile system is a precise assembly of multiple complex sub-systems. The missile sub-systems are designed adequately to meet overall missile system configuration and mission objectives resulting in optimal performance complying with the specific needs and characteristics of the program [3,4]. The rapid technological changes and advancements in structural design, analysis and product development always look for improved, efficient, optimised, and reliable structures [5]. The strength-to-weight ratio should be as high as possible for an optimised aerospace structure to satisfy the mission requirements [5, 6]. The reduction in inert weight is useful for a higher mass ratio, which in turn means more incremental velocity for a given efficiency and can be converted into higher payload capability or augmented range [7]. Current advanced technology uses composites in a range of structural and thermal applications for missiles and space [5 & 6].

1.2. Solid Rocket Motor (SRM)

SRM is a rocket engine that uses solid propellants. SRM is used in most of the missile systems and LVs for their simplicity in construction, operational readiness, and reliability [8]. SRM operates on the energy conversion principle [9, 10], oxidizer, binder and other ingredients are mixed and packed into a metallic/composite casing. SRM falls under the classification of a non-air breathing type propulsion system i.e., atmospheric oxygen is not needed for the combustion of fuel. The combustion takes place within the chamber. The propellant contains chemical energy which gets converted into pressure and thermal energy through the combustion process after grain ignition [10]. Once the propellant grain is ignited, it burns with a specified rate till the propellant is completely burnt and produces high-pressure hot gases as a combustion by-product. The hot gases thus produced are subsequently expanded through a convergent-divergent nozzle and pass through the exit of the nozzle with very high velocity. The nozzle first reduces the exit area to increase the velocity of exhaust gases and subsequently gases attain supersonic velocity at the nozzle throat. Thereafter, the nozzle area is further increased to increase the gas velocity. In this process, the pressure and thermal energies of the combustion gases convert into kinetic energy imparting upward reaction thrust for the LV [10]. The thrust generated by an SRM is the most fundamental measure of its performance and it is expressed as

$$F = \int P \, dA = \dot{m} v_e + (P_e - P_a) A_e \qquad \text{…….. } \textbf{Equation 1}$$

Where $\dot{m}$ (mass flow rate) is the amount of mass moving through a given plane over a time and equals to density (ρ) * area (A) * velocity (V). V_e is the velocity of gases at the exit, P_e is exit Pressure, P_a is ambient pressure and A_e represents the area of the nozzle exit. The left-hand term in equation 1, represents the integral of the pressure forces acting on the rocket motor and nozzle, along an axis normal to the nozzle axis of symmetry, as shown in Figure 1.1.

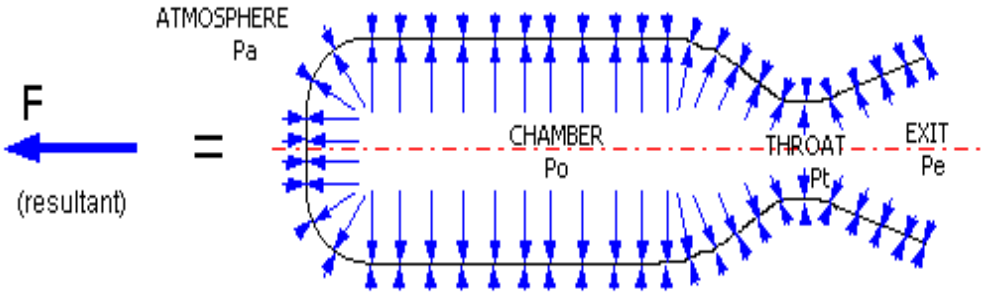

Figure 1.1. Principle of Thrust.

The maximum internal pressure within the motor case decreases steadily along the nozzle axis. The external environmental pressure is uniform all over the outside surfaces. The second term on equation 1 represents pressure thrust, and for a nozzle with an optimum expansion ratio i.e., when P_e=P_a, the pressure becomes zero. According to the concept of conservation of mass at the nozzle throat, equation 1 can be rewritten as

$$F = \rho^* A^* v^* v_e + (P_e - P_a) A_e \quad \text{..... Equation 2}$$

SRM consists of five major sub-systems viz. Motor casing, Internal insulation system, Propellant grain, Nozzle, and Igniter as shown in Figure 1.2 [10].

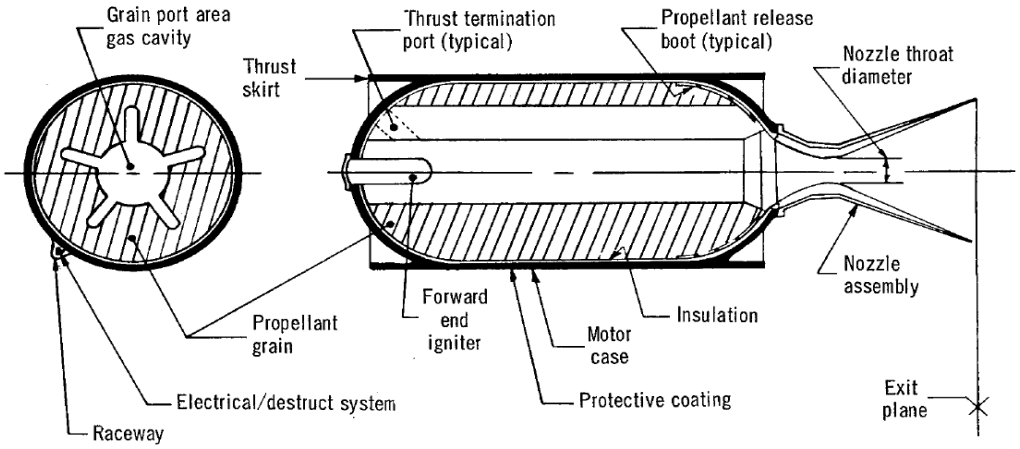

Figure 1.2. A Typical SRM Assembly (Courtesy: NASA Report).

1.2.1 Rocket Motor Casing (RMC)

It works as a combustion chamber and contains propellant grain. The burning of propellent takes place within the RMC and it also works as a flight vehicle structure designed to withstand the handling, transportation, and flight loads [7 & 11].

1.2.2 Internal Insulation System

It is a thermal barrier configured between the RMC internal surface and the propellant grain. It is designed to limit temperature on the internal surface within the allowable limit during the rocket motor operation. The insulation thickness protects the motor case structure until pressure –time curve tails off. The temperature of gases produced inside the motor cases ranges from approximately 3500 K. The primary function of internal insulation is to inhibit heat transfer towards the motor case and to protect its structural integrity. The secondary function of the insulation system is as follows:

- Inhibits the propellant grain surface, where burning is non-essential
- Inhibits transfer of case strain into the propellant grain
- Restricts the migration of chemical species
- Acts like sealing agent
- Guide the combustion flow into the nozzle

1.2.3 Solid Propellant Grain

The large-size propellant grain is usually case bonded and produces high-pressure hot gases through combustion. The propellant grain is a shaped processed mass cast inside the RMC. The material and geometrical configuration of the propellant grain determines the ballistic performance characteristics of SRM [10]. There are two types of grain:

- Cartridge loaded grains, which are manufactured separately and then assembled into the case [10]
- Case-bonded grains where the propellant is cast directly into the case

1.2.4 Nozzle

The high-pressure hot gases are expanded through the nozzle and pressure energy is converted into kinetic energy. The primary function of a nozzle is to accelerate the combustion products to maximize the exit exhaust velocity to supersonic velocity [10].

1.2.5 Pyrogen Igniter

It is a small SRM required for the ignition of a large SRM. The pyrogen igniter acts as a heat source to diffuse the large-size propellant grain. These efficient and reliable energy

systems provide heat flux and induce pressure in the chamber which is necessary to ignite the propellant and produce sustained combustion within the required time limit [10].

1.2.6 Advantages

The SRMs are most widely used due to the following advantages:

- Simple configuration and design
- Offers flexibility as preparation time is nil
- Negligible moving parts
- Relatively less overall weight
- Design possibility for very high thrust for shorter action time
- Conducive for the long storage period
- Design with thrust vector control is possible
- Combustion instability is less
- Better production rate

SRMs are having vast applications as propulsion stages for LVs, spacecraft, long-range and tactical missile systems, and to meet a wide range of thrust magnitude. They are specifically used as strap-on boosters apart from the main booster of LVs to achieve high initial thrust and to meet the requirement of payload and range.

1.3 Rocket Motor Casing (RMC)

The LV and missile system consists of primary structures namely, metallic, composite airframe sections and rocket motors for each stage. The primary structures are equipped with various subsystems and designed to meet all expected load [10, 11]. The primary objective is to select the materials with the highest possible specific strength and stiffness [12]. The design and development of missile and LV structures is the most fundamental task to achieve improved mission performance. The motor case material is the most crucial element in the design of the RMC and its selection involves various considerations like high specific strength, high specific stiffness, failure modes, machinability, weldability, availability, service conditions, and thermal properties. The critical loads are MEOP and buckling loads depending on mission objectives and the location of the RMC within the vehicle [13]. There are two types of materials for RMC application, viz., metals and composite materials. The various option for metallic RMC is:

- Low alloy steels such as 4130, D6AC, 15CDV6
- High-strength steels such as Maraging steel grade 250
- Titanium alloys

The SRM casings are traditionally being realized with ultra-high-strength steels such as maraging steels to gain in range and payload capabilities. The advent of high-strength steels which are highly fractured prone has brought a significant change in the design methodology as well as in the Quality Assurance (QA) philosophy [13]. The design methodology calls for fracture-based design in addition to strength-based design [14]. The metal cases have been conducive for rough handling and possess certain advantages like good ductility permits yielding to occur before failure, can withstand relatively High Temperatures (HT) (700-1000˚C), good machinability and weldability. Maraging steel is most preferred and contains a very low percentage of carbon and a very high percentage of nickel, cobalt and molybdenum (Ni-Co-Mo) as alloying elements and high strength is achieved through ageing at relatively low temperatures (LT) [15]. The percentage of carbon is kept at a minimum to minimize the formation of titanium carbide (TiC) which can otherwise have a detrimental effect on strength, ductility, and toughness. The fracture toughness, weldability, and machinability of maraging steel are also excellent. The maraging steels provide superior yield strengths ranging from 1030 to 2420 MPa [15]. The fracture toughness is comparatively better than all other conventional steels and makes it a suitable choice for a wide variety of space applications. Maraging steel grade 250 is most preferred among all variants because of its availability, cost, machinability, and strength aspects [14].

Aluminium and Titanium alloys are also used for various space applications. Titanium alloys also have a high strength-to-density ratio and are predominantly preferred for Composite Overwrapped Pressure vessels (COPV) and air bottle applications. The RMC serve two purposes [7, 10 & 11]:

- Acts as a combustion chamber
- A vented portion through which gases are expanded and provides forward thrust

1.3.1 Configuration

The configuration of RMC is based on the following considerations:

- Load envelope

The load envelope shall comprise of handling, storage, and operational loads [10,11 & 14]. The representative types of loads include:

  - Operating pressure, temperature, and other environmental considerations
  - Motor thrust and structural load produced by the lower-stage motors
  - Buckling, aerodynamic bending, acceleration loads and axial loads including handling, transportation, storage, and flight environment
  - Kinetic heating

- Nominal diameter and Length

The nominal diameter and length shall meet the overall vehicle configuration. The length-to-diameter ratio is chosen to maximise the vehicle performance as determined by the trade-off optimization concerning weight, drag loss, buckling stiffness and cost-effectiveness.

- Pole opening and end contour

The end closure configuration is chosen to optimise the size and shape, satisfying the requirements of:

  - Propellant grain design
  - Clearances for associated subsystems and interfaces

- Envelope volume

The external envelope shall be optimally designed to facilitate [14]:

  - Integration with ongoing and spent stages
  - Ease of fabrication, handling, transportation, and integration with launch facilities

- Propellant Mass Fraction:

The indicative casing weight shall arrive from the specified propellant mass fraction. The minimal case–weight design shall consider:

  - Use of ultra-high strength materials
  - Use of minimum design factors
  - Minimising stress concentrations
  - Minimising weight and end closure profile

A typical SRM case comprises of [10, 14]:

1. Cylindrical shells
2. Igniter End (IE) dome and Nozzle End (NE) dome
3. IE skirt and NE skirt
4. Attachments

Bridging the gap between high strength and light weight is a crucial challenge to the material and design engineers for strategic aerospace operations. The search for better material is exposed to increasingly tougher challenges for designing an optimal, robust, and reliable structure. Polymeric composite materials (Carbon, Kevlar, Glass) are an ideal choice and display an immense potential to become a key material for RMC.

1.4 Composite Rocket Motor Casing (CRMC)

Composite-made structures are receiving greater attention in aerospace industries due to their enhanced performance capabilities compared to their metallic counterparts [6]. The

design of RMC with composites is an ideal choice for rockets/aerospace applications. The polymeric composites consist of reinforcement and matrix. The Carbon & Kevlar fibres have high strength and high modulus, are ideally suited as reinforcement along with epoxy resin and are suitable candidate materials for CRMC [16, 17]. The design of composite structures unlike that of metals goes hand in hand with the selection of material and process options as both materials synthesis and processing occur simultaneously [16]. Composite casing's primary design load is the maximum expected operating pressure (MEOP) and the worst structural load. The casing is an axis-symmetric thin shell which is predominantly under a biaxial state of tensile stresses under normal operating conditions and these stresses vary along the axis of the casing [5]. The end attachments facilitate assembly with adjoining airframe sections.

FW is an obvious choice for manufacturing CRMC as it provides an efficient netting system of fibres in which the benefit of the variability of directional strength is utilized [5]. CRMC is a pressure vessel with unequal pole openings and specially designed metallic end attachments namely polar bosses and skirts [5, 6]. The CRMC consists of hoop and helical plies. The angles of helical winding in the cylindrical portion of the casing are small and non-uniform. The hoop winding is carried out only at the cylinder portion since the hoop components of helical layers are not sufficient to meet the strength requirements. Since the hoop winding is not possible at the end domes, additional layers (doily) of high-strength fabric are laid up interspersing the helical layers from the cylinder–to–dome transition (CDT) to the pole opening [17]. Among the various types of winding methods, helical winding provides iso-tensoid contour at the domes. The constraint of unequal pole opening at both ends, calls for non-geodesic helical winding.

The FW technique offers a high production rate and is ideal for fibre placement in the required orientation as per design requirements [18]. The resin-impregnated continuous fibres are laid down over a male rotating mandrel according to a winding program in a predetermined and sequential manner, under tension to yield a surface of revolution with the desired thickness. The winding program is evolved considering the stresses and design requirements [5]. This allows for an optimal Fibre Volume Fraction (V_f) in the required directions [16]. The general architecture and configuration details of a typical CRMC are given in Figures 1.3, 1.4 (a), (b) and (c) respectively.

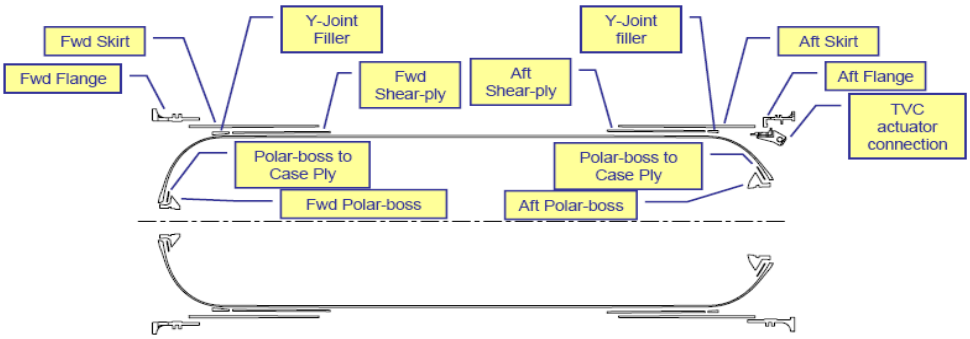

Figure 1.3. General Architecture of a Typical CRMC for Space Application (Source: Research gate).

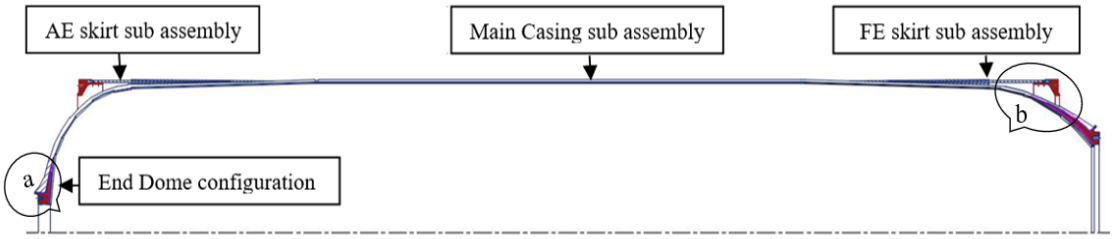

(a)

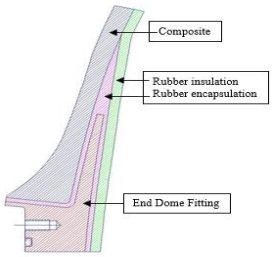

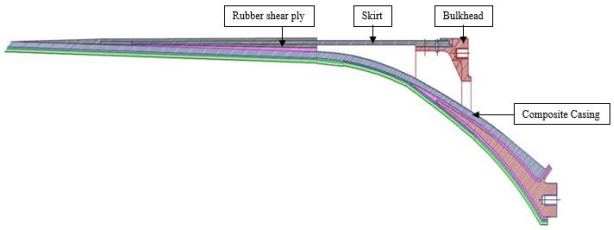

(b) **(c)**

Figure 1.4. (a) (b) and (c) Configuration of CRMC.

1.4.1 Material Selection

FW is possible either with tow-pregs (dry wining) or with wet winding. The most suitable candidate materials used as reinforcements are i) E – glass fibre, ii) Kevlar– 49 and iii) Carbon fibres of various grades [5]. Resins with longer gel time and better mechanical properties are the most suitable for the FW process to produce the casing. Therefore, epoxy resin is the most suitable candidate for this purpose [5].

➢ **Advantages**

- Longer gel time and better mechanical properties
- Low viscosity and flow rate
- Low volatility during curing
- Low shrinkage

- Easy availability

The Poly Acrylo Nitrile (PAN) based High strength carbon fabric is used for the lay-up of doilies. Aluminium alloy, titanium and low alloy steels are the candidate materials for the fabrication of end polar bosses. The aluminium alloy made end skirt rings are used as end attachments. Composites are highly process sensitive, non-repairable and susceptible to environmental factors and defects. The design and structural analysis of CRMC needs a conclusive methodology concerning the configuration, mission requirements, raw material system and filament winding methodology, [6, 17, 19 & 20]. The FW parameters influence the physical and mechanical properties of cured composite and affect the overall quality and reliability of CRMC [21-24].

1.4.2 Sub-Assemblies

- **Polar boss sub-assembly**

The metallic end dome fittings are used for fastening the igniter and nozzle and to carry the unsupported blowout load. The end domes are fabricated by contour machining. The metallic polar boss and the composite casing undergo differential deformation under high pressure and axial loads, to take care of this problem. The polar bosses are encapsulated with an elastomeric rubber layer.

- **Skirt sub-assembly**

The composite skirt along with a metallic attachment is attached near the junction of the dome and the cylinder at each end. The skirts serve as the primary structure to convey loads between various stages of missile systems [6]. The metallic end attachments i.e., bulkheads are provided on both ends to facilitate the rocket motor casing integration with adjacent sections. The skirts are fabricated by the FW process/fabric lay-up process on a separate mandrel or through the in-situ winding. The skirts are bonded and fastened with metallic attachments. The bearing strength of the composite skirt is enhanced by fabric layup in between filament wound layers. The shear plies at the joint between the skirt and the casing take care of dilations of the casing during internal pressure. The inner shear ply is laid up on a specially shaped mandrel over which the winding, interspersed with fabric lay ups is carried out. The skirt along with the mandrel is cured in an oven, extracted, and machined.

- **Y Joint**

The primary two methods of joining the skirt to the casing are:

  - Adhesive bonding
  - In situ winding on the main casing

1.5 Composite Materials

Composite material is a combination of two or more constituents not soluble in each other and differing in form or composition on a macroscale but acting in concert in combined form, retaining their identities across the interface between one another. One is called the reinforcement and the other one in which it is embedded is called the matrix. The reinforcements are principal load-bearing members and matrix acts as a load transfer medium, keeping reinforcement intact at required locations and orientations [6, 16]. The reinforcing material may be in the form of fibres, particles, or flakes. The matrix phase materials are generally continuous. Examples of composites include concrete reinforced with steel and epoxy reinforced with carbon fibres, etc. Composite material combines several properties not usually found in a single material. Composites have high specific strength and high specific stiffness, non-corrosive, and superior thermal and electrical insulation properties. The constitution of the composite is shown in Figure 1.5.

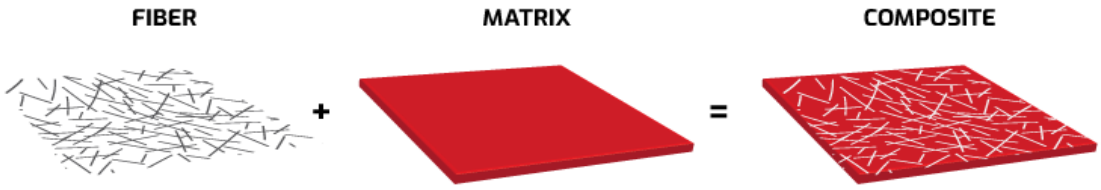

Figure 1.5. Constituents of Composite.

1.5.1. Reinforcements:

Composites are classified based on reinforcement geometry as

- **Particulate**

Composites consist of particles immersed in the matrix such as alloys and ceramics as shown in Figure 1.6 (a). Particulate composites have improved strength, increased operating temperature, oxidation resistance, etc. Examples include aluminium particles in rubber and silicon carbide particles in aluminium.

- **Flake**

Composites consist of flat reinforcements of the matrix as shown in Figure 1.6 (b). Typical examples are glass, mica, aluminium, and silver. The advantages are high out-of-plane flexural modulus, higher strength, and low cost. However, flakes cannot be easily oriented and so only a limited number of materials are available for use.

- **Fibre**

Composites consist of a matrix reinforced by short (discontinuous) or long (continuous) fibres as shown in Figure 1.6 (c). Examples of fibres are carbon, boron, and aramids etc. The particulate, flake and fibre composites are shown in Fig 1.6 (a), (b) & (c).

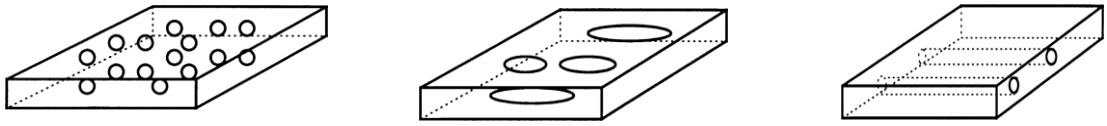

(a) **(b)** **(c)**

Figure 1.6. (a) Particulate Composite (b) Flake Composite (c) Fibre Composite.

Further, fibre can be classified as continuous and discontinuous types of fibre. Continuous and aligned fibres are the most widely used reinforcement, especially in high-performance applications.

1.5.2 Matrix Materials

Matrix is the continuous phase of composites [16] and can be classified as:

- Metal Matrix Composites (MMC)
- Ceramic Matrix Composites (CMC)
- Polymer Matrix Composites (PMC)

Primary functions

- Acts as a binder, holds fibres together and facilitates load transfer
- Provides rigidity
- Keeps fibres separated to act individually and arrests crack propagation
- Matrix aids to surface finish
- Protects the fibres from environmental effects
- Influences ductility, impact strength, and toughness of composite
- Dictates the mode of failures in composites

1.5.2.1 Metal Matrix Composites

MMCs have metal as a matrix. Examples are aluminium, magnesium, and titanium. Typical fibres include carbon and silicon carbide. Metals are used as reinforcement to increase or decrease their properties to meet design requirements.

Advantages

- Higher elastic properties
- Higher service temperature
- Insensitive to moisture

- Better electric and thermal insulation properties
- Improved wear, fatigue, and flaw resistances

Disadvantage

- Higher processing temperatures and higher density

Applications

The applications are magnesium matrix composites for space, titanium matrix composites in aircraft, aluminium matrix composites in automotive and aerospace etc.

Manufacturing Process

There are different fabrication methods for MMCs. One of the methods is diffusion bonding which is used in the manufacturing of boron/aluminium composite parts (Figure 1.7). A boron fibre mat is placed between two thin aluminium foils. A polymer holds the fibres together. The layers of these metal foils are stacked according to design. The laminate is first heated in a vacuum bag to remove the binder and hot pressed in a die under pressure and temperature.

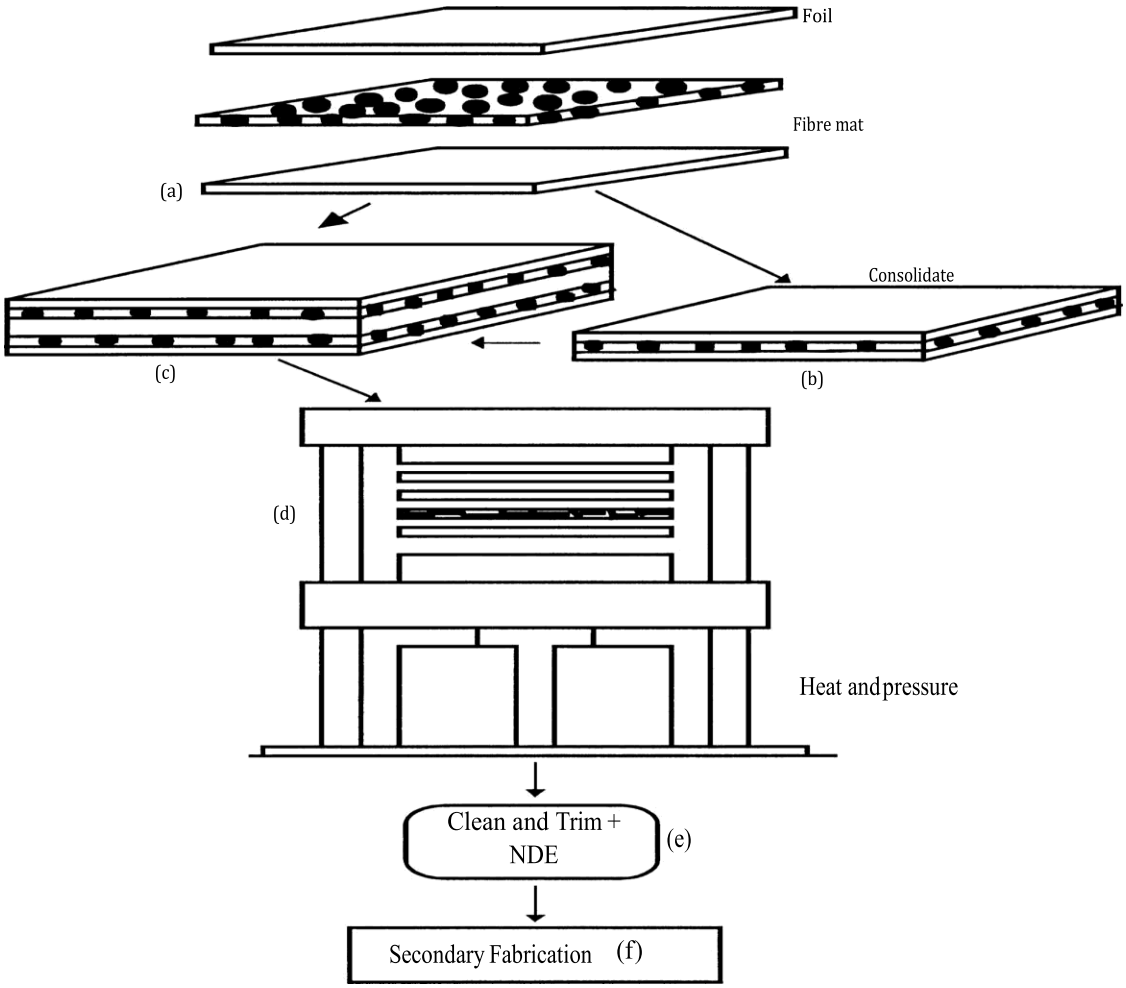

Figure 1.7. Diffusion Bonding Process – MMCs [16].

1.5.2.2 Ceramic Matrix Composites (CMC)

CMC consist of ceramic fibres reinforced with particulates, fibres, etc. CMCs have high strength, good crack resistance, improved thermal and erosion properties at HT. CMCs are fabricated through vapour phase deposition techniques. Examples are carbon fibre-reinforced carbon matrixes, silicon carbide fibre-reinforced silicon carbide matrixes etc. The ceramic matrix examples are zirconium carbide, alumina, zirconia, glass etc.

Advantages

- High strength and hardness
- High service temperature
- Chemical inertness

Applications

The applications are thermal and ballistic, aero engines, gas turbines, process equipment, furnaces, nuclear components and re-entry shielding etc.

1.5.2.3 Polymer Matrix Composites (PMC)

The PMCs consist of a polymer reinforcement of thin diameter, an example is carbon-epoxy composites. They are also known as Fibre Reinforced Plastics (FRP) [16].

Advantages

- High strength and stiffness
- Ease of manufacturing complicated shapes
- Low density

Disadvantages

- Low operating temperatures
- High coefficients of thermal and moisture expansion
- Low elastic properties

Applications

The applications are Carbon Epoxy (C/E) and Glass epoxy (G/E) composites in aerospace, airframes, payload bay doors, ablative liners, and for marine application such as fiberglass in speed boats etc.

1.5.3 Fibre

The development of various types of fibre with varying properties gives a competitive advantage to composites vis-à-vis conventional materials. The key fibres are glasses, carbons, aramids, and ceramics [16].

Primary functions

- Act as the main load-carrying element
- To contribute to the structural properties
- To provide other properties like electrical conductivity or insulation etc

1.5.3.1 Glass Fibre

The glass fibre made polymeric composite is also known as Glass Fibre Reinforced Plastic (GFRP). The E and S glass fibre is widely used for many mechanical applications. E-glass fibres are originally developed for electrical insulation applications. E-glass is calcium alumni borosilicate with good tensile strength, generally used in industrial, aerospace and defence products. The S type is magnesia-aluminosilicate glass with high tensile strength and stiffness, used in aerospace. The thermal and electrical conductivities of glass fibres are low, and GFRPs are often used as thermal and electrical insulators. The manufacturing process of glass fibre is shown in Figure 1.8.

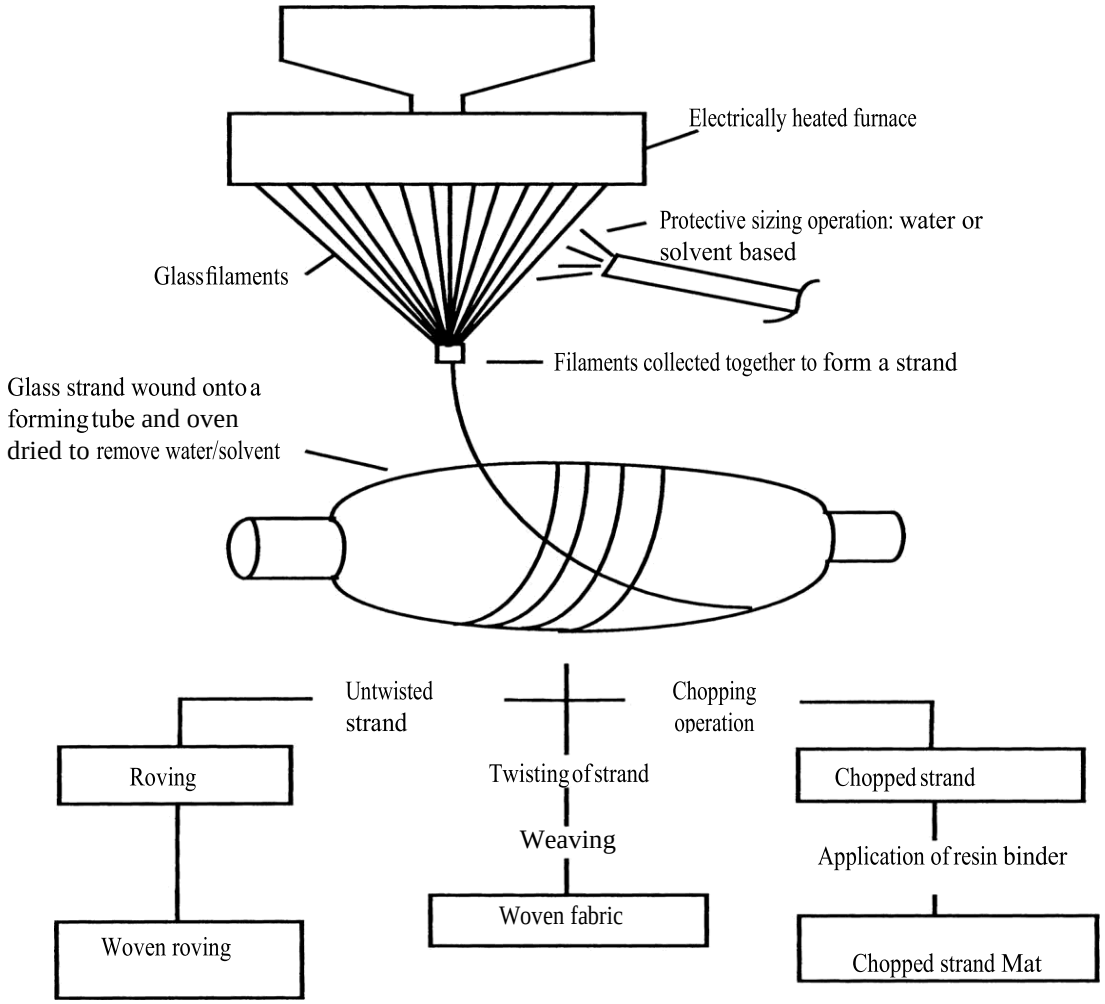

Figure 1.8. Manufacturing Process - Glass Fibres (Source: Research gate).

1.5.3.2 Carbon Fibre

The carbon fibre also called graphite fibre, is used as reinforcement for polymers, metals, ceramics, and carbon matrix composites. Carbon fibres are widely used in aerospace and defence applications. The carbon fibres have excellent resistance to creep, stress rupture, fatigue, and corrosive environments. The axial stiffness, tension, compression strength and thermal conductivity of carbon fibre are much greater than the corresponding properties in the radial direction [16]. The carbon fibres are made primarily from three key precursor materials: PAN, petroleum pitch, and coal tar pitch. The carbon fibre is produced by the controlled oxidation, carbonisation, and graphitisation of carbon-rich organic precursors.

1.5.3.3 Boron Fibre

Boron fibres are primarily used to reinforce polymers and metals. Boron fibres are produced as monofilaments by the Chemical Vapour Deposition (CVD) of boron on a tungsten wire. They have relatively large diameters compared to E-glass and carbon fibres.

1.5.3.4 Silicon Carbide based Fibre

Silicon-Carbide based fibres are primarily used to reinforce metals and ceramics. There are varieties of fibres available based on silicon carbide. The silicon-carbide-based fibres are made by a variety of processes such as the pyrolysis of preceramic polymers. This fibre also contains varying amounts of silicon, carbon, titanium, nitrogen, and zirconium.

1.5.3.5 Alumina Based Fibre

Alumina-based fibres are primarily used to reinforce metals and ceramics. For example, alumina-based titanium matrix composites, and alumina fibre-reinforced aluminium alloy composites. The primary constituents, in addition to alumina, are boria, silica, and zirconia. These are primarily used for better wear and tear properties.

1.5.3.6 Aramid Fibre

Aramid fibres are synthetic organic fibres prepared from aromatic polyamides by spinning a solid fibre from a liquid chemical blend. This is a high-strength and high-modulus fibre primarily used as reinforcement in aerospace and for ballistic protection. The aramid fibre also offers good resistance to abrasion, chemical and thermal degradation. There are several commercial aramids fibres such as Kevlar 29, 49 and 149 (Dupont).

1.5.4 Resin System

Resin is used as a matrix in PMC. The resin can be further classified as thermoset and thermoplastic. Thermoset resin once cures, forms irreversible chemical bonds and cannot be re-moulded, whereas thermoplastic can be remoulded and recycled. The resin shall have:

- Good mechanical and toughness
- Good adhesive properties
- Good resistance to environmental degradation

Examples

- Polyesters, epoxy, phenolic, cyanate esters, polyamides and bismaleimides resins

1.5.4.1 Epoxy Resin

Epoxy resins are usually two-part systems consisting of an epoxy and a curing agent i.e., a hardener. The hardener mostly an amine, facilitates curing. The epoxy largely dictates the properties of the resin, and the curing agent determines the cure temperature. The term epoxy refers to a chemical group consisting of an oxygen atom bonded to two carbon atoms [16]. The epoxy class of resins is the main workhorse for aerospace components.

Advantages

- Higher fracture toughness and superior fatigue performance
- Low cure shrinkage
- Longer gel time and better mechanical properties

1.5.4.2 Polyester Resin

Polyester resins are the most widely used resin systems for marine applications. Orthophthalic polyester is a standard resin and is widely used. Isophthalic polyester resin is preferred in marine applications. Polyester resin is also used in many applications.

1.5.4.3 Phenolic Resin

Phenolic resin is suitable for high service temperatures, and good electrical and moisture resistance applications. There are two types of phenolic resins Viz. Novolac and Resol. They are primarily used for thermal barriers and ablation purposes in aerospace due to their high char yield.

1.5.4.4 Cyanate Ester

Cyanate ester-based composites have high Glass Transition Temperature (T_g), low moisture absorption, good mechanical properties, and excellent dielectric properties. Due to low dielectric properties glass/quartz-reinforced cyanate esters are suitable for radome applications.

1.5.4.5 Polyamide Resin

The polyamide type of resin is suitable for high-temperature applications. The thermal stability results in service temperatures of about 300^{o} C. It is mainly used for missile and aero-engine components.

1.5.4.6 Bismaleimides

It can be used for service temperatures up to 230^{o}C. They are primarily used in engine inlets and high-speed aircraft flight surfaces.

1.6 Advantages and Disadvantages of Composites

The advantages and disadvantages of composites are as follows [16]:

Advantages

- Light Weight
- Corrosion Resistance
- Design Flexibility
- Part Consolidation
- Dimensional Stability
- Radar Transparent
- Durability

Disadvantages

- High Cost
- Complex Design, analysis, and characterisation
- Complex fabrication
- Process intensive
- Composite metal joining
- Sensitive to environmental factors
- Repair process is not established
- Non-Destructive Testing (NDT) and Inspection requirements
- Re-cycling infrastructure is not well established

1.7 Advanced Composites

Advanced composites are primarily used in aerospace applications. Epoxy resin is used as a matrix material for many of the high-performance applications. Advanced composites are polymeric matrix (epoxy, bismaleimide, phenolic) reinforced with high-modulus or high-strength carbon fibres.

Examples

- Graphite/epoxy, Kevlar/epoxy, boron/ aluminium composites etc.

1.8. Manufacturing process - PMC

There are many different material options in composite concerning resins, fibres and cores, etc to meet the requirements of strength, stiffness, toughness, heat resistance, cost, production rate etc. The broad manufacturing options are shown in Figure 1.9.

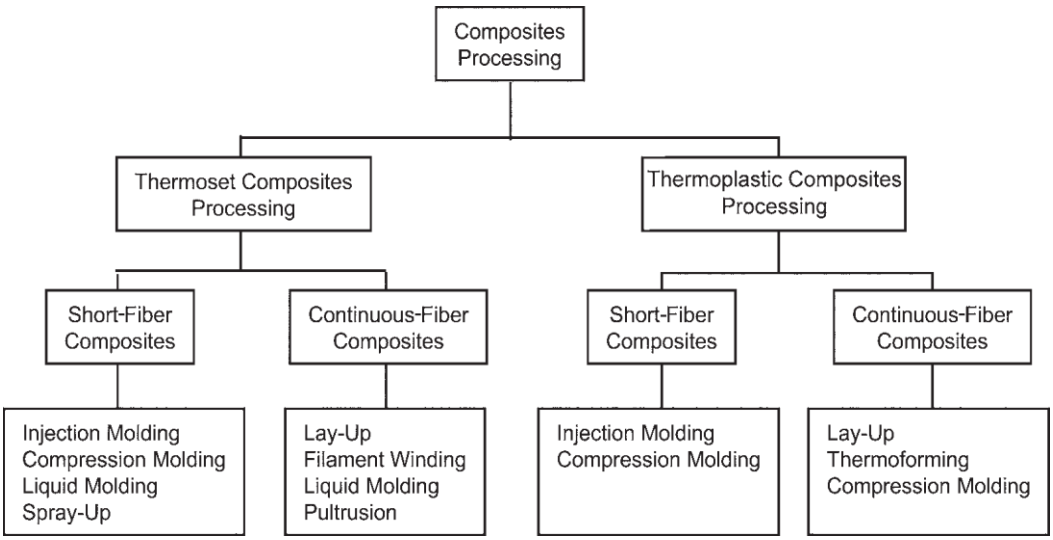

Figure 1.9. Different Manufacturing Processes - PMCs.

1.8.1. Wet Lay-up

Description

Resins are impregnated by hand into fibres which are in the form of woven, knitted, stitched, or bonded fabrics. This is usually accomplished by rollers for impregnation. The laminates are cured at ambient conditions. The wet lay-up manufacturing process is shown in Figure 1.10.

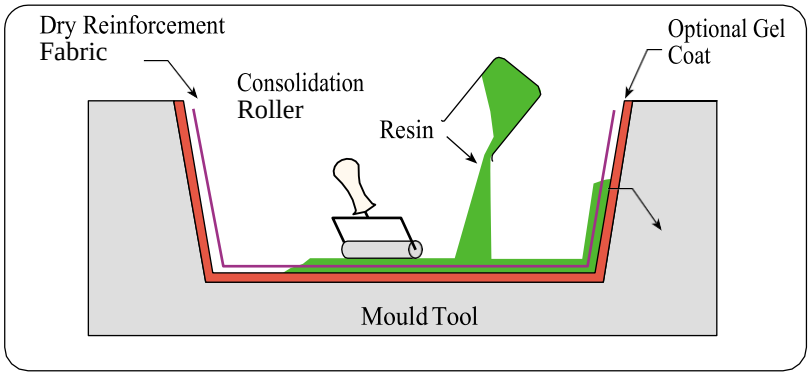

Figure 1.10. Wet Lay-up (Source: Research gate).

Material Options

- Resins: epoxy, polyester, vinyl ester, phenolic
- Fibres: glass, carbon etc

Advantages

- Simple
- Low tooling cost
- Wide choice of material
- Higher V_f

Disadvantages

- Processing is skill dependent
- Health and safety considerations
- Low viscosity

Applications

- Wind-turbine blades, commercial boats, infrastructure components etc

1.8.2. Vacuum Bagging

Description

In this case of wet lay-up, external pressure is applied for curing. The laminate is sealed with plastic film and then pressure is applied. The vacuum bagging process is shown in Figure 1.11.

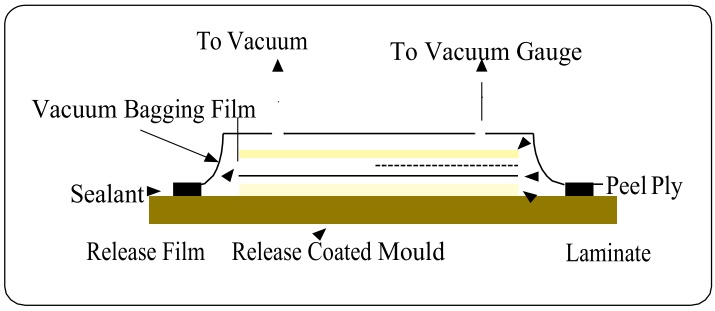

Figure 1.11. Vacuum Bagging (Source: Research gate).

Materials Options

- Resins: Epoxy, Phenolic etc
- Fibres: Glass, Carbon etc

Advantages

- Higher V_f
- Low void contents and improved consolidation
- Improved fibre wet-out
- Safety

Disadvantages

- Highly costly
- Sensitive to the operator

Applications

- Automotive, naval, and infrastructure applications

1.8.3. Pultrusion

Description

The bunch of fibres are pulled from a creel through a resin bath and then pass through a heated die. The die completes the impregnation, controls the resin content and cures into the required shape. The pultrusion is a continuous process and produces a profile of constant cross-section. The pultrusion process is shown in Figure 1.12.

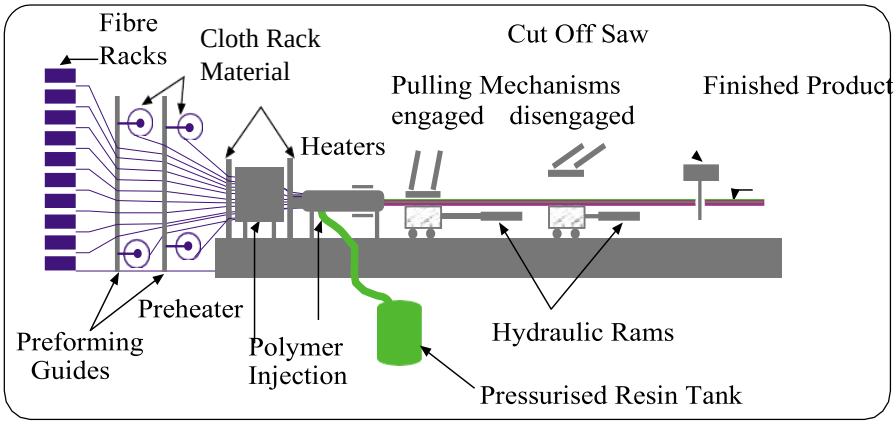

Figure 1.12. Pultrusion (Source: Research gate).

Materials Options

- Resins: Epoxy, Polyester, Vinyl ester, Phenolic etc
- Fibres: Any

Advantages

- Fast and economical
- Controller resin content
- Minimum fibre wastage
- Better structural properties and high V_f can be achieved
- Less volatiles

Disadvantages

- Limited to constant or near-constant cross-section components
- High tool cost

Applications:

- Beams and girders, bridges, ladders etc

1.8.4. Resin Transfer Moulding (RTM)

Description

In the RTM process, fabrics are laid up as input stock of materials. These fabrics are then pressed to the desired mould and held together using a polymeric binder. The other half of the mould is then placed over the first, the resin is injected into, and a vacuum is applied to improve the consolidation. Both resin flow and curing take place at either ambient or elevated temperatures. The RTM process is shown in Figure 1.13.

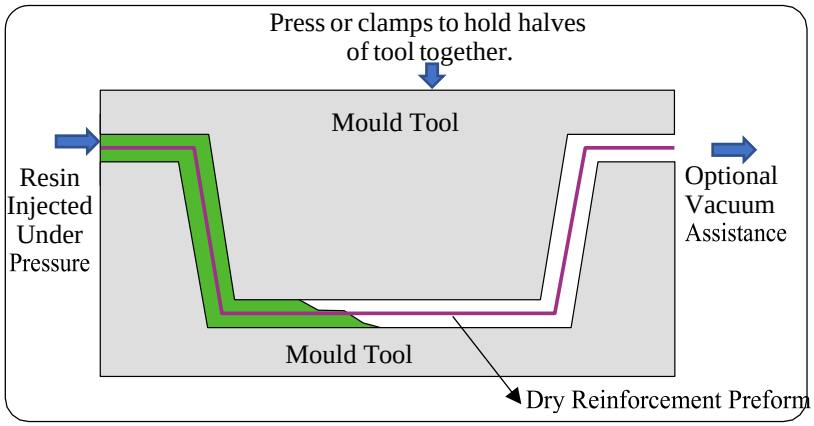

Figure 1.13. RTM (Source: Research gate).

Materials Options

- Resins: Epoxy, Polyester, Vinyl ester and Phenolic
- Fibres: Any stitched materials

Advantages

- Laminates with High V_f and very low voids
- Better health, safety, and environmental control
- Low labour cost
- Better surface finish

Disadvantages

- Expensive tooling
- Generally limited to smaller components
- Poor efficiency as likely chances of scrap is more

Applications

- Aircraft and automotive components

1.8.5. Vacuum-Assisted Resin Transfer Moulding (VARTM)

Description

VARTM is an extension of the RTM process where the top half of the mould is replaced with vacuum bagging to assist resin flow. It provides better consolidation. The fabrics are loaded on the bottom mould and covered with peel ply and a non-structural fabric. The assembly is then vacuum bagged, and resin is allowed to flow and makes the laminate wet. The manufacturing process is shown in Figure 1.14.

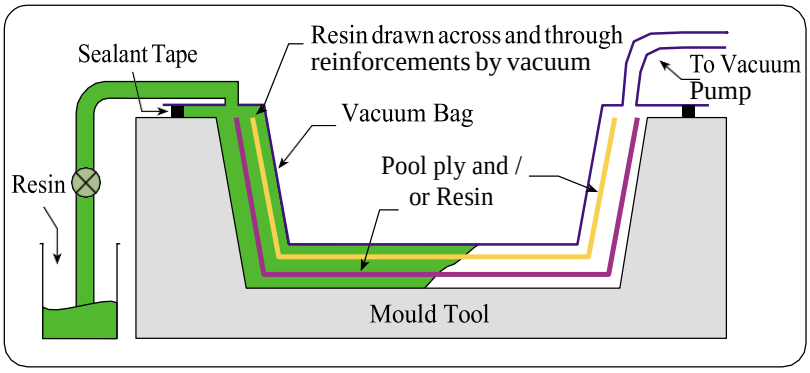

Figure 1.14. VARTM (Source: Research gate).

Materials Options

- Resins: epoxy, polyester, and vinyl ester
- Fibres: Any

Advantages

- Laminates with high V_f
- Low tooling cost does not require autoclave
- Large parts can be manufactured
- Better surface finish
- Easy tooling

Main Disadvantages

- Relatively complex process
- Requires resin with low viscosity

Typical Applications

- Transportation, wind energy, marine infrastructure, and aerospace

1.8.6. Prepregs

Description

The fibres and fabrics are pre-impregnated with a resin system in a controlled environment under heat, pressure, catalyst and cured. The prepregs are recommended to be stored at low temperatures as the resin is usually at the B stage. The prepregs can be processes

in a different way depending on end use. The prepregs are laid up onto a mould surface, vacuum bagged and then heated according to the resin cure cycle. This allows the resin to flow over the surface and the application of heat accelerates the curing [16]. The prepreg requires autoclave curing where temperature, pressure and vacuum are applied simultaneously. The prepreg processing setup is shown in Figure 1.15.

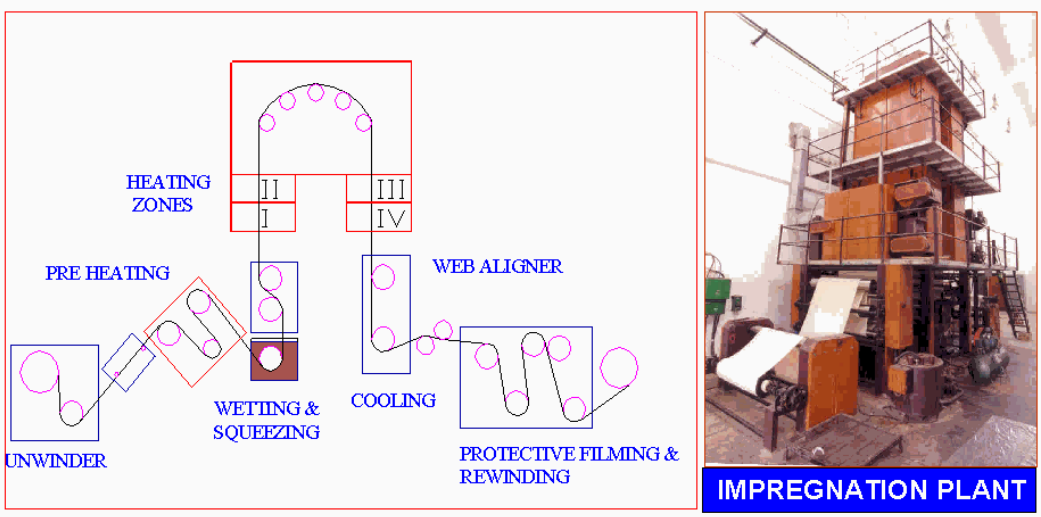

Figure 1.15. Prepreg Processing Setup and Impregnation Plant.

Materials Options

- Resins: epoxy, polyester, phenolic, polyimides, cyanate esters and bismaleimides etc
- Fibre and Fabric: glass, carbon, and aramid etc

Advantages

- Controlled properties
- High V_f can be achieved
- Efficient and repeatable process
- Uniform and better surface finish
- Optimised mechanical and thermal performance
- Less volatiles, voids and defects and good consolidation
- Complex parts can be manufactured
- Can be automated and labour costs can be minimised

Disadvantages

- High material cost
- Requires Autoclaves for curing – an expensive and time-consuming process
- Sensitive to shelf life

- Customised Tooling

Applications

- Aero-structures, aerospace, missiles, defence and automotive

1.8.7. Filament Winding (FW)

Filament wound composites are used as pressure vessels in chemical plants, missile/space vehicles and in the oil, gas, and nuclear industries. FW is most suited for the manufacturing of surface of revolution, open or closed-end structures. It involves the winding of filaments under tension over a rotating male mandrel. The mandrel rotates around the spindle while a delivery eye on a carriage transverse horizontally in line with the axis of the rotating mandrel, laying down fibres. Once the desired thickness is achieved, the component along with the mandrel is cured [5]. The controlled variables are fibre, resin content, wind angle, bandwidth, and thickness of the fibre bundle. The hoop winding (0°) shall provide circumferential strength, while angle winding provides greater longitudinal/ axial tensile strength. FW is possible either with tow-pregs (dry winding) or with roving along with a wet resin system (wet winding). Tow-pregs provide better frictional properties to carry out non-geodesic winding.

Description

This is primarily used for hollow, circular or oval-sectioned components, the examples are pipes, tubes, gas cylinders, storage tanks and air bottles. The fibres are passed through a resin bath and wound onto a mandrel in a variety of orientations, controlled by the feeding mechanism, and mandrel rotation [5]. The FW process is shown in Figure 1.16

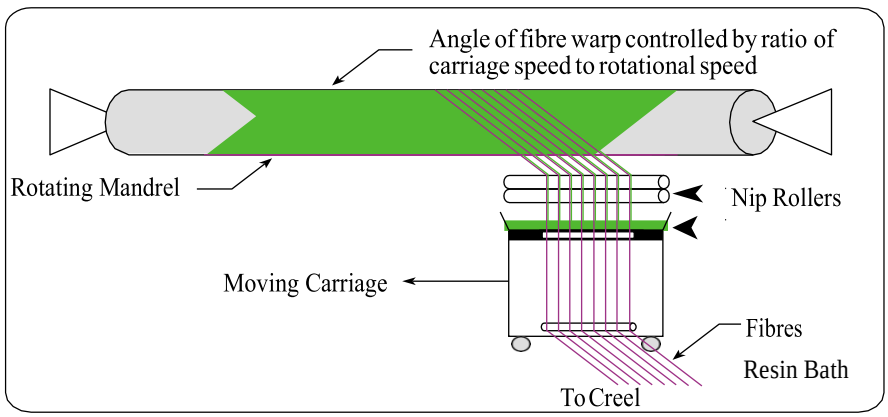

(a)

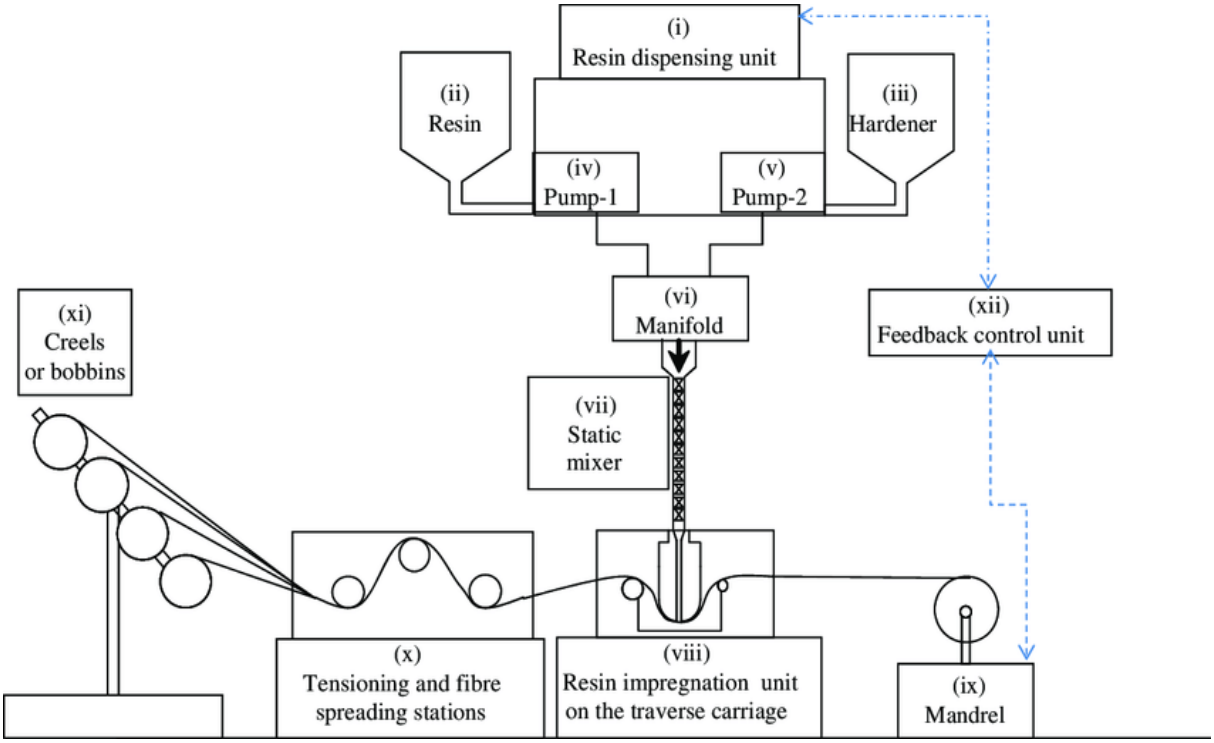

(b)

Figure 1.16. FW (a) Under Progress (b) Manufacturing Setup [Source: Research gate].

1.8.7.1.Different Types of Winding Methods

The wet and dry winding are two different winding methods shown in Figures 1.17 and 1.18, respectively.

Wet winding

- Fibres are passed through a resin bath and wound on a rotating mandrel. This is generally used in commercial and aerospace applications. The process is sensitive to resin viscosity, roller pressure, winding tension, ply sequence and bandwidth etc.

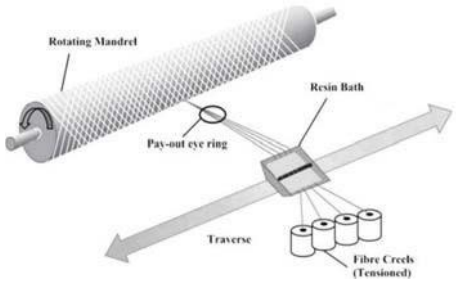

Figure 1.17. Wet Winding Method (Source: Research gate).

Dry winding (Tow-preg)

In dry winding, pre-impregnated fibre tows are placed on the rotating mandrel and cured.

Advantage:

- Superior quality
- Reproducibility in terms of process parameters and consistent properties
- Better resin content control

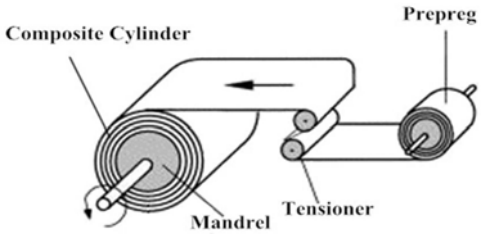

Figure 1.18. Prepreg Winding Method.

1.8.7.2. Winding pattern

There are three types of winding patterns: circumferential, helical, and polar winding.

- **Circumferential winding**

Circumferential winding is a special winding with a winding angle of 90° and is also known as hoop winding [5]. The circumferential winding is shown in Figure 1. 19.

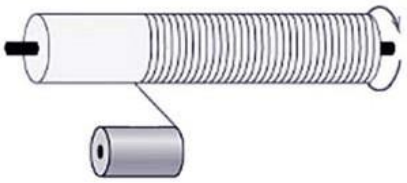

Figure 1.19. Circumferential winding.

- **Helical winding**

In helical winding, the mandrel rotates at a constant speed while the carriage unit traverses back and forth at a regular speed to generate the desired helical angle [5].

The helical winding is shown in Figure 1. 20.

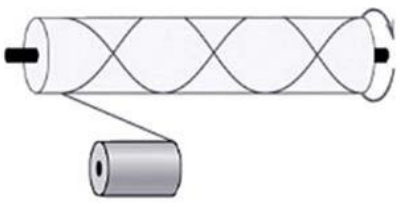

Figure 1.20. Helical winding.

- **Polar winding.**

In polar winding, composite fibres pass tangentially to the pole opening at one end in the reverse direction and pass tangentially to the opposite pole opening. The composite fibres are wound from one pole to another pole, while the mandrel rotates around the longitudinal axis. The polar winding is shown in Figure 1.21. [5]

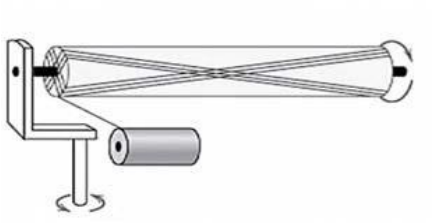

Figure 1.21. Polar winding.

1.8.7.3. Materials for Fabrication

FW requires continuous fibre reinforcement and a suitable resin system for impregnation. The suitable reinforcements are glass, carbon, and aramids etc. The fibre properties affect the stiffness and strength of composites.

Advantages

- Faster rate of production
- Controlled Resin content
- Minimum fibre wastage
- Superior structural properties
- Precise layup

Disadvantages

The process is limited to convex shape components, the cost of the mandrel is high, generally has a poor surface finish and is limited to low - temperature applications.

1.9 Introduction to Composite Pressure Vessel (CPV)

Pressure vessels are important structures as liquids and gases can be stored under high pressure. For low pressures applications, the pressure vessel is constructed in tubes and sheets rolled form. However, special attention is given to building adequate strength to prevent rupture. In recent days filament-wound lightweight and high-strength pressure vessels are replacing conventional metallic pressure vessels. FW is an effective fabrication technique for creating cylindrical composite structures such as pipes, chemical storage tanks and RMCs. The FW technique is one of the emerging manufacturing methods with a high degree of effectiveness and automation and with wide applications in space, defence, transportation, petroleum, naval and shipping industries [18].

1.9.Effect of Environmental Exposures on Composites

The moisture penetrates the composite by the physical diffusion process and affects the matrix, and fibre-matrix interface and leads to bond failure. The presence of voids/cracks initiates a capillarity flow of moisture into the composites. The diffusion process is temperature - dependent and Maximum moisture content is dependent on ambient conditions. The hygro-thermal behaviour of composite is a function of temperature and humidity and exposure to hygrothermal conditions affects the thermal & mechanical properties and decreases the structural performance [16].

1.9.1. Effect of Exposures on Resin

Primarily, moisture is absorbed by the matrix and all thermosetting matrix materials absorb moisture. The curing agents, catalysts and plasticizers also influence the moisture uptake. The toughening elements such as Blends with elastomers, thermoplastics etc substantially change the hygro-thermal behaviour of the composite. Many hardeners are not suitable for hot & humid service conditions. The epoxy resin systems are mixed with a variety of hardeners such as aliphatic, amines and sulfones to produce a cross-linking structure, these functional groups provide are sensitive to moistures [5, 16]. The few prominent functional groups in PMCs are, hydroxyl (O-H), phenol groups (O-C), amine groups (N-O) and sulfone groups (O-S), these group provides sites for hydrogen bonding and water molecules.

1.9.2. Effect of Exposures on Reinforcements

The effect of exposures on reinforcement is widely varying depending on the type of fibre, glass and carbon fibre is mostly inert by nature whereas aramid fibre is hygroscopic in nature. The form of reinforcement such as continuous, discontinuous, and braided mat types absorbs comparatively more moisture. The coupling and finishing agents also affect the moisture exposure and affect the adhesion with the resin system [5,16]. The effect of environmental conditions on different types of fibre is given in Table 1.1.

Table 1.1 Effect of Environmental Conditions on Different Types of Fibres.

Glass	Carbon	Aramid
Not affected by moisture but the adhesion of resin to glass is critical.	PAN Carbon is inert by nature whereas Rayon absorbs moisture	Absorbs a higher weight percentage of moisture than matrix
Surface coating: Sizes, finishes and binders largely influence the hygrothermal behaviour	Does not degrade in a moist environment Adhesion promoted by sizes/couplings	Aramid fibre loose strength under Ultraviolet (UV) exposures

1.11 Ageing Mechanisms

Composites are sensitive to the ageing phenomenon. Heat gets conducted & moisture gets absorbed into the composites when they are subjected to HTs, and wet conditions and the lamina strength and interface properties degrade. Hygro-thermal exposures induce hygro-thermal stresses affecting the properties and geometry of laminates and induce bending [24]. The service life assessment of filament wound composite is important as the change in material properties is expected when exposed to hygro-thermal conditions which lead to irreversible degradation in material strength.

Delamination and other manufacturing defects which get embedded during service life also damage the composite structures [25]. Delamination is usually induced at relatively low load levels, well before the full load capacity of the fibres is attained. As the presence of defects and their growth may adversely affect safety and durability, a comprehensive understanding of the effect of environmental conditions on the structural performance of the composite is of fundamental importance.

1.12 Service Life of Composites

Composites are sensitive to environmental conditions, and it affects the service and operational life of CRMC. Composites also degrade with time. The Factors that effects are temperature, humidity, UV exposures etc, accordingly it is essential to know the useful service life of a Composite Structure under service environments. It is essential to determine the effect of environmental and service conditions on the enviro-mechanical durability of composites ensuring their long-term reliability [25].

1.13 Need Aspects of the Proposed Research Work

Composite-made structures are receiving greater attention in missiles and space systems due to their enhanced performance capabilities. The advent of composites is highly process-dominant and non-homogeneous in nature [5, 6,17 & 26]. The in-service performance of the polymeric composite is sensitive to environmental factors; the strength and other properties degrade due to environmental factors [27-28]. Environmental conditions degrade the mechanical properties and affect the structural performance of polymeric composites [29-30]. The selection of the raw materials calls for detailed characterisation, evaluating all the design properties considering the fabrication methodology and process parameters. During the service life, the composite gets exposed to moisture and temperature variations, affecting its physical and mechanical properties. To understand the effect of environmental exposure on the structural performance, of composites, an extensive study is essential. Further, any defect embedded during the manufacturing service life of composite motor casing may endanger its structural integrity resulting in a huge loss. The damage initiation may occur at any time during the processing stage, curing or subsequent life and may also arise from a wide variety of external causes. The structural degradation can further cause premature failure of the structure resulting in catastrophic incidents during the actual operation of missile systems. There are no laid down acceptance criteria for the acceptability of the casing and hence the effect of service and storage life on the performance of CRMC is to be explored post-prolonged storage. To assess the in-service life of CRMC, an ageing and surveillance program is mandatory [2]. Hence in this context, the proposed research work is initiated to study the life aspects of CRMC - one of the main elements of the SPSs.

1.14 Research Work Plan

In the comprehensive literature review, various research papers, review papers, articles and NASA technical reports are studied concerning composites, RMC, composite processes, materials, characterisation, and life aspects. An extensive literature survey is carried out to study the effect of various environments and the ageing phenomenon of composites.

Unfortunately, in the available literature, efforts to understand the behaviour of the composite casing exposed to different conditions using static firing and natural ageing studies on product levels are extremely rare. The burst test method is used to examine the effect of environmental conditions on the structural performance of CRMC [27]. However, the burst does not simulate the instantaneous pressure rise and combustion environments. On the contrary, a static test resembles actual operational conditions, as expected during flight.

Accordingly, the present study is carried out on a subsystem level resembling the actual flight hardware configuration. The overall effect of environmental conditions and the ageing phenomenon, on the performance of CRMC, is experimentally validated in an integrated way through static firing and full-scale pressure test (for C/E CRMC).

The primary objective of this study is:

- To characterise filament wound C/E and G/E composites – to confirm the design properties and for raw material acceptance
- To study the effect of maximum expected service temperature on mechanical properties of C/E composites
- To study the dynamic behaviour of CRMC during PPT
- To study the effect of natural ageing on the performance of C/E CRMC
- To qualify the G/E composite cases for different service and operational conditions of missile systems such as
    - Vibration
    - Acceleration
    - Shock
    - Temperature environments
    - Thermal cycling
    - Tropical exposures
- To Study the effect of natural ageing and accelerated ageing environment on the performance of G/E CRMC

Finally, the implementation of research findings is applied to validate the useful life of CRMC without affecting its quality and reliability.

Present research work is carried out as per the plan given below

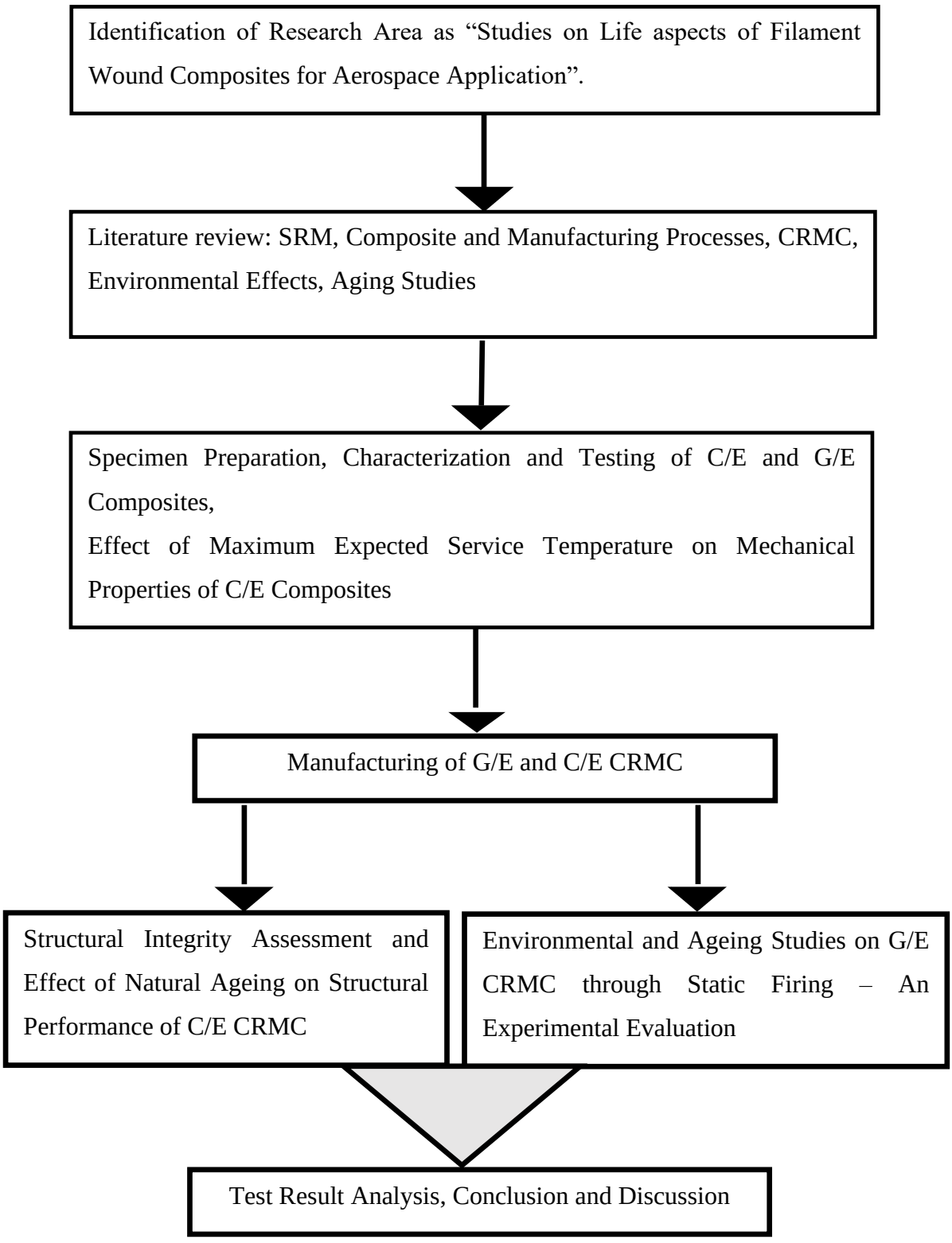

1.15 Organisation of Thesis

The current study deals with studies on the life aspects of filament wound composites for aerospace applications. The effect of various environmental conditions on the performance of CRMC is experimentally evaluated. The expected environmental conditions during the service and operational life of CRMCs are temperature, thermal cycling, tropical exposure, dynamic conditions and natural ageing.

Chapter 1, Introduction

This chapter includes an introduction to Aerospace LVs and Missile systems, Solid propulsion systems, Rocket Motor Casing, CRMC, Composite Materials, Manufacturing Processes and Applications, Ageing of Composites, Needs, Aspects, the relevance of present research work, Road Map and Organization of the Thesis.

Chapter 2, Literature Review

This chapter includes a brief on various published research and technical papers in the field of Solid propulsion systems, Rocket Motors, Failure Mechanisms, Design, Analysis, Development and Qualification of CRMC, Polymeric Composites, Ageing, Service Life, the effect of Environmental Exposures, Accelerated Ageing etc.

Chapter 3, Characterisation Studies on C/E and G/E Composites

This chapter includes objectives, manufacturing of composite laminates/specimens, mechanical properties testing and detailed characterisation of fibre, epoxy resin and Carbon/ Glass epoxy composites, Comparison with test results of naturally aged composite specimens, Effect of temperature on mechanical properties and summary of test results.

Chapter 4, Manufacturing of CRMC

This chapter includes a detailed manufacturing process of Glass-epoxy and Carbon epoxy Composite Rocket Motor Casing, Acceptance and Qualification procedure.

Chapter 5, Structural Integrity Assessment and Natural Ageing Studies on C/E CRMC

This chapter includes objectives and natural ageing studies on carbon epoxy CRMC. CRMC manufactured through the established procedure is exposed to natural ageing. As a part of service life evaluation under natural ageing, CRMCs are subjected to periodic structural integrity assessment and performance evaluation is carried out through periodic pressure tests and results are analysed.

Chapter 6, Environmental Studies on G/E CRMC

This chapter includes the effect of different environments on the performance of CRMC. The CRMCs are subjected to temperature, thermal cycling, vibration, acceleration, shock, and tropical exposure environment. Post-exposure, performance evaluation is carried out through static firing.

Chapter 7, Accelerated Ageing Studies on G/E CRMC

The chapter is about accelerated ageing studies on SRM with G/E composite cases. The CRMCs are subjected to accelerated ageing environments and performance evaluation is carried out through static firing.

Chapter 8, Summary and Conclusions

This chapter includes a summary of the test results from the above tests and conclusions based on studies carried out to meet the research work objectives.

Chapter 9, Future Scope of Work

This chapter further discusses the broad scope for future studies.

CHAPTER 2

LITERATURE REVIEW

With reference to the road map and research objectives discussed in the previous chapter, a systematic literature review is carried out in the field of composites, SRM, CRMC, environmental effects on composites, ageing and accelerated trials and summarised in the succeeding section.

2.1 Introduction

The missile systems are single-shot devices and are designed to perform reliably within the stipulated life cycle. Missile systems are designed optimally and demand the use of high specific strength and high specific stiffness materials to minimize the inert weights resulting in a significant reduction in structural mass. Accordingly, the effect of storage, service, and operational life, on the performance of missile systems is to be evaluated and considered during the design phase [8].

2.2. Solid Rocket Motor (SRM)

SRM is the main workhorse for long-range ballistic missiles and LVs. The RMC, internal insulation system, ignition system, solid propellant grain, and nozzle are the major elements. The RMC works as a combustion chamber and acts as a primary structural member. The motor case is designed to withstand the high-pressure and HT combustion environments

to sustain all expected flight loads and facilitate attachments with other sub-systems/systems [31].

2.3. Rocket Motor Casing (RMC)

RMC is one of the significant and critical sub-systems of SRM and Launch LVs. The design, material systems, manufacturing process, in-process QC, qualification, and acceptance test procedures are the key driver for a robust and reliable product [15, 16]. From the literature survey, it is evident that Failure mode and effects analysis (FMEA) and (Failure mode, effects, and criticality analysis (FMECA) are the key necessity and must be conducted during the design phase considering the operational aspects. FMECA with Risk Priority Number (RPN) approach has been widely applied for the safe design of critical components of Solid Rocket Boosters (SRB) [3]. This is essential for reliable and repeatable performance; probable and catastrophic failures need to be detected and mitigated at an early stage of design and processing. Various open kinds of literature are available on the application of the FMECA concept for the design and development of SRBs [3]. The probable cause of various defects and their failure modes are explored, and suitable preventive actions are adopted during the design and development phase. Ishikawa's approach is adopted to identify and analyse the potential cause of defects. The consequences of different failure modes are identified and the corresponding RPN number is calculated concerning the severity, criticality, and occurrence [2, 3 and 4]. For the critical defect, suitable measures are taken to mitigate the possibility of potential defects. The long-term durability of rocket motor cases for the intended operational and service environment is an essential aspect of space application [16]. This emphasises the need for a comprehensive development program and qualification frame for the development of RMC. Suitable reliability improvement techniques and validation techniques (such as accelerated test methods) are employed to validate the CRMC performance for the intended service life [27].

2.4. Composites

The research for better materials drives the use of composite materials as it displays immense potential with very attractive high strength, high stiffness, and many other superior properties. A brief review of available literature explores the unique and broad application of composites such as polymers, aramids, composites, and carbon and glass based FRP. It is noted that the composite raw materials properties are dictated by microstructure, and it plays a significant role in defining their applications. Alberto [32] studied the physical changes in the molecular structure of the epoxy-based matrix and evaluated their influence on the

performance of the composite. He concluded that the development of aerospace polymeric composites, calls for trade-off decisions concerning the design, materials, processing, and functional aspects. Composites are process-sensitive and are non-repairable in nature, accordingly, the manufacturing and assembly process evolved to meet the functional requirements. The various available reliability and process improvement techniques such as a cause-effect diagram, fault tree analysis, and FMEA are to be adequately adopted as a part of risk mitigation plans to prioritize manufacturing of errors free FRP products [8].

2.5. Composite Rocket Motor Casing (CRMC)

Filament wound composite cases are replacing the conventional metallic RMC, as the required properties can be tailored according to design [6 & 17]. The use of advanced composites improves the performance factor (n = PV/W) of CRMC as compared to metallic ones [6 & 7]. Filament wound composites are the prominent choice due to their high-performance factor (n=12-15) resulting in weight reduction. However, composites are more prone to damage accumulation such as matrix cracking, delamination, de-bonding, porosity, fibre buckling, fibre breakage etc [28]. This calls for detailed characterisation and identification of suitable NDT methods for process control and defect diagnosis. The UT, RT and Acoustic Emission Testing (AET) are the primary NDT techniques with a credible history of usage for process and quality control of composite structures. A detailed test plan to be evolved and different specimens to be made simulating the processing environment and the corresponding NDT signatures shall be recorded for future comparison and evaluation purposes.

This design, development and qualification procedure of filament wound high-performance CRMCs with augmented payload capabilities meant for VEGA SRM gives an insight into various design, process and technology-related challenges [7]. Biagi et al [11] discuss the development and qualification framework for VEGA P80 composite motor case. He outlined major milestones in, a development plan with a special focus on structural qualification and burst pressure tests for composite cases. The design and analysis philosophy of CPVs with integrated and unequal end domes needs special attention. The unequal pole opening dictates the filament winding parameters. Madhavi et al [17] discuss a process design approach to understand the behaviours of composites, studied the implication of filament winding parameters and predicted the corresponding burst pressure. The results are significant in understanding the structural characteristics of filament wound pressure vessels. The design, material system and manufacturing process affect the structural integrity of CPVs for long-

term use. The structural integrity is a function of materials microstructure; inspection methods; load spectrum; the consequences of impact, fatigue, environmental conditions, and the nature of inherent flaws [33]. The optimal ply design of the composite shall affect the burst pressure. The determination of appropriate winding angle and ply thickness is an important aspect of structurally efficient filament wound composites [34]. The various winding parameters such as winding tension, ply angles, V_f, viscosity and temperature etc affect the structural performance of filament wound CPVs. Both analytical solutions and experimental validation are essential to design and developing structurally efficient composite cases. Onder et al [26] studied the optimal angle-ply orientations of symmetric and anti-symmetric G/E composite for maximum burst pressure. The study deals with the influences of processing temperature and winding angle on filament wound CPVs. Both analytical and experimental solutions were carried out. The Finite Element Analysis (FEA) results are validated with an experimental burst pressure test and demonstrate a good correlation. Park et al [35] studied the importance of appropriate winding angles and achieved ply thickness for structurally efficient filament wound composites. FEA is carried out to predict the behaviour of filament wound structures and results are validated with strain data acquired from the experimental pressure test.

2.6. Acceptance and Qualification – Composite Motor Case

There are many design and development-related challenges associated with the FW process and those challenges need special attention [18]. It is essential to understand the various design, and process-related challenges to realise a reliable filament-wound composite [36]. The CRMCs are required to be realised with consistent quality and high order of repeatability. In the process, QC and an efficient NDT methodology are to be established to realise high-performance CRMC with consistent quality [6]. The NDT techniques are complementary to each other; a comprehensive NDT scheme is essential for structural integrity assessment [6]. Ibrahim [37] studied various types of defects that may arise during manufacturing and also studied in service usage of composite materials for marine environments. To understand the likely distribution of various flaws, their characteristics and functional implication, various type of flaws are characterised using different NDT techniques and their corresponding signatures are recorded.

In open sources, several pieces of literature are available with an outline, development plan, applicable NDT techniques and suitable mathematical models, with specific emphasis on full-scale qualification methodologies for large-size CRMCs. Huang [38] highlights the relevance of AE for the Non-Destructive Evaluation (NDE) of PMC, various available

techniques, applications, and future trends. He describes the AE fundamentals and techniques suiting PMC. A typical AE testing process is described and compared with other available NDE methods. Waller [39] discusses the use of AE to monitor progressive damage accumulation in Kevlar composites. The significant AE events are the outcome of microstructural change and defect prognosis. The progressive damage is monitored during tensile tests of Kevlar/epoxy specimens, and different AE parameters such as AE event rate and energy parameters are monitored. The test results are analysed, and the location of active sources is identified based on energy attenuation and arrival time differences of significant events.

Chou [40] studied the damage Analysis of CPVs Using AE as an in-service inspection method, AE sensors, strain gauges and optical sensors are used during the pressure tests. Post-pressure test and acousto-ultrasonics are also carried out for Structural Health Monitoring (SHM). The concept is useful to evaluate damage accumulation and assess health degradation over some time. Furthermore, the potential of performing life assessment of CPVs using AE is demonstrated. The test results are also useful for failure prediction. Chou et al [41] studied the effect of constant and cyclic loads on the performance of CPVs using AE. AE tests revealed that the development of damage is highly variable under constant pressure and affects the behaviour of the carbon fibre rupture process. Mane et al [42] studied the SHM of SRM using AE during PPT. The dynamic behaviour of RMC is recorded using Acoustic AE techniques and the active zones are identified. Online structural integrity monitoring of CRMCs is carried out to evaluate the effect of the dynamic behaviour of flaws and to validate the manufacturing process and final acceptance. The strain, dilations, and acoustic behaviours are measured online during the pressure test and post-test, detailed comparison of NDT signatures is carried out indicating the soundness of the structure. Weathers et al [43] studied the damage assessment of RMC using the Felicity Ratio (FR), which indicates the soundness of motor casing and monitored any growing and active defects. AE is widely used as a diagnostic and predictive tool for the burst prediction of CPVs.

The development and qualification procedures for qualifying VEGA igniters are studied. To realise an optimised composite case, a new concept for manufacturing composite casing is adopted. The design is validated through no. of repeatable and successful ground static firing [44]. The results demonstrate a good correlation between the prediction and static firing test results. The post-test inspection is carried out and observations are recorded [45]. Tam et al [46] give an insight into the design and manufacturing philosophy of titanium lined Composite Overwrapped Pressure Vessels (COPV) for high-pressure helium storage tanks intended for

spacecraft application. The non-linear modelling techniques are evolved to predict the Margin of Safety (MoS) for the end application. A qualification program is evolved to verify design adequacy and to evaluate design margins through destructive burst pressure tests. Jush et al [47] studied the structural design philosophy and experimental validation procedure for E glass based COPV. This study highlights the COPV design, probable failures, manufacturing process and operational aspects.

2.7. Effect of Environmental Conditions

PMCs have many types of binding and reinforcement systems. In general, fibre is inert, does not absorb moisture and is resistant to many chemical solutions making them particularly suited to the adverse environment. It is learnt from the available literature that the interface between fibre and matrix plays an important role in dominating the final performance of composites and it is also sensitive to hygrothermal exposures. Maxwell A et all [48] discuss various failure mechanisms experienced in PMCs and relevant techniques for life prediction. These failure and degradation mechanisms help to develop suitable predictive models for service life estimation [49]. Environmental exposures affect the mechanical and physical properties of composites [50]. The various internal factors like the V_f and its orientation to the moisture diffusion path also influence the functioning of composites. The observed trends can be explained in terms of typical fibre permeabilities, and the diffusion paths preferred by moisture [51]. The physical ageing phenomenon in composites affects their mechanical properties, viscoelasticity, fracture toughness, thermal expansion coefficient, volume and enthalpy relaxation and moisture absorption capabilities [52]. As composite structures are optimally designed, the damage and degradation mechanisms shall be considered during the design phase. Several kinds of literature show applications of the probabilistic framework to predict damage accumulation in CPVs. These models are supported by the experimental test results on different specimens. AE and NDT signatures are obtained, and suitable failure prediction models are generated [36].

Parhi et al [24] carried out Finite element analysis FEA based on the first-order shear deformation theory to obtain the free vibration and transient response of multiple delaminated composites under a hygrothermal environment. The analysis considers the lamina material properties at elevated moisture concentration and temperature. The results show a reduction in the fundamental frequency with an increase in the percentage of uniform moisture content as well as temperature for simply supported anti-symmetric cross-ply and angle-ply laminates and it is independent of delamination size. Chamis et al [53] developed a statistical predictive

model to determine the significant hygrothermal variables influencing the tensile durability of epoxy composites and its comparison with tested data. Davison [54] studies the effect of temperature and moisture variation on strength degradation and fatigue behaviour of C/E composites. The fatigue and damage accumulation tests are also carried out and a mathematical model is generated for failure prediction.

The expected harsh environments during service life such as saline environments and HT also affects the structural performance of the epoxy composite. Exposure to a saline environment affects the absorption characteristics, and microstructure properties and contaminates the composites. It degrades the chemical and physical bonding at the interface and mechanical properties [29, 30]. Idrisi et al [30] tested different composite specimens for seawater environments. The effect of environmental exposures is investigated in terms of seawater absorption, microstructure, and mechanical property degradation. The test results form the basis for formulating a mathematical model for predicting the strength degradation. The temperature and moisture affect the tensile strength of graphite epoxy composites. The ultimate tensile strengths are measured for different temperature ranges and moisture contents [55]. The temperature and moisture affect the interlaminar delamination toughness [56]. Dry and moisture-saturated composite specimens are tested over a temperature range. The effect of delamination is evaluated in terms of load-carrying capabilities and strain energy release rate [56]. The strength degradation of G/E composites against a hygro-thermal environment is experimentally evaluated. The composite specimens are subjected to various hygro- thermal environments and tested for mechanical and Inter Laminar Shear Strength (ILSS) properties. The test results are compared with virgin specimens and degradation in properties is experimentally evaluated [28]. No. of mechanical tests are performed to evaluate interlaminar fracture toughness indicating the degradation in fibre/matrix bond strength. The results demonstrated that the moisture absorbed by the laminates causes either reversible or irreversible plasticization of the matrix. The humidity combined with the temperature may also cause significant changes in the T_g of the matrix and toughness affecting the laminate strength. This behaviour is investigated by Scanning Electron Microscopy (SEM) and Dynamic Mechanical Analyser (DMA) [41]. Sethi S [57] studied the effect of high & low temperature, UV, and different strain rates on mechanical responses of C/E and G/E composites. It is concluded that fibre/matrix microstructure influences the amount of thermal energy absorbed and consequently affects the mechanical properties. Also, the effect of environmental variants on fibre/matrix interfaces and stability is studied.

Singh [58] studied the strength deterioration of GFRP sandwich composites due to temperature, sunshine, water/moisture, alkalinity and applied load. An experimental investigation is carried out to study the combined effect of moisture and temperature & also to study the rate & magnitude of damage in G/E composites under hygrothermal loading conditions. Li [59] studied the effect of temperature and moisture on composite-made wind turbine blades. The effect of temperature and moisture is evaluated on E- glass fibre with different combinations of the resin system. He made different types of specimens, and no. of mechanical tests are conducted to evaluate interlaminar fracture toughness and fibre/matrix bond strength. He also performed micro-debonding tests both on dry and wet specimens and discussed various aspects of improving delamination resistance.

In the literature, various studies are reported describing the effects of moisture, temperature and hygrothermal conditions on the strength, durability, and structural integrity of C/E composites. The changes in fatigue strength are evaluated on the composite specimens aged under humid and elevated temperatures [60]. The static and cyclic performance of composite with embedded defects is investigated at room temperature both in dry and wet conditions [61]. Patel et al [60] studied the effects of moisture variation, temperature cycling and hygrothermal ageing on the strength and durability of a graphite/epoxy composite. The specimens are exposed to humid and HT environments and fatigue and residual strength are evaluated; the corresponding damage mechanisms and respective failure modes are identified [47].

Hizli [27] studied the effect of various applicable environmental factors on the structural performance of CRMC. The no. of prototypes is realised and subjected to different environments such as high/low-temperature cycle, thermal shock, high-temperature humidity, icing, salt fog and vibration. Post-environmental test, the burst test is conducted to identify the burst pressure and burst mode. The result showed that LT cycle and salt fog tests have a significant effect on burst pressure whereas icing tests have negligible effects [27].

2.8. Ageing studies

For predicting and evaluating the long-term durability of composites, for different climatic conditions, robust modelling and experimental methodology are mandatory. Several mathematical models are developed by several researchers using Arrhenius principles to predict the degradation in C/E composite under hygrothermal exposure under applied stresses. Chawla [62] developed a mathematical model incorporating synergistic interactions between temperature, moisture, and stress effects, predicting strength and stiffness degradation under

different ageing conditions. A proven modelling concept and life-predicting methodologies are the keys to predicting and estimating the degradation in composite properties over some time. A test program is designed to validate the model with experimental results of degradation in composite properties under hygro-thermal and other environmental conditions [28]. Gates et all [63] discuss the application of accelerated test methods for polymeric composites for high-temperature environments. He discussed different screening methods suitable to identify new material systems intended for the long-term duration and extreme environments such as elevated temperature, moisture, oxygen and mechanical load. Bilkstad M et all [64] studied the effect of long-term moisture absorption in graphite/epoxy composites. The moisture content vs. square root of exposure time is estimated using Fick's equation of moisture diffusion. A three-dimensional solution is used to predict the moisture absorption for specimens of a small width-to-thickness ratio.

Reilly et al [65] studied the effect of ageing on the mechanical properties of C/E composites. The C/E specimens are exposed to an accelerated ageing environment, subsequently, DMA and short beam shear tests are carried out to quantify the degradation. The test results show a significant loss in the T_g and the short beam shear test revealed a significant decrease in ILSS. The influence of an accelerated hygrothermal ageing environment on G/E composite is evaluated through water absorption, DMA, Thermo Gravimetric Analysis, and short-beam shear strength tests [66].

The long-term behaviour of FRP composites against a hygro-thermal environment is evaluated by conducting no. of mechanical tests. Based on test results, a correlation model is developed indicating the effects of deionized water and humidity on the long-term durability of composites [67]. The effect of long-term moisture absorption in epoxy composites is evaluated by observing the change in moisture content vis-à-vis the square root of exposure. The long-term durability of CFRP is evaluated for low earth orbit environments consisting of high vacuum, atomic oxygen and Ultra Violet (UV) light exposures. Accelerated ageing tests are carried out and based on the test results, long-term mechanical behaviour is predicted Ethylene Propylene Diene Monomer (EPDM) [68].

Various accelerated test methods are adopted to characterise the effect on the functionality of advanced composite materials [69]. The long-term ageing phenomenon affects the performance of CPVs. Different tests are carried out to evaluate the ageing effect on overwrap tensile strength on epoxy-based specimens. Further, several kinds of literature are reported demonstrating the effect of ageing on mechanical properties on the performance

of COPV [70]. From the literature, it is observed that the service and operational life of CPVs is a function of ageing and expected service and operational environments.

2.9. Gap Analysis

The above papers and literature have enlightened various concepts, fundamentals, and ideas to formulate the present research work. The explicit details of the following experimental research works are not available in the open literature:

- Evaluation of drop in mechanical properties of C/E composites against the maximum expected service temperature
- Study on dynamic behaviour of C/E CRMC against designed load
- Effect of natural ageing on the structural performance of C/E CRMC
- Experimental validation of the impact of environmental conditions on the structural performance of CRMC through static firing resembling flight hardware configuration (Integrated subsystem level studies)
- Accelerated ageing studies on CRMCs

2.10.Summary:

In the comprehensive literature review, various research papers, review papers, articles and NASA technical reports are studied related to SRM, RMC, CRMC, Polymeric composite materials, characterisation, manufacturing processes, structural integrity assessment, the effect of environments on polymeric composites, ageing and evaluation of long-term degradation using accelerated test methods. Based on literature studies, and functional and operational-related considerations, it is concluded that a specific life study program is to be initiated to establish the long-term durability of CRMCs considering the specific storage, service and operational conditions. The various concepts learned from the literature review are taken as a reference to formulate the research objectives for the present research work.

CHAPTER 3
CHARACTERISATION STUDIES ON C/E AND G/E COMPOSITES

This chapter discusses the specimen preparation, characterisation and testing of filament wound C/E and G/E composites. This study is initiated to validate the design properties, and correlation and to generate acceptance test data of starting raw materials.

3.1. Material Selection

The primary material and processing technique for realising the CRMCs are C/E, G/E and FW respectively. FW is possible either with tow pregs or with a roving and wet resin system. In the present study, wet winding with T-700 Poly Acrylo Nitrile (PAN) based carbon fibre (12K) and epoxy resin are considered for large size RMC for booster and upper-stage applications. For, smaller Solid Rocket Motors (SRMs), wet winding with E- glass epoxy is considered. The small SRMs are used for the ignition of large SRMs.

3.2. C/E Composites

For, C/E composites, two different material systems are studied:

- T-700 (PAN-Based) Carbon fibre with LY556 and HY5200 epoxy resin system
- T-700 (PAN Based) Carbon fibre with Epo1555 and FH5200 epoxy resin system

3.2.1. Acceptance Test Procedure - Carbon Roving (T-700)

The carbon roving is visually inspected for defects such as stains, discoloured patches, fibre cuts etc. The Tex of the roving's is determined by weighing 1 Km length of the roving. The filament diameter is determined using Tex and density of roving. The carbon content is measured using a CHNS-O elemental analyser. The average test results of T-700 (12K) PAN based carbon fibre are given in Table 3.1

Table 3.1 Technical Specifications and Test Results - T-700 Carbon Fibre.

Parameter	Specification	Avg. Test Results	ASTM Standard
Tex	800 gm/km (min.)	798	--
Fibre Diameter	6–8 microns	6.88	--
Carbon Content	94% (min.)	94.5	--
Sizing Content	1%	1.1	--
Specific Gravity	1.7 –1.8	1.75	D792 [71]
Impregnated Tow Tensile Strength, (MPa)	3000 (min.)	3015.85	D4018 [72]
Hoop Tensile Strength (MPa)	1200 (min.)	1667	D2290 [73]
ILSS (MPa)	40 (min)	52.0	D2344 [74]

* The above results are QC and acceptance parameters, generated from in-house testing. The Impregnated tow test, hoop tensile strength and ILSS results are corresponding to T-700 & LY556/HY5200 resin system for a V_f of 0.6.

3.2.2. Acceptance Test Procedure - Epoxy Resin System

- **LY 556 and HY 5200 Resin System**

LY556 epoxy resin (DGEBA Based) is based on Bisphenol-A and Hardener HY5200 is a non-MDA-based liquid aromatic diamine with low viscosity. Resin LY556 and Hardener HY5200 are mixed in a ratio of 100:24 and gel time is recorded. The resin mix is subsequently heated to 160°C for 20 minutes and the mass loss is recorded as volatile content. The cure cycle followed is: 120ºC /2 hrs +180ºC /4hrs. The technical specification and average test results of epoxy resin (LY556 & HY5200) system are given in Table 3.2.

Table 3.2 Technical Specification and Test Results - LY556/HY5200 Epoxy Resin System.

Parameter	Specification	Avg. Test Results	ASTM Standard
Epoxy Resin LY 556			
Viscosity at 25 °C, cPs	8000-12000	8600	D2393 [75]
Specific Gravity at RT	1.10 -1.20	1.16	D891 [76]
Volatile Content, % Wt	<0.75	0.08	
Epoxy content, Eq./kg	5.0 to 5.9	5.5	D1652 [77]
Hardener HY5200			
Viscosity at 25 °C, cPs	150-180	156	D2393
Specific Gravity at RT	1.0-1.1	1.02	D891
Gel time at 100°C, (min.) (Mix ratio LY556: HY5200=100:24)	120 (min.)	150	--

- **Epo 1555 and FH 5200 Resin System**

Epo -1555 is a modified distilled liquid epoxy resin. It contains hydroxyl groups, creating flexible sites on the cross-linked polymer. Chemically, Epo 1555 is 2-[[4-[2-[4-(Oxiran-2-ylmethoxy) phenyl] propan-2-yl] phenoxy] methyl] oxirane (Figure 3.1).

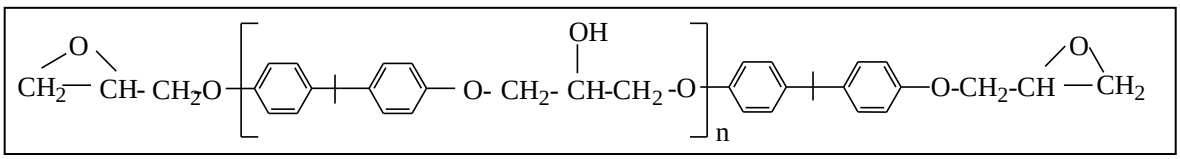

Figure 3.1. Chemical Structure of Epo 1555/FH 5200 Resin System.

It is based on Bisphenol- A. Epo-1555 gives a partly flexible system without compromising the T_g of the cured system. Fine hardener FH 5200 is a formulated aromatic amine and acts as a curing agent. The viscosity of Epo-1555 has been studied at various temperatures and the variation against temperature is shown in Figure 3.2.

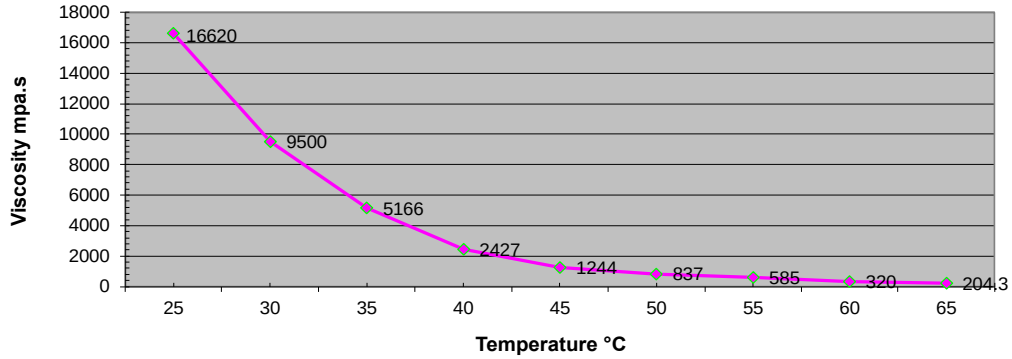

Figure 3.2. Viscosity vs Temperature of Epo 1555 Resin.

Epo 1555 reacts with FH 5200 to form a semi-interpenetrating polymer network (SIPN). This system has a long pot life making it suitable to produce large composite structures. This Resin system retains high mechanical strength at elevated temperatures and has T_g of about 160-170ºC. Accordingly, Epo 1555/ FH 5200 resin system is considered here for the FW process, the stability is studied at 45ºC, and the results are shown in Figure 3.3.

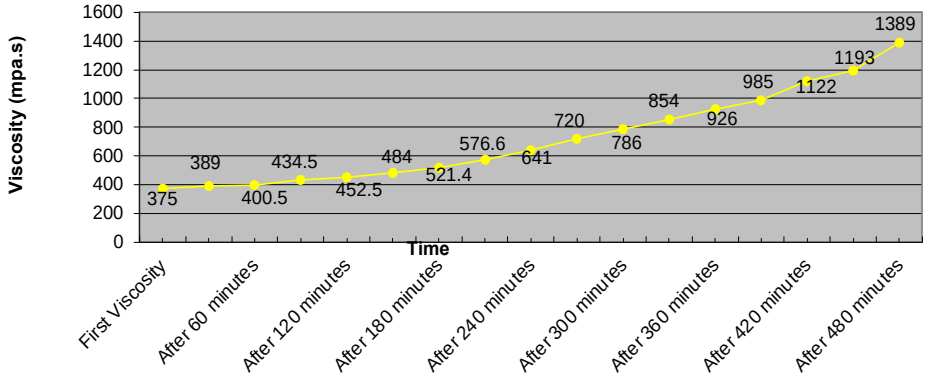

Figure 3.3. Viscosity vs Time – Epo 1555 and FH5200 Resin System.

The technical specification and average test results of Epo1555 and FH5200 Epoxy resin systems are given in Table 3.3.

Table 3.3 Technical Specification and Test Results - Epo1555/FH5200 Resin System.

Parameter	ASTM Standard	Specification	Avg. Test Results
Epoxy Resin 1555			
Specific Gravity at 25°C	D891	1.15-1.20	1.17
Viscosity at 25°C (cps)	D 2393	15000-18000	16400
Volatile Content (% by wt.)	--	<1	0.19
Epoxy Content (Eq/Kg of resin)	D1652	4.8-5.9	5
Hardener FH 5200			
Specific Gravity at 25°C	D891	1-1.1	1.02
Viscosity at 25°C (cps)	D2393	150-200	180
Initial mix viscosity - Resin & Hardener, at 25°C (cps)	D2393	5000-7000	6500
Initial mix viscosity - Resin & Hardener, at 45°C (cps)	D2393	800-1200	900
Gel time of Resin mix at 100°C (min.) (Mix ratio of Epo1555:FH5200=100:27) (min.)	D 2471 [78]	120	140
T_g by DSC (°C)	E 1356 [79]	155-170	161

3.2.3. Mechanical Testing - Neat Resin System

The tensile test specimens are made from a neat epoxy resin system and tensile strength, modulus, and elongation are evaluated in accordance with ASTM D 638 [80]. The mould used for preparing mechanical samples, test specimens, and mechanical testing procedure is shown in Figure 3.4.

(a) (b) (c) (d)

Figure 3.4. Mechanical Testing of the Neat Resin System (a) Mould (b) Test Samples (c) Mechanical Testing (d) Failed Specimens.

- **Mechanical Properties of LY556 and HY5200 Resin system**

The mechanical property test results of LY556/HY5200 resin system are given in Table 3.4.

Table 3.4 Test Results - Mechanical Properties of LY556/HY5200 Epoxy Resin System.

Properties	ASTM Standard	Avg. Test Results
Tensile strength (MPa)	D 638	50
Tensile Modulus (GPa)	D 638	3
(%) Elongation		2.1

- **Mechanical Properties of Epo1555 and FH5200 Resin system**

The tensile Strength vs strain (%) plot for neat epoxy resin (Epo1555/FH5200) is shown in Figure 3.5.

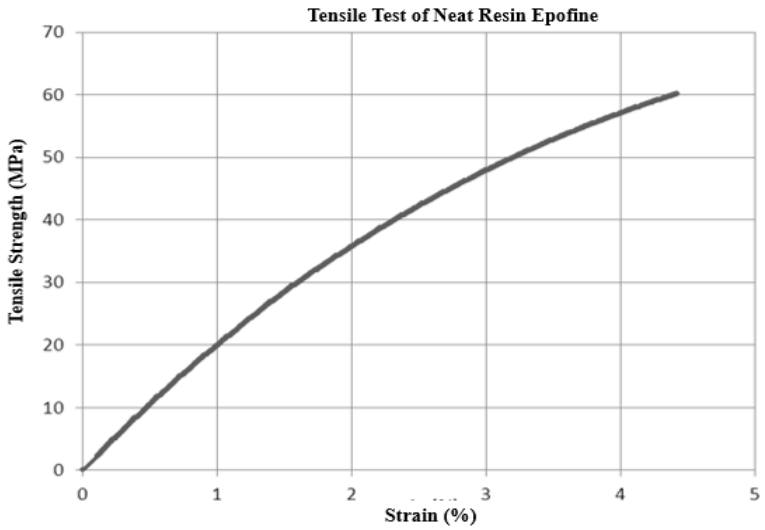

Figure 3.5. Tensile Strength vs Strain (%) Plot for Neat Resin (Epo1555/FH5200).

The test results for mechanical properties of the neat resin system are given in Table 3.5.

Table 3.5 Test Results - Mechanical Properties of Epo1555/FH 5200 Epoxy Resin System.

Properties	ASTM Standard	Avg. Test Results
Tensile strength (MPa)	D 638	60
Tensile Modulus (GPa)	D 638	2.8
% Elongation		4.2

3.2.4. Characterisation

A comprehensive study is carried out to understand the behaviour and properties of composite raw materials. The detailed material characterisation of C/E and G/E composite is carried out to generate necessary data to validate the design properties and for raw material acceptance. For minimum characterisation of a uni-directional (UD) composite, the following properties are required:

- Longitudinal Elastic Modulus, Transverse Elastic Modulus, In-plane shear modulus, and major Poisson ratio
- Longitudinal Tensile Strength, Longitudinal Compressive Strength, Transverse Tensile Strength, Transverse Compressive Strength, and In-plane shear strength

The mechanical testing is carried out on a calibrated universal testing machine (Instron UTM) to evaluate the ultimate properties of different specimens in accordance with applicable ASTM standards.

3.2.5. Method

The road map followed for the characterisation study is given in Figure 3.6.

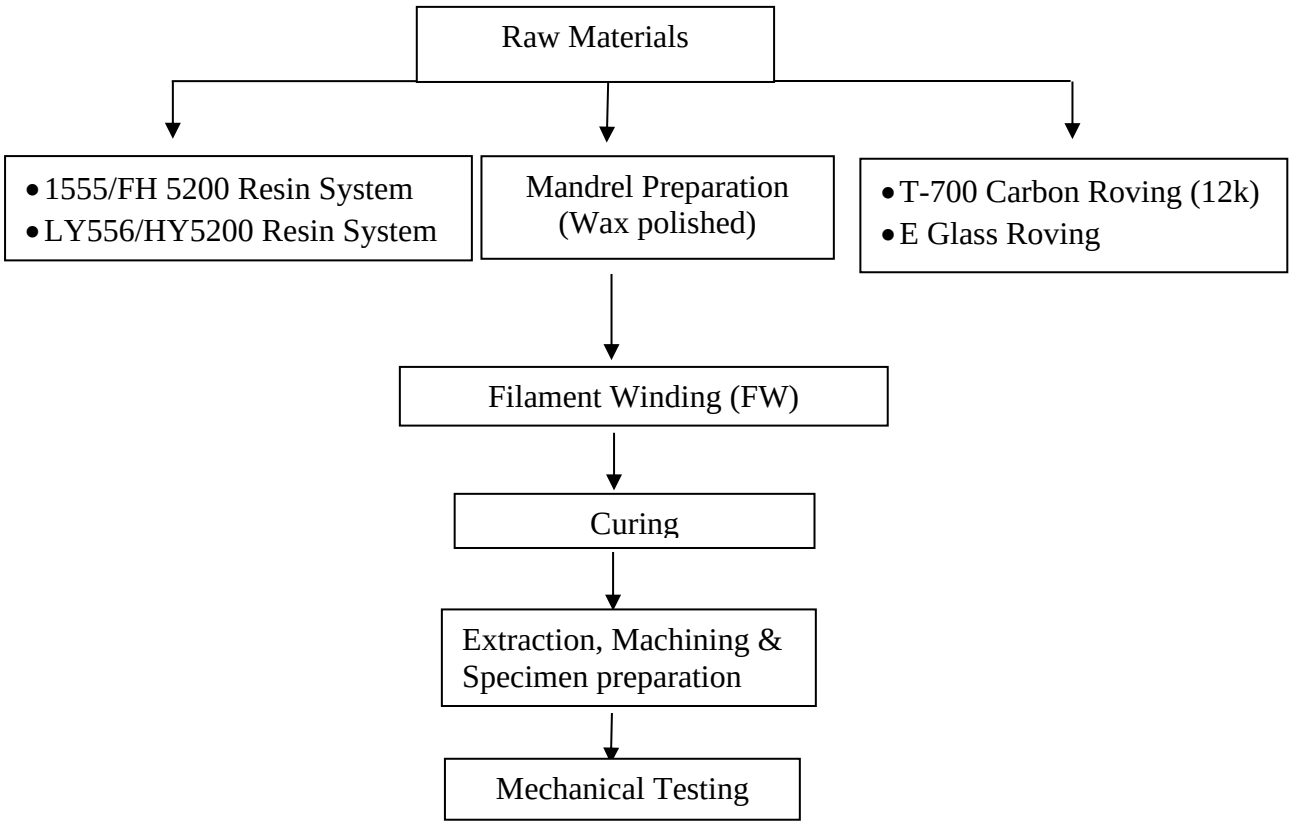

Figure 3.6. Road Map for Characterisation Studies of Filament Wound Composites.

3.2.5.1. Manufacturing Process

To, test and generate the various properties mentioned in para 3.2.4, and to evaluate ILSS, flexural and hoop tensile strength, the required number of laminate/ ring specimens is worked out. The test specimens are manufactured using the FW process. The fibre spools are kept on the creel stand, several roving's are drawn and passed through the resin bath and pulled from the pay-out eye and placed on the flat/rectangular/cylindrical mandrel. The mandrel and pay-out eye motions are started, and the thickness builds up as the winding progress (Figure 3.7). Different UD laminates (with fibre orientation of 0°) of 2, 3 and 4 mm thickness and 2mm thick laminate with fibre orientation of ± 45º is prepared.

(a) **(b)** **(c)** **(d)**

Figure 3.7. Manufacturing Process of Test Laminates using FW Method: a) Resin bath b) Creel stand c) FW d) Laminate.

3.2.5.2. Curing

The test laminates are cured in a calibrated oven according to a predetermined cure cycle as per resin cure characteristics. The cure cycle of LY556/HY5200 resin system is shown in Figure 3.8.

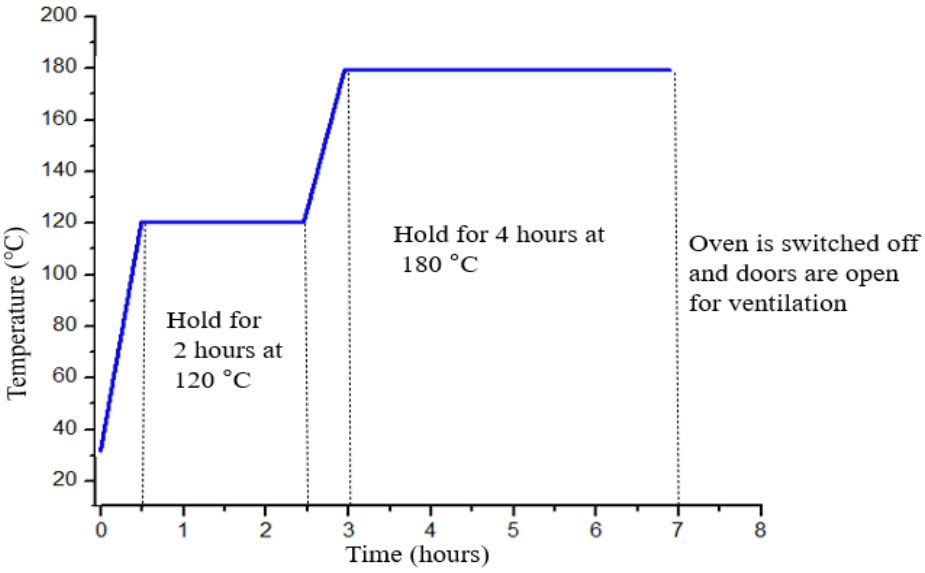

Figure 3.8. Curing Cycle - Carbon Fibre /Epoxy Resin (LY556 & HY5200).

The Epoxy resin systems (EPO1555 and FH 5200) are mixed in a ratio of 100:27 and the cure cycle followed is: 120ºC /3hrs +160ºC /3hrs.

3.2.5.3. Non-Destructive Testing

The test laminates are inspected with both UT and RT. Through Transmission UT is carried out with test frequency of 0.5 Mega Hertz (MHz) and a probe of dia. of 10 mm is used. The Threshold level and gains are set as 90% and 58 Decibel (dB) respectively. The Laminates are found to be free from delamination, resin rich areas, cracks, and other defects.

Post UT, RT is carried out to detect internal defects like de-bond, voids, delamination, etc. KODAK made fine-grained radiographs used and processed as per the standard procedure. The radiographs are viewed by a viewer in subdued lighting and laminates are free from any defects.

3.2.5.4. Quality Requirements

The FW is highly process-intensive and quality requirements are stringent. The requirement is as follows:

- Inspection and clearance of mandrel
- Trial winding and validation
- Verification of life and clearance of all the raw materials

- Verification of ply sequence
- In process QC checks
    - Resin & hardener mix. ratio
    - The viscosity of Resin mix
    - Carbon roving tension for each spool (Spec: 0.5 kgs/spool).
    - Resin bath temperature 45±5°C

3.2.5.5. Specimen Preparation

Post curing, laminates are cut, trimmed and laminates of 400 mm×400 mm sizes are made. The test specimens are cut using a diamond tip cutter and aluminium tabs are bonded using AW 106 and HV 953U resin system. For, longitudinal test specimens, laminate is cut in the fibre direction, and for transverse direction specimens, laminate is cut in the transverse direction as shown in Figure 3.9.

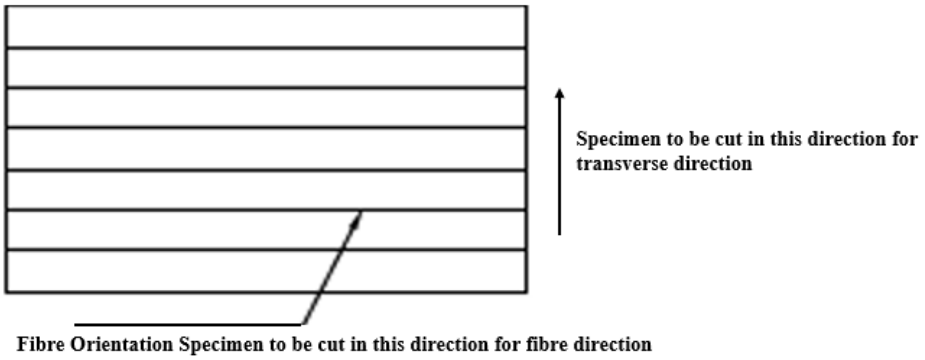

Figure 3.9. Fibre Orientation in Laminates.

3.2.6. Physical Properties Testing

The resin content, V_f and density are checked from the cured sample representing each laminate as per ASTM D3171 [81] and ASTM D 792, respectively. A sample of C/E composite is dried and weighed, immersed in an acid solution to dissolve the matrix. The residue is filtered, washed, dried, and weighed, and the V_f = (Wf/pf)/(Wc/pc) is calculated, Where, Wf = Weight of fibre, Wc = Weight of composite, pc=Density of composite, and pf = Density of fibre. The T_g is investigated as per ASTM E 1356, by the Differential Scanning Calorimeter (DSC) method. The heat flow is recorded vis-à-vis the temperature rise. In addition to DSC, for one time validation, T_g is also evaluated using Thermo-Mechanical Analyser (TMA) in accordance with ASTM E 1545 [82]. TMA estimates the T_g of a material by measuring the changes in its coefficient of thermal expansion (CTE) vis-à-vis the temperature rise. The DSC setup, DSC, and TMA scan of the composite sample are shown in Figure 3.10 and the value of T_g for one of the samples is 161.5 °C (DSC).

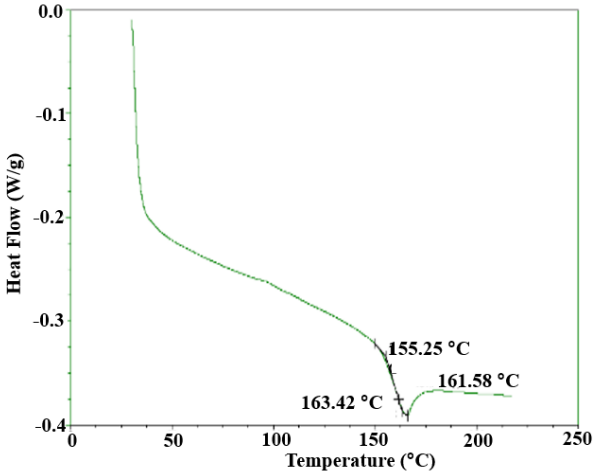

(a) **(b)**

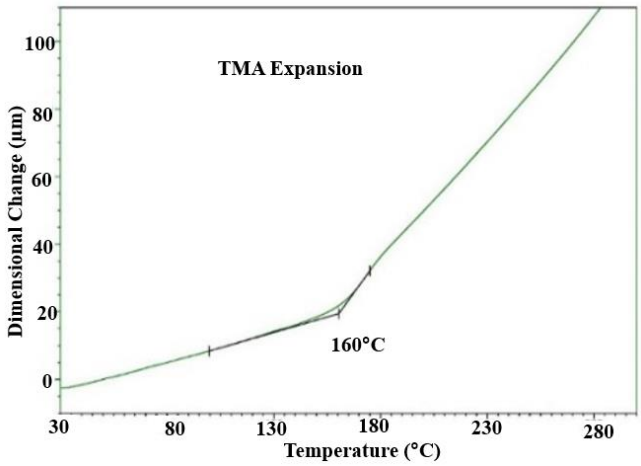

(c)

Figure 3.10. (a) DSC Test Setup (b) DSC Scan (c) TMA Scan.

The physical property test results of T-700 carbon fibre with LY556/HY5200 epoxy resin system are given in Table 3.6.

Table 3.6 Test Results - Physical Properties T-700 with LY556/HY5200.

Contents	Sample-1	Sample-2	Sample-3	Average	Specification
Resin Content (% wt.)	35.9	36.2	35.5	35.86	35-45
Density (Kg/m^3)	1408	1490	1480	1480	1500 ± 50
DSC	No residual exothermic peak in DSC				
T_g of Composite (^{0}C)	163	161.5	163.5	163	

The results of the physical properties test of T-700 Carbon fibre with Epo1555/FH5200 epoxy resin system are given in Table 3.7, respectively.

Table 3.7 Test Results - Physical Properties T 700 with Epo1555/FH5200.

Sl. No	Parameter	Average Value
1	V_f (%)	60
2	Density (Kg/m^3)	1350
3	T_g (^{0}C) (By DSC)	161-168

3.2.7. Mechanical Properties Testing

All test samples are dried in a moisture removal chamber (Figure 3.11) and moisture content is calculated. First Sample is weighed at the ambient temperature (Wa), Samples are dried and weighed again (Ws). The Moisture content % (weight) is = (Wa- Ws)/ Ws *100 is calculated and a moisture content of ≤0.1% is reported.

(a) **(b)**

Figure 3.11. (a) Moisture Removal Chamber (b) Samples inside the Chamber.

3.2.7.1. Longitudinal (0°) Tensile Test and Transverse (90°) Tensile Test

The longitudinal tensile test (Figure 3.12) is conducted to evaluate the tensile strength (σ11) along the fibre direction (0°), Modulus (E11), and major Poisson's ratio (ν12) in accordance with ASTM D 3039 [83]. The dimension of the tensile specimen is as follows:

Length: 250 mm, Width: 15 mm for Longitudinal (0°) Tensile Test Specimen and 25 mm for Transverse (90°) Tensile Test Specimen, Thickness: 2 mm. For, strain measurement, rosette strain gauges are used. The longitudinal tensile strength is calculated from the corresponding ultimate load and longitudinal tensile modulus is evaluated from stress-strain curve. The major Poisson ratio (μ_{12}) is obtained from lateral and longitudinal strains using an extensometer. The longitudinal test is shown in Fig 3.12.

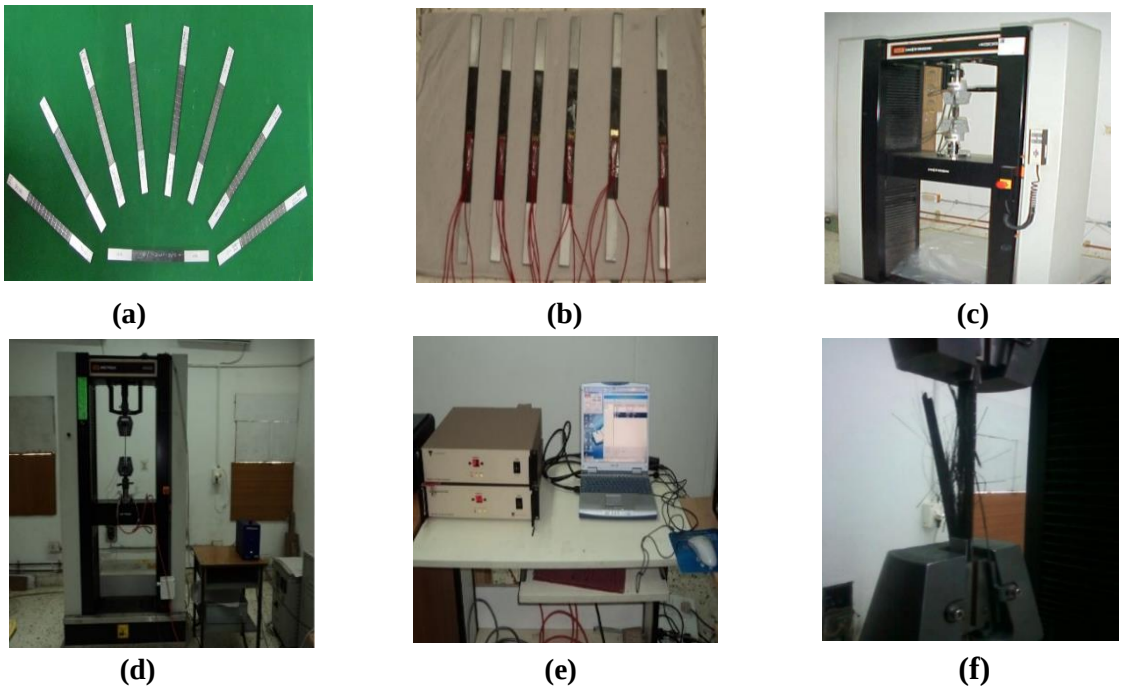

(a) **(b)** **(c)**

(d) **(e)** **(f)**

Figure 3.12. Tension Test on Longitudinal Specimens - (a) and (b) Test Specimen (c) UTM (d) Tension Test under progress (e) Test Set-up (f) Failed Specimen.

- **LY556 and HY5200 Resin System**

The transverse vs longitudinal strain plot from longitudinal tensile test of one of the composite specimens (LY556/HY5200) is given in Figure 3.13.

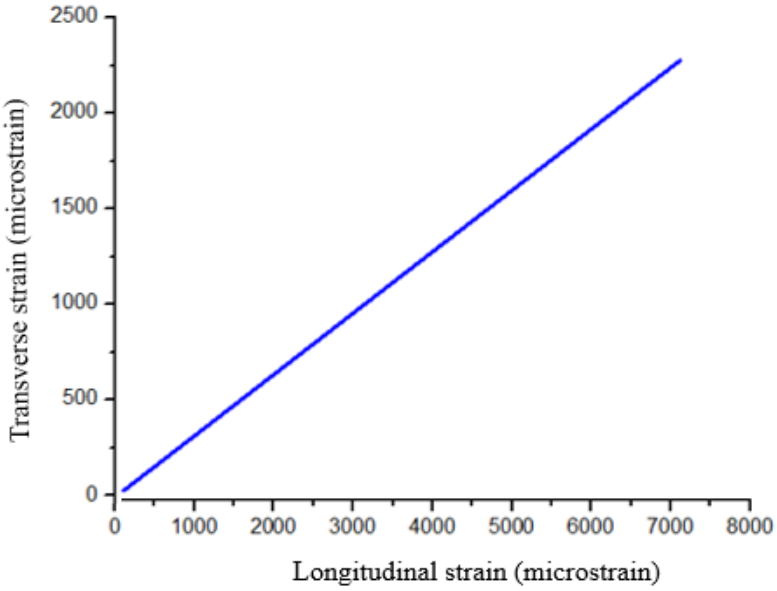

Figure 3.13. Transverse Strain vs Longitudinal Strain Plot - Longitudinal Tensile Test.

The test results of longitudinal strength, modulus, and Poisson ratio for T-700 and LY556/HY5200 composite are given in Table 3.8.

Table 3.8 Test Results of Longitudinal Tensile Test (LY556/HY5200).

Specimen No.	UTS (MPa), σ_{11}	Modulus (GPa), E_{11}	Poisson Ratio (ν_{12})
1	1564	160.00	0.33
2	1582	159.10	0.30
3	1620	162.00	0.31
4	1543	166.80	0.32
5	1552	155.00	0.31
6	1482	160.60	0.32
7	1640	158.20	0.28
8	1580	162.40	0.31
9	1655	156.20	0.29
10	1625	160.00	0.32
Average	**1584.3**	**160.03**	**0.30**
Standard Deviation	**52.36**	**3.33**	**0.01**

Flat Transverse (90°) specimens are used to perform the transverse tensile tests. The transverse tensile strength is determined from the corresponding failure load and the modulus is evaluated from the stress-strain curve. The transverse tensile specimens are shown in Figure 3.14.

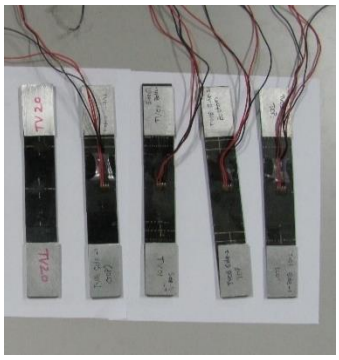

Figure 3.14. Transverse Tensile Test Specimens.

The test results of transverse tensile strength and modulus of T-700 with LY556/HY5200 composite are given in Table 3.9.

Table 3.9 Test Results of Transverse Tensile Test (LY556/HY5200).

Specimen No.	UTS (MPa), σ_{22}	Modulus (GPa), E_{22}
1	18.60	5.65
2	14.74	5.24
3	16.06	4.72
4	16.27	5.53
5	13.16	5.87
6	14.78	4.99
7	12.66	4.79
8	15.03	4.58
9	12.80	4.71
10	18.65	5.07
Average	**15.27**	**5.11**
Standard Deviation	**2.16**	**0.44**

- **Epo 1555 and FH 5200 Resin System**

The test result of one of the longitudinal tensile specimens is shown in Figure 3.15. Ultimate tensile strength (UTS) (σ_{11}), Tensile Modulus (E_{11}), Poisson Ratio (ν_{12}) and Failure Strain is found to be 1988 MPa, 132 GPa, 0.29 and 14750 με respectively.

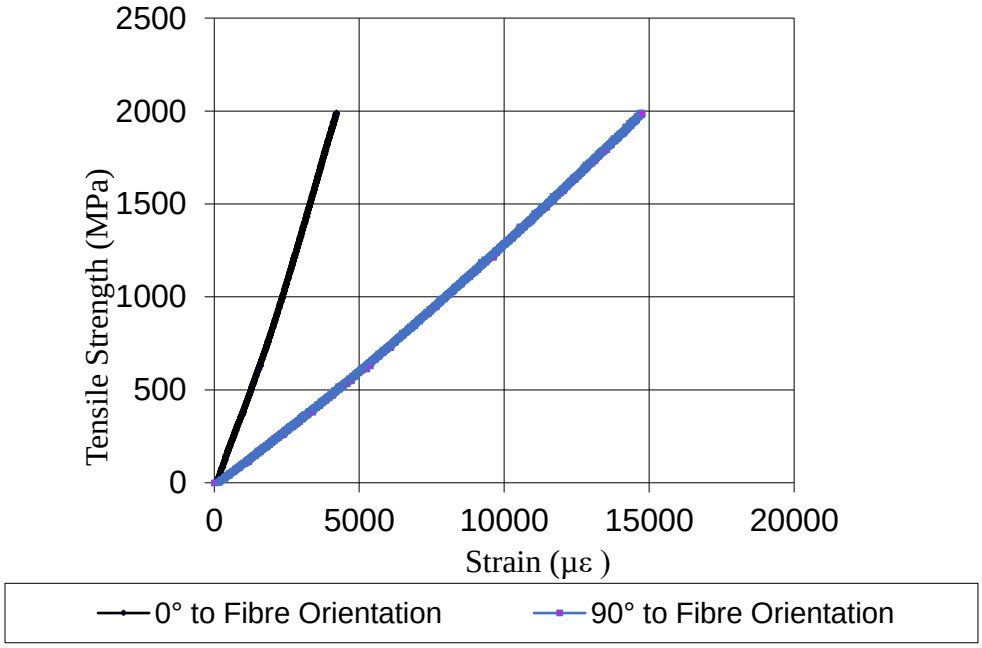

Figure 3.15. Test Result of Longitudinal Tensile Test – Carbon fibre and Epo1555/FH5200 Resin System.

The test results for longitudinal tensile Strength, modulus, and passion ratio of Epo1555/FH5200 resin system are given in Table 3.10.

Table 3.10 Test Results of Longitudinal Tensile Test (Epo1555/FH5200)

Specimen No.	Ultimate Tensile Strength, σ_{11} (MPa)	Tensile Modulus, E_{11} (GPa)	Poisson Ratio, ν_{12}
1	2258	132	0.32
2	1988	134	0.29
3	2168	131	0.32
4	2100	132	0.29
5	2341	128	0.30
6	2376	125	0.32
7	2430	129	0.28
8	2220	128	0.28
9	2477	124	0.29
10	2312	125	0.29
Average	**2267**	**128.8**	**0.29**
Standard Deviation	**151.97**	**3.42**	**0.01**

The transverse Tensile strength and modulus of T-700 carbon fibre/Epo1555/FH5200 resin system is given in Table 3.11.

Table 3.11 Test Result of Transverse Tensile Test (Epo 1555/FH5200).

Specimen No.	UTS σ_{22}, (MPa)	Modulus, E_{22} (GPa)
1	17.60	8.40
2	17.60	8.50
3	15.40	8.28
4	15.70	8.0
5	15.50	8.63
6	15.80	8.52
7	16.30	9.50
8	18.0	10.30
9	18.70	10.31
10	17.95	8.67
Average	**16.85**	**8.91**
Standard Deviation	**1.23**	**0.82**

3.2.7.2 Longitudinal (0°) Compressive Test and Transverse (90°) Compressive Test

The compression test on longitudinal specimens (0°) (Figure 3.16) and on transverse specimens (90°) (Figure 3.17) are carried out to determine the longitudinal and transverse compressive strength, respectively. The specimen preparation and testing methodology is carried out in accordance with ASTM D3410 [84]. The longitudinal and transverse compressive strengths are calculated from the corresponding failure loads.

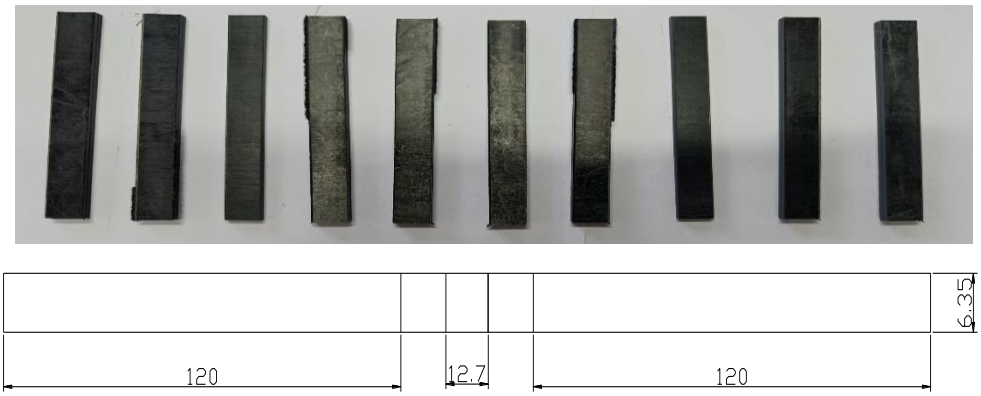

Figure 3.16. Longitudinal Compressive Specimen (all dimensions are in mm).

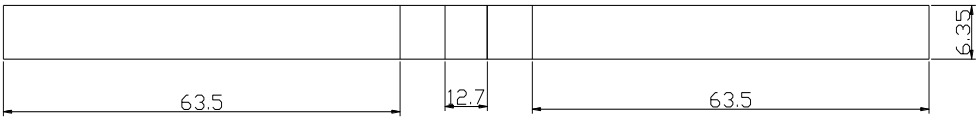

Figure 3.17. Transverse Compressive Specimen (all dimensions are in mm).

- **LY556 and HY5200 Resin system**

The test results of longitudinal and transverse compressive strength for LY556 and HY5200 resin systems are given in Table 3.12.

Table 3.12 Test Results- Longitudinal & Transverse Compressive Strength LY556/HY5200.

Specimen No.	Longitudinal Compressive Strength (MPa)	Transverse Compressive Strength (MPa)
1	581.5	59.26
2	502.6	56.41
3	484.5	69.43
4	563.8	71.27
5	454.6	68.04
6	499.1	65.56
7	522.2	67.88

8	497.7	64.61
9	443.16	67.48
10	466.67	48.48
Average	**501.58**	**63.84**
Standard Deviation	**44.51**	**7.06**

- **Epo1555 and FH5200 Epoxy Resin System**

The test result of longitudinal compressive strength of one of the specimens is shown in Figure 3.18.

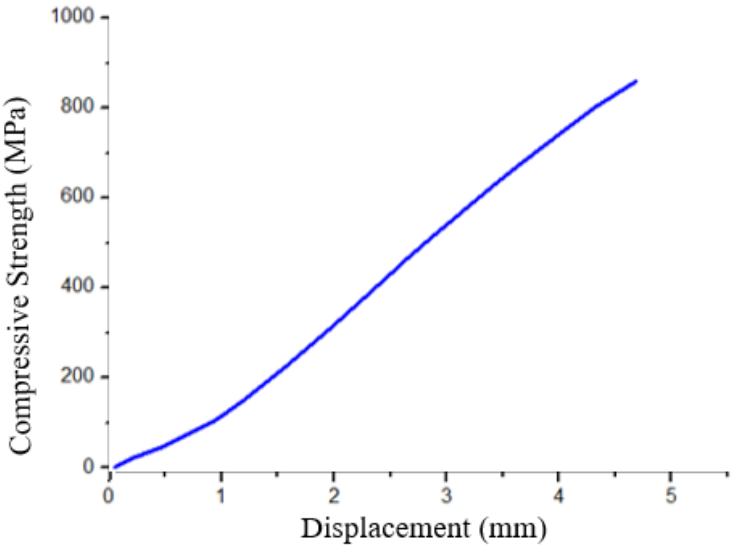

Figure 3.18. Test Result - Longitudinal Compressive Strength.

The average test results of 10 specimens for Longitudinal and Transverse Compressive Strength for Epo1555/FH5200 epoxy resin system are given in Table 3.13.

Table 3.13 Test Results of Longitudinal and Transverse Compressive Strength (Epo1555/FH5200).

Specimen No.	**Longitudinal Compressive Strength (MPa)**	**Transverse Compressive Strength (MPa)**
Average	966	149.6

3.2.7.3. In-Plane Shear Test

The test specimens (Figure 3.19) are prepared from a test laminate with ± 45° ply sequence and In-plane shear strength is evaluated from a tension test in accordance with ASTM D 3518 [85]. The rosette Strain gauges are bonded on the specimens for strain

measurement along the loading (0°) and perpendicular (90°) directions. The in-plane shear modulus is determined from the corresponding stress-strain curve. An extensometer is used to measure strains along the loading and perpendicular direction.

Shear Stress $\sigma_{LT} = \frac{1}{2} \sigma_X$, where $\sigma_{X\ is}$ applied stress,

Shear Strain $\varepsilon_{LT} = \varepsilon_X - \varepsilon_{y,}$ Where ε_X = Strain in 'X' direction and ε_y = Strain in 'Y' direction

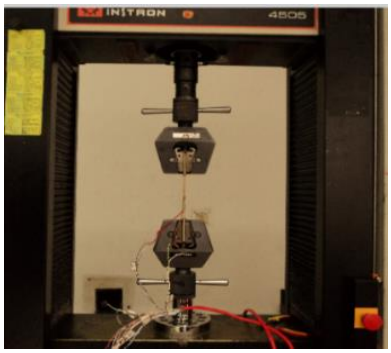

(a)

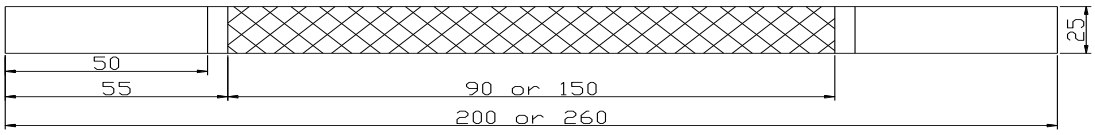

(b)

Figure 3.19. In-Plane Shear Test (a) Shear Test (b) Test Specimen.

The shear strength vs shear strain for one of the LY556/HY5200 composite specimen is shown in Figure 3.20.

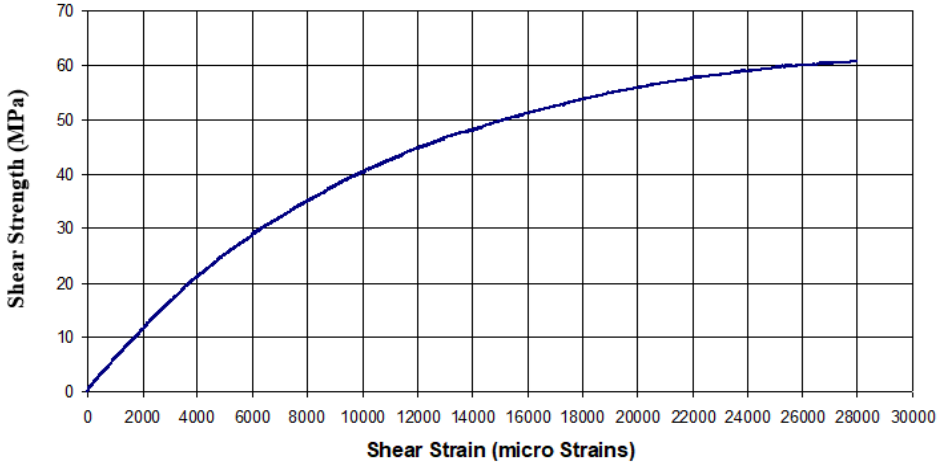

Figure 3.20. In-Plane Shear Stress vs Shear Strain Plot.

The results for In-plane Shear test of T-700 and LY556/HY5200 resin systems are given in Table 3.14, respectively.

Table 3.14 Test Results of In-plane Shear Test (LY556/HY5200).

Specimen No.	Shear Strength (MPa)	Shear Modulus (GPa)
1	65.16	4.95
2	67.54	5.46
3	74.88	5.30
4	63.66	4.37
5	54.61	5.09
6	76.10	5.48
7	79.18	4.95
8	61.65	4.80
9	67.80	5.08
10	61.20	4.90
Average	**67.17**	**5.13**
Standard Deviation	**7.63**	**0.33**

The average test results of 10 specimens of In-plane Shear test of T-700 and Epo1555/FH5200 resin system are given in Table 3.15, respectively.

Table 3.15 Test Results of In-plane Shear Test (Epo 1555/FH5200).

Sl. No	Shear Strength (MPa)	Shear Modulus (GPa)
Average	**46.8**	**2.98**

3.2.7.4 Interlaminar Shear Strength (ILSS)

This test is carried out using a three-point support fixture with short beam specimens in accordance with ASTM D 2344 [74] (Figure 3.21). Flat specimens are oriented along the length dimension and a span/depth (l/d) ratio of 4:1 is selected to minimise the effect of bending. ILSS = 3P/4bd where, P **=** maximum load**,** b = Specimen width, and d = Specimen thickness.

(a) **(b)** **(c)**

Figure 3.21. ILSS Test (a) Test Specimen (b) Test Setup (c) Failed Specimens.

The ILLS test result for T-700 Carbon Fibre with LY556/HY5200 and Epo1555/FH5200 resin systems are given in Table 3.16.

Table 3.16 Test Results - ILSS of T-700 Carbon Fibre with LY556/HY5200 and Epo 1555/FH5200.

Sl. No	ILSS (MPa) (LY556/HY5200)	ILSS (MPa) (1555/FH5200)
1	53.86	58.41
2	49.94	59.94
3	53.46	60.83
4	50.74	58.11
5	50.98	62.78
6	48.91	61.49
7	50.66	59.98
8	48.85	59.80
9	51.55	60.62
10	50.02	60.39
Average	**50.89**	**60.23**
Standard Deviation	**1.68**	**1.36**

3.2.7.5 Flexural Strength

The test is carried out using a three-point bend test setup in accordance with ASTM D 790 [86]. The support span-to-depth ratio (l/d) selected is 16:1, to maximize bending. The specimen width is selected appropriately to get the sensitivity of the load vs deflection curve. A crosshead speed of 2.0 mm /minute and a nose roller of diameter 10 mm are selected for this test. The observed failure mode is in tensile mode in the bottom side of the specimen and compression mode in top side of the specimen, respectively. The test specimens are shown in Figure 3.22.

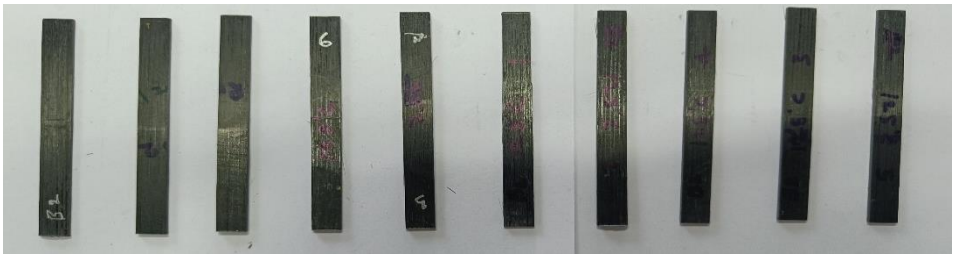

Figure 3.22. Flexural Strength Test Specimens.

The Flexural Strength Test Result of one of the specimens (T-700 & Epo1555/FH5200) composite) is shown in Figure 3.23 and the corresponding flexural strength is 1302 MPa.

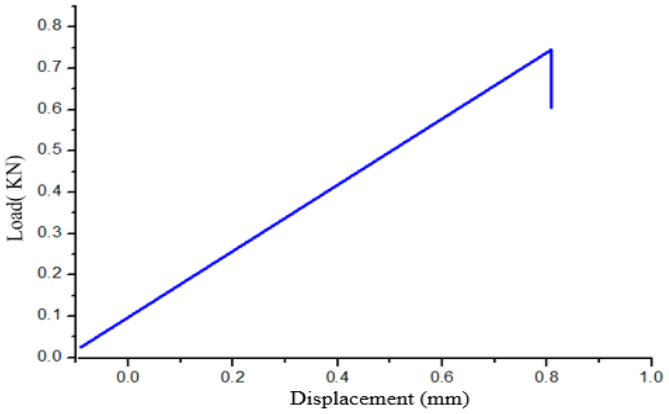

Figure 3.23. Load vs Deflection Curve for Flexural Test.

The flexural test results of T-700 Carbon Fibre with LY556/HY5200 and Epo1555/FH5200 resin systems are given in Table 3.17

Table 3.17 Test Results - Flexural Strength T-700 Carbon Fibre with LY556/HY5200 and Epo 1555/FH5200.

Specimen No.	Flexural Strength (MPa) (LY556/HY5200)	Flexural Strength (MPa) (Epo1555/FH5200)
1	880	1221
2	888	1302
3	913	1311
4	908	1299
5	925	1261
6	907	1265
7	1037	1344
8	882	1329
9	904	1389
10	917	1359
Average	**916**	**1307**
Standard Deviation	**45.03**	**50.16**

3.2.7.6 Hoop Tensile Strength Test

The hoop tensile rings (fibre orientation 0° are realised through FW process and tested in accordance with ASTM D 2290. This test evaluates apparent hoop strength. The rings are loaded in a longitudinal direction using a specially designed split disk-type test fixture. This

test is used as a Quality Control (QC) indicator for acceptance of COPV. The crosshead speed selected is 2.5 mm/minute. The rings failed mostly in the circumferential direction.

Hoop Tensile Strength = Max. tensile Load/ (2 * width * thickness)

The test specimens, setup, and load vs displacement curve for one of the Epo1555/FH520compositeste are shown in Figure 3.24.

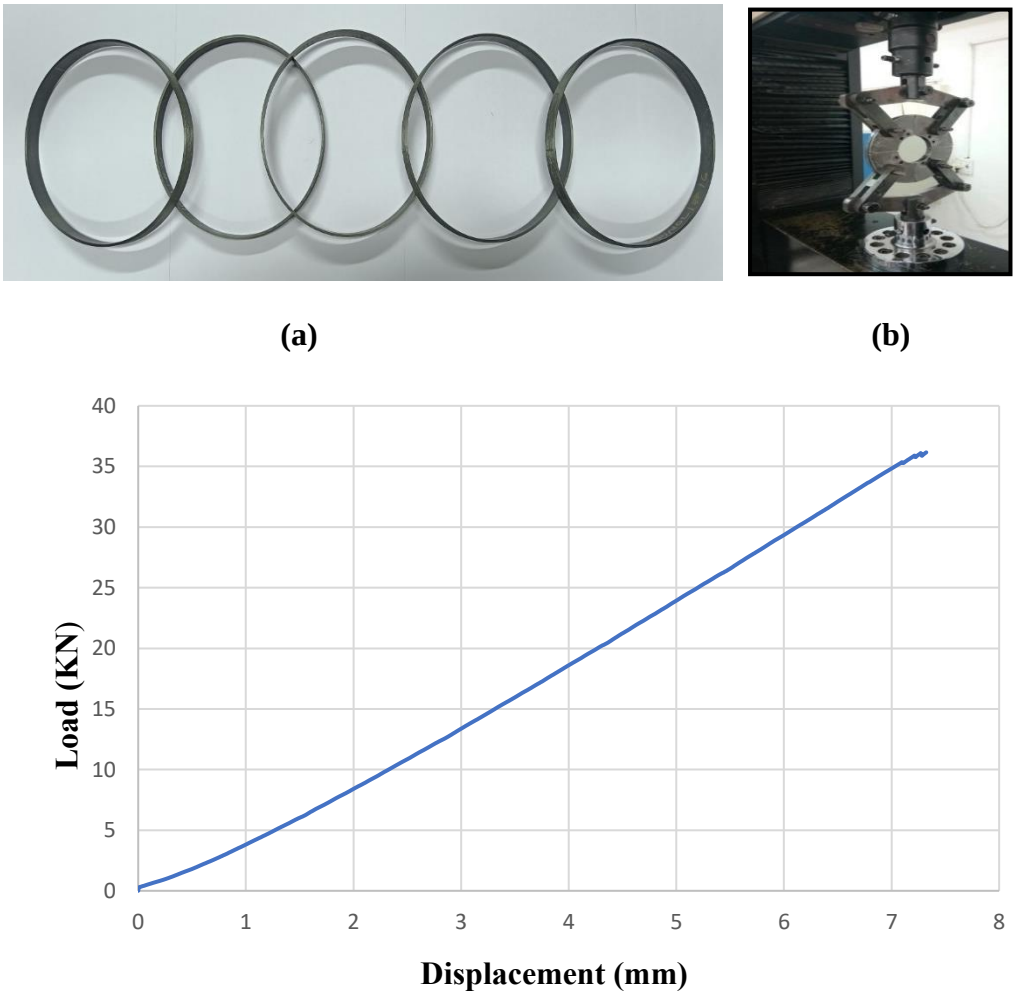

Figure 3.24. Hoop Tensile Strength Test a) Test Specimens (b) Test Setup (c) Load vs Displacement Plot.

The test results of the hoop tensile strength of T-700 Carbon fibre with LY556/HY5200 and Epo1555/FH5200 resin systems are given in Table 3.18.

Table 3.18 Test Results - Hoop Tensile Strength of LY556/HY5200 and Epo1555/FH5200.

Specimen No.	Hoop Tensile Strength (MPa) T-700 and LY556/HY5200	Hoop Tensile Strength (MPa) T-700 and Epo 1555/FH5200
1	1516	2017
2	1610	2124
3	1493	2299
4	1492	2050
5	1559	2012
6	1566	2063
7	1567	2291
8	1528	2201
9	1583	2108
10	1572	1990
Average	**1548**	**2116**
Standard Deviation	**39.48**	**113.09**

3.3. Mechanical and Physical Properties Testing of Glass Epoxy (G/E) Composite

G/E laminates are prepared in accordance with the manufacturing process described in para 3.2.5.1. From G/E laminates, the required no. of specimens is tested in accordance with relevant ASTM standards. The E- Glass fibre specimens are tested as shown in Figure 3.25. The average results are given in Table 3.19.

(a) (b)

Figure 3.25. (a) G/E UD Laminate (b) Tensile Test setup.

Table 3.19 Test Results of E Glass Roving [17].

Sl. No	Property	Test Results (Average)
1.	Tex (gm/km)	1200 ± 20
2.	Tensile strength (MPa)	1000 (Min)
3.	Specific gravity	2.5 to 2.6

3.3.1. Design Properties: Glass Epoxy Composites

Flat unidirectional laminates are made by the wet FW method using a flat/ rectangular mandrel. From the test laminates, various samples are made and tested in accordance with applicable ASTM standards. The test results are shown in Table 3.20.

Table 3.20 Properties for E - Glass/Epoxy (LY556/HY5200) Composite.

Sl. No	Parameter	Avg. Result	ASTM No.
1.	Longitudinal Modulus (GPa)	44	D3039
2.	Transverse Modulus (GPa)	10	D3039
3.	Shear Modulus (GPa)	8	D3039
4.	Poisson's Ratio	0.24	D3039
5.	Longitudinal Tensile Strength (MPa)	590	D3039
6.	Transverse Tensile Strength (MPa)	18	D3410
7.	Longitudinal Compressive Strength (MPa)	400	D3410
8.	Transverse Compressive Strength (MPa)	85	D3518
9.	Shear Strength (MPa)	44	D3518
10.	Density (Kg/m^3)	2100	D792

3.4 Evaluation of Mechanical Properties of C/E Composite for Maximum Expected Service Temperature

During the operational service life, the C/E CRMC is subjected to aerodynamic kinetic heating during the actual flight profile and its external surface gets heated. The rise in service temperature is a function of the mission profile and objectives. To evaluate the effect of maximum expected service temperature on mechanical properties, samples are dried and then heated up to 50, 75, 100 and 125ºC, soaked for 5 min. and then tested. The test results are compared with the results of virgin specimens (without any exposure). The test results for strength degradation of C/E composite are considered for structural layer design considering a kinetic heating effect, provide input for the design of external thermal protection system and account for adequate FoS in design. The specimen testing is shown in Figure 3.26.



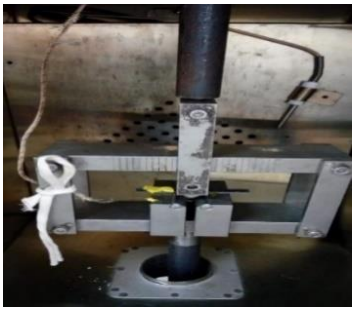

Figure 3.26. High Temperature Testing.

3.4.1 Test Results

Results of longitudinal tensile, ILSS, Flexural and hoop tensile strength tests for LY556/HY5200 and Epo1555/FH5200 resin system, under HT exposures (max 125°C) are given in Table 3.21, 3.22, 3.23, 3.24, 3.25, 3.26, 3.27 and 3.28, respectively.

Table 3.21 Effect of Temperature on Longitudinal Tensile Strength (LY556/HY5200).

Temperature	Tensile Strength (MPa)	Avg. (MPa)	Standard Deviation	Drop in Properties (%)
Room Temperature	Refer Table 3.8	1584	52.36	-
@ 50˚ C	1606, 1600, 1592, 1512, 1550	1572	40.07	0.7
@ 75˚ C	1527, 1485, 1593,1479, 1500	1516	46.45	4.2
@ 100˚ C	1506, 1396, 1385, 1427,1465	1435	50.05	9.4
@ 125˚ C	1286, 1291, 1409, 1365, 1310	1332	53.14	15.8

Table 3.22 Effect of Temperature on Longitudinal Tensile Strength (Epo1555/FH5200).

Temperature	Tensile Strength (MPa)	Avg. (MPa)	Standard Deviation	Drop in Properties (%)
Room Temperature	Refer Table 3.10	2267	151.97	-
@ 50˚ C	2207, 2315, 2182, 2167, 2218	2217	57.93	2.2
@ 75˚ C	2231, 2091, 2185, 2249, 2135	2178	65.79	3.9
@ 100˚ C	2207, 2078, 2049, 2120, 2085	2107	60.94	7
@ 125˚ C	2005, 1887, 1905, 1850, 1867	1902	60.76	16

Table 3.23 Effect of Temperature on ILSS (LY556/HY5200).

Temperature	ILSS	Avg. (MPa)	Standard Deviation	Drop in Properties (%)
Room Temperature	Refer Table 3.16	50.89	1.68	-
@ 50˚ C	50.25, 50.05, 49.02, 49.0, 48.6	49.38	0.72	3.8
@ 75˚ C	48.25, 47.5, 48.02, 47.84, 47.5	47.8	0.32	6.54
@ 100˚ C	45.05, 44.03, 43.5, 43.8, 43.32	43.94	0.67	14
@ 125˚ C	40.04, 38.95, 39.7, 38.5, 38. 2	39.07	0.78	23.2

Table 3.24 Effect of Temperature on ILSS (Epo1555/FH5200).

Temperature	ILSS	Avg. (MPa)	Standard Deviation	Drop in Properties (%)
Room Temperature	Refer Table 3.16	60.23	1.36	-
@ 50˚ C	60.05, 58.45, 59.46, 59.4,58.9	59.25	0.60	1.6
@ 75˚ C	58.95, 58.54, 57.98, 57.25, 57.5	58.04	0.70	3.6
@ 100˚ C	53.25, 54.05, 54.49, 54.07, 54.29	54.03	0.47	10.2
@ 125˚ C	49.85, 49.05, 47.4, 47.05, 47.23	48.11	1.25	20.1

Table 3.25 Effect of Temperature on Flexural Strength (LY556/HY5200).

Temperature	Flexural Strength	Avg. (MPa)	Standard deviation	Drop in Properties (%)
Room Temperature	Refer Table 3.17	916	45.03	-
@ 50˚ C	940, 880, 920, 850, 840	886	43.35	7
@ 75˚ C	889, 850, 798, 843, 820	840	34.18	9.3
@ 100˚ C	850, 720, 785, 765, 707	765	57.03	16.48
@ 125˚ C	707, 720, 690, 648, 676	688	27.98	24.89

Table 3.26 Effect of Temperature on Flexural Strength (Epo1555/FH5200).

Temperature	Flexural Strength	Avg. (MPa)	Standard Deviation	Drop in Properties (%)
Room Temperature	Refer Table 3.17	1307	50.16	-
@ 50˚ C	1305, 1240, 1298, 1274, 1260	1275	26.82	2.4
@ 75˚ C	1189,1265, 1249, 1180, 1220	1220	36.82	6.6
@ 100˚ C	980, 1035, 1045, 1020, 1087	1033	38.86	20.9
@ 125˚ C	950, 885, 965, 985, 867	930	51.58	28.8

Table 3.27 Effect of Temperature on Hoop Tensile Strength (LY556/HY200).

Temperature	Hoop Tensile Strength (MPa)	Avg. (MPa)	Standard Deviation	Drop in Properties (%)
Room Temperature	Refer Table 3.18	1548	39.48	-
@ 50˚ C	1500, 1583, 1496, 1445, 1480	1500	50.81	3.1
@ 75˚ C	1519, 1445, 1420, 1520, 1406	1462	54.31	5.5
@ 100˚ C	1426, 1327, 1309, 1391, 1320	1354	51.14	12.53
@ 125˚ C	1256, 1306, 1346, 1291, 1276	1295	33.985	16.34

Table 3.28 Effect of Temperature on Hoop Tensile Strength (Epo1555/FH5200).

Temperature	Hoop Tensile Strength (MPa)	Avg. (MPa)	Standard Deviation	Drop in Properties (%)
Room Temperature	Refer Table 3.18	2116	113.09	-
@ 50˚ C	2150, 2096, 2078, 1950, 1942	2044	92.64	3.4
@ 75°C	2068, 1990, 1986, 1950, 1942	1987	49.91	6
@ 100˚ C	1975,1896, 1825, 1805, 1786	1857	77.80	12.2
@ 125°C	1880, 1800, 1750, 1747, 1720	1779	63.22	15.92

3.5 Discussion

A detailed experimental study is carried out to confirm design properties, for raw material acceptance and to validate the FW manufacturing process. C/E composite material system is considered for large size CRMC intended for booster and upper stage applications, whereas G/E composite material system is considered for small rocket motor applications. The various type of composite specimens such as flat plates, hoop tensile rings etc., are manufactured using FW and tested. The mechanical properties of neat resin system, physical properties and mechanical properties of cured composites are generated in-house and summarised. The following material systems are considered for this study:

- T-700 with LY556/HY5200 Resin System
- T-700 with Epo1555/FH5200 Resin system
- E glass with LY556/HY5200 Resin System

The Material Properties of Cured composite – Carbon Fibre T700 12K/LY556 & HY5200 and Epo 1555 & FH5200 are given in Table 3.29 and 3.30, respectively. The results are average of 10 specimens and suitably normalised for a V_f of 0.6.

Table 3.29 Material Properties of Cured Composite – Carbon Fibre T700 12K/LY556 & HY5200.

Parameter	Design Value	Test Data (Avg.)
Longitudinal modulus, E_1, (GPa)	155±5	160.0
Transverse modulus, E_2, (GPa)(min)	5	5.0
Shear modulus, G_{12}, (GPa)(min.)	5	5.0
Poison's Ratio, v_{12}	--	0.3
Longitudinal tensile strength, T_1, (MPa)(min.)	1200	1580
Longitudinal compressive strength, C_1, (MPa)(min.)	450	500
Transverse tensile strength, T_2, (MPa)(min)	12	15
Transverse compressive strength, C2, (MPa)(min.)	50	60
In-plane shear strength, S_{12}, (MPa)(min.)	50	65
Hoop tensile strength (MPa)(min.)	1200	1550
Interlaminar shear strength (MPa)(min.)	40	50
Flexural Strength (MPa)(min.)	700	900
Fibre volume fraction (V_f)(min.)	0.5	0.60
Density, ρ, ($Kg/m^{3)}$	1450 ±50	1480

Table 3.30 Material Properties of Cured Composite – Carbon Fibre T700 12K/Epo1555 & FH5200.

Parameter	Design Value	Test Data (Avg.)
Longitudinal Modulus, E_1, (GPa)	130±5	128.0
Transverse Modulus, E_2, (GPa)(min.)	5	9.0
Shear Modulus, G_{12}, (GPa)(min.)	3	3.0
Poison's Ratio, v_{12}	--	0.29
Longitudinal Tensile Strength, T_1, (MPa)(min.)	1800	2260
Longitudinal compressive strength, C_1, (MPa)(min.)	750	960
Transverse tensile strength, T_2, (MPa)(min.)	15	17
Transverse compressive strength, C_2, (MPa)(min.)	80	150
Flexural Strength (MPa)(min.)	900	1300
In-plane shear strength, S_{12}, (MPa)(min.)	45	46.8
Hoop tensile strength (MPa)(min.)	1800	2100
Inter laminar shear strength (MPa)(min.)	55	60
Fibre volume fraction (V_f)(min.)	0.5	0.60
Density, ρ, ($Kg/m^{3)}$	1400 ±50	1350

The consolidated physical and mechanical properties of G/E composite are shown in Table 3.19 and 3.20, respectively.

3.6 Summary

The findings are summarised as follows:

- The test results are validated with design properties and the correlation between the physical/mechanical properties of neat resin system and physical/mechanical properties of cured composite is established.
- It is observed that the T-700 carbon fibre and Epo 1555 & FH 5200 resin system exhibits longer gel time, longer pot life and superior mechanical properties (due to higher % elongation of 4.1% of neat resin system) and also evident from the summary of consolidated properties indicated in Table no 3.29 and 3.30. The Epo1555 and FH 5200 resin system is considered for further system-level studies (at casing level) due to enhanced performance factor and requirements of superior mission performances.
- The decreasing trend from the specified tensile strength of Carbon fibre - C/E tensile specimens - C/E hoop tensile ring specimen is as expected, and corresponds to V_f and is attributed to the effects of manufacturing process. The filament wound hoop tensile rings simulate process and fibre orientations. The test results of longitudinal tensile specimen and hoop tensile rings are comparable and the observed trend is as expected.
- All the test results are repetitive and consistent and meet the design specifications.
- During service and operational life, the motor is expected to see a maximum service temperature of 125°C during flight in accordance with the mission profile. The tensile specimens, hoop tensile rings, ILSS and Flexural properties are heated at 50, 75, 100 and 125°C, soaked for 5 minutes and tested to evaluate drop in properties. The ILSS and flexural testing are carried out to study the effect of service temperature on fibre/matrix interfacial strength.
- Increase in temperature affects the rigidity and stiffness of the epoxy resin matrix a and drop in mechanical properties is observed. The drop in properties is noted and a noticeable degradation is evident after 100°C. The strength degradation is more sensitive in the case of ILSS and flexural test specimens due to shear forces, bending and the effect of delamination.
- It is found that strength degradation follows the same degradation trend in the case of both the epoxy resin system (LY556/HY5200 and Epo1555/FH5200). This input is important for design consideration, and to realise a safe and reliable high-performance CRMC to meet mission requirements.

CHAPTER 4

MANUFACTURING OF CRMC

The manufacturing of CRMC throws up several challenges in front of the designer and process engineers. The efficient design requires consideration of configuration, interfaces, load envelope, material, process, and quality. The brief aspects of design, material and process options, manufacturing, process control and quality are discussed in this chapter.

4.1 Manufacturing of C/E CRMC

These are large-size structures, ideally suited for long range missile systems and LVs. The CRMC is fabricated in the form of a cylindrical shell with end domes at both ends and configured with an unequal pole opening. The smaller opening on the HE side accommodates the igniter assembly and the larger pole opening on the NE side accommodates the nozzle assembly [5, 6]. The composite casing is primarily consisting of three major sub-assemblies:

- Main Casing Sub-Assembly
- Skirt Sub-Assemblies
- Polar Boss Encapsulations Sub-Assemblies

CRMCs are designed to sustain a high mass flow rate and high heat flux with an instantaneous pressure rise in the shortest possible time [6, 8]. The stresses vary along the axis of the casing.

The casing meridional contour is divided into three zones: one central cylinder and two contoured end domes. The cylinder provides seating for the two skirts, the junction at the end of the cylinder and the contour end dome is called CDT (cylinder-to dome-transition). The composite skirt along with a metallic bulkhead is attached near the CDT region at both ends. The typical configuration with unequal pole opening calls for a modified non-geodesic helical winding at the cylindrical portion between IE to NE CDT region. The helical layers are continuous from the IE pole opening to the NE pole opening with variable thickness at each station. The hoop layer is chosen for the cylinder region. The hoop along with non-geodesic helical winding and doily lay-up is the processing method adopted for CRMC. The doily is a planar reinforcement applied to local areas to provide additional strength, usually in the hoop direction [5]. The cylindrical shell is realised with multi-layers of hoop, helical winding, and doilies. Additional layers of high-strength doilies (PAN-based carbon fabrics) are laid up interspersing the helical layers around the dome and cylinder to take care of the circumferential and meridional stresses [5].

4.1.1 Material and Process Options

The efficiency of an RMC is judged in terms of a performance factor (n= PV/W), where ‘n’ is the performance factor, ‘P’ is the internal pressure, ‘V’ is the volume and ‘W’ is the weight of the casing [5]. The higher value of ‘n’ indicates an efficient system, for metallic RMC, ‘n’ is in the order of 5, whereas for CRMC (realised with wet winding), ‘n’ can be as higher as 12-15. The high specific strength and stiffness give a higher performance factor. The various parts, materials and process options are given in Table 4.1.

Table 4.1 Various Parts, Materials and Process Options – C/E CRMC [7].

S. No.	Part	Material	Process
1.	Casing	T-700 (12K) carbon fibre with a Epo 1555/FH5200 epoxy resin system (Wet FW process)	Helical non-geodesic winding between IE & NE CDT point, geodesic elsewhere Hoop winding Hoop winding for UD sheets Doily lay-ups Collapsible mandrel: Metallic shaft with foam disc and Plaster of Paris (POP)
2.	Skirts	T-700 (12K) carbon fibre with a Epo 1555/FH5200 epoxy resin system (Wet filament winding) PAN-based carbon fabric	Hoop winding Helical Fabric layup In-situ winding
3.	Metallic end dome and end Bulkheads (BH)	AA2014 Aluminium alloy	Machining, ageing, drilling and tapping
4.	Encapsulation for end dome (Polar boss)	EPDM Rubber	Lay-up of rubber sheets Vulcanization in the press
5.	Skirt to BH joints	Araldite (AW106) and hardener (HV953U) Composilok	In-situ winding on bulkhead followed by fastening
6.	Casing-skirt Y joint	T-700 carbon/ glass fibre and epoxy resin systems EPDM Araldite (A16) and hardener (k5)	Local machining of sacrificial composite layers In-situ winding with hoop and doily layup

4.1.2 Design and Process Considerations

The filament wound structures are known to provide very high strength-to-weight ratio. The design criterion is concerned with fibre direction. The CRMC is an axisymmetric thin shell under a biaxial state of tensile stresses during the normal operating condition. The basic aim is to orient the fibres in the direction of the principal stresses. At high stress levels, resin fails due to the transverse strain. The composite case design is worked out based on netting theory with the assumption that the casing comprises of fibres alone and the contribution of resin toward strength is neglected [5].

One of the primary objectives is to exploit the property of the composite materials to the maximum possible extent to achieve an optimum design. Main Casing Sub Assembly is primarily designed for internal pressure (MEOP-Maximum Expected Operating Pressure) and skirts are designed for the worst expected structural load considering the entire load envelope. Based on the ballistic prediction of SRM, a pressure time profile is generated. For a given temperature bound, propellant characteristics and nozzle throat diameter, ballistic performance prediction is carried out. Based on the predicted performance bounds, the MEOP is worked out and the composite casing is designed to withstand the predicted pressure time profile. For a given MEOP, the allowable total thickness of the casing (comprising of the hoop and helical plies) is at first theoretically calculated. The theoretically calculated total ply thickness is then divided into no. of hoop and helical plies. The helical and hoop ply thickness (including the resin system) is then calculated using [5].

$$t_{helical} = \frac{n_a\,(csa)}{w_a * v_{fa}} \qquad \textbf{……. Equation 3}$$

The hoop ply thickness is estimated using:

$$t_{hoop} = \frac{n_{90}\,(csa)}{w_{90} * v_{f90}} \qquad \textbf{……. Equation 4}$$

- $t_{helical}$: Helical ply thickness
- n_a: Number of spools for helical winding
- csa: Cross-sectional area of one carbon tow
- w_a: Bandwidth for helical winding
- vf_a: Fibre volume fraction for helical winding
- t_{hoop}: Hoop ply thickness
- n_{90}: Number of spools for hoop winding

- w_{90}: Bandwidth for hoop winding
- vf_{90}: Fibre volume fraction for hoop winding

In the case of geodesic winding, the ply angles for helical winding are obtained using Clairaut theorem, $r \times \sin\alpha = r_o$, where r: radius at the point, α: angle of winding and r_o: radius at the pole opening. In the case of non-geodesic helical winding, the computation of the fibre path angle, the contour of the casing and fibre stresses are interlinked. An optimum design solution is evolved considering the design and FW parameters. The winding angle, friction, end dome contours, composite mechanical properties and expected internal pressure are the key parameters that affect the ply design. The FW process design shall be experimentally validated with trial winding concerning the various winding parameters such as fibre tension, resin mix ratio, viscosity, temperature, fibre path, ply sequence, winding pattern, etc and the angle for non-geodesic helical winding portion is arrived numerically.

- **Polar Boss**

The two-end metallic dome facilitates the fibre reversal and provides attachment provision for the igniters and nozzle and sustains the unsupported blowout load. The inside and outside contours are chosen to match the end dome contour and to provide the minimum required flange thickness at different points. The polar bosses are encapsulated with an elastomeric shear layer providing an interface between polar bosses and the composite casings and are designed considering the differential stiffness of composite/metal and the maximum expected stresses.

- **Composite Skirt**

The skirts are attached to the casing using bonding and winding, and a low cone angle of (1-2°) blends the cylinder with the end dome contour. This provides a smooth transition for the skirt-to-case interface and also minimises discontinuity stresses. The composite portion of the skirt consists of hoop and helical layers interspersed at an approximate 50:50 ratio. In addition, carbon fabric layers are provided to improve the bearing strength at the holes provided for the bolts to connect the skirt to the metallic bulkhead. The load envelope for the skirt consists of worst-case axial inertial force plus bending moments.

- **Design of Y joint (Shear Plies)**

The joint between the skirt and the composite casing is designed with a nitrile rubber shear layer. The transmission of thrust between the skirt and the casing is through the shear plies. The proportion of the load shared by the shear ply depends on the stiffness of the

casing/skirt. The deflection at the 'Y' joint is a function of meridional membrane strains in the case and the axial movement of the skirt.

4.1.3 Manufacturing Process

Several tools and fixtures are used in the realisation of components and subsequent assemblies. Several Foam discs are stacked together on a central shaft on which Plaster of Paris (POP) is cast, followed by contour machining and bonding of encapsulated rubber polar boss to get the desired shape as per the inner profile of the casing. Subsequently, FW is carried out on the mandrel according to the validated winding program as per the designated ply sequence. Dry tows are drawn through a resin bath containing an epoxy resin system, collimated into a band and then wound on a rotating mandrel in a pre-described and sequential manner. In-situ skirt winding is carried out after placing rubber shear ply at the interface zone. After the FW operation is completed, CRMC is cured at elevated temperature in an oven to get a highly cross-linked high strength structure. The major steps of the manufacturing process are mentioned in Figure 4.1.

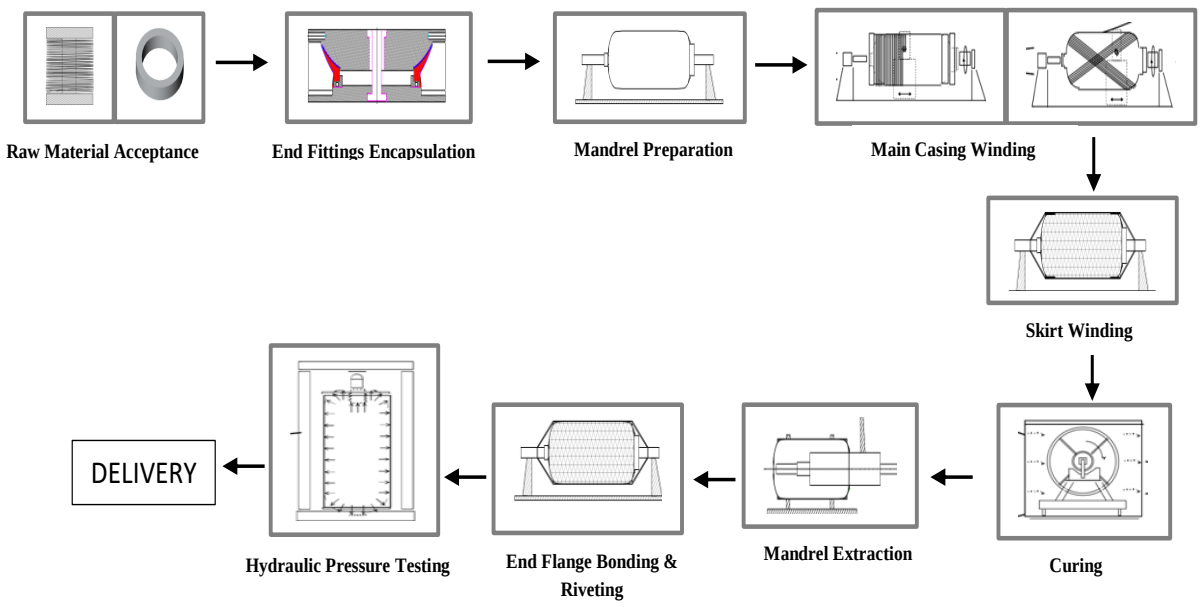

Figure 4.1. Manufacturing process flow of CRMC.

4.1.4. Failure mode effect analysis of CRMC

CPVs are multi-layered, multi-material and multi-interface structures, these structures are large-sized, contour shaped and have variable thicknesses all over which makes fabrication complicated [6]. Concerning the previous studies and research done by experts, the following are the broad areas and the possible failure modes:

- Main composite casing shell: hoop and helical fibre failure, compressive strength failure and buckling
- Fore End (FE) and Aft End composite skirts: compressive strength failure and buckling
- Encapsulated Polar Boss joint: boss blow-out & excessive stress in metal/rubber
- Skirt joint: strength failure of composite and bond failure
- Metallic bulkhead to composite skirt joint: composite bearing failure & fastener

Detailed FMEA and FMECA studies (Appendix 1 and 2) are carried out concerning various probable failure modes. FMEA activity combines technology and experience to identify potential failure modes, enabling the designer to eliminate those, thereby reducing development time and cost [4]. It improves the quality and reliability of the product [87, 88]. Two methods have been adopted:

- A Qualitative method using Military Standard (MIL-STD) 1629A, Task 105 [89]
- A Quantitative method using RPN.

Failure mode-driven design and process approach reduces the service and operational risk of polymeric composite products and makes the products more robust and reliable for the intended objectives [87, 88]. In addition to the above, process and configuration-oriented defects are also indicated in Figure 4.2.

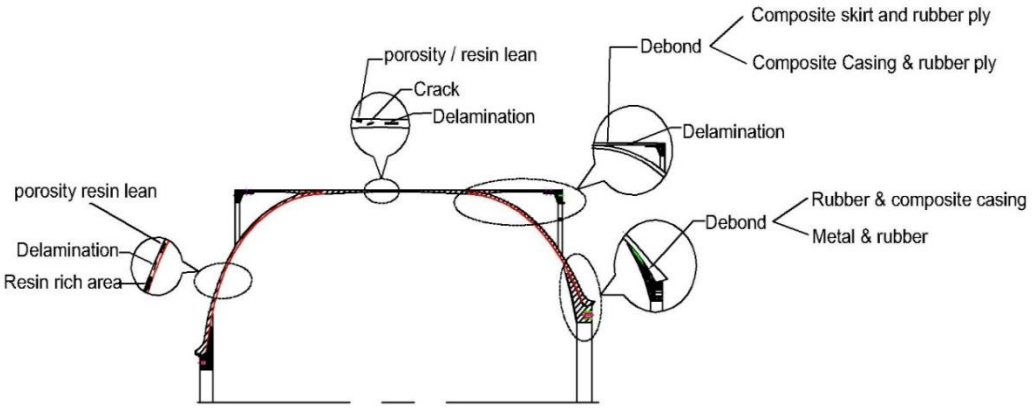

Figure 4.2. Process and Configuration Oriented Defects – Typical CRMC.

FMEA study as per MIL 1629A standard, Task 105 The study have been carried out to perform FMEA of CRMC using MIL 1629A standard as per Task 105 [89]. Various failure modes in different sub-systems of CRMC are populated in the FMEA worksheet enclosed as Annexure-I along with its effects i.e., local, next higher level and end effects and severity of each failure mode is categorized into 4 subcategories as per MIL 1629A standard, i.e., Category-I (Catastrophic), Category-II (Critical), Category-III (Marginal) and Category-IV (Minor).

FMECA studies are carried out using RPN methods to quantify the risk associated with each potential failure mode. The above studies give an insight into the most critical failure modes. It is observed that the main casing shell and boss blow failures are the most critical and frequently occurring failure modes., accordingly acceptance test procedure, NDT and instrumentation plan are evolved. The outcome of the FMEA & FMECA studies highlights the high priority failure modes, accordingly appropriate improvement in process design can be done as a risk mitigation plan.

4.1.5. Quality Assurance:

The desired level of Quality is built in CRMC through several stages of stringent process and QC, the key stages are:

- QC at the Tooling, fixture, and mandrel stage
- QC at the Raw material stage
- Process control
- QC at Component stage

The specification of all raw materials, including their storage condition and shelf life is to be verified. At the time of processing, certain required material properties are tested for raw material verification. The FW process is carried out in accordance with approved procedures. The representative samples are made as travel coupons and tested for physical properties and cure characteristics evaluation. The casing is subjected to metrology inspection for dimensional attributes and accepted. The casing is finally accepted based on a detailed structural integrity assessment and acceptance pressure test, elaborated in Chapter 5.

4.2Manufacturing of G/E CRMC

4.2.1 Product Description and Design Details

SRM

The G/E CRMC is used as a motor case for small SRM. This small SRM is an efficient energy release system, contains solid propellant [44, 45] and is used for ignition of large SRM. The small SRM consists of four primary elements. The different sub-systems are shown in Table 4.2.

Table 4.2 Different sub-systems of SRM with the composite case.

Sl. No	Components	Material
1.	HE Flange	Maraging Steel (M-250)
2.	Filament Wound Composite Casing	Glass Epoxy
3.	**Thermal Protection System (TPS)**	
	HE & NE Insulation	Nitrile Rubber
	Insulation Boot	Asbestos Phenolic
	Nozzle Insert (NI)	Carbon Phenolic
	Synthetic Resin Bonded Paper Tube (SRBP) tube	Kraft paper & Synthetic resin
4.	Propellant	Hydroxy Terminated Polybutadiene -based Composite grain

HE flange is a metallic interface configured with assembly and attachment-related features. The HE flanges are machined out of M-250 forgings, heat-treated, and aged. It is configured with multiple adaptor ports for pressure transducer and pyro cartridge mounting. The pyrotechnic-based initiation system actuates the ignition process by converting the mechanical energy into chemical energy, which ignites the propellant grain [44, 45]. The HE flanges are insulated with nitrile rubber for thermal protection. The thermal protection system consists of an insulator boot, HE insulation, NE insulation and carbon phenolic NI. NI is realised through the compression moulding process using rayon-based carbon fabric/phenolic resin prepreg and bonded to the composite case. The carbon phenolic-made NI also works as an energy discharge system The paper tube is made of Kraft insulation paper impregnated with polyester resin. SRBP tube holds the propellant grain as well as acts as an insulator to restrict the interface temperature of the composite case within the T_g of the resin system. The propellant grain is bonded to the SRBP tube and then assembled with HE flange sub-assembly and SRM is realised. A small SRM with the composite case is shown in Figure 4.3.

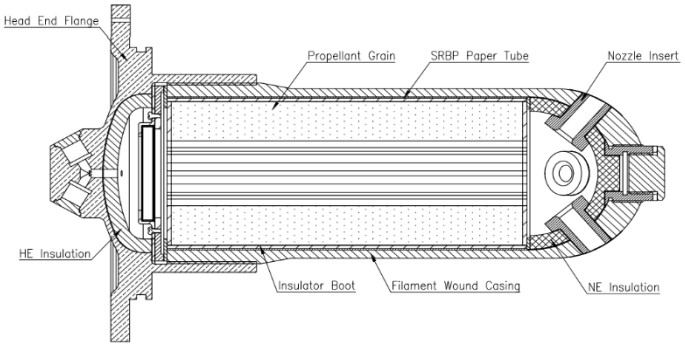

Figure 4.3. A Small SRM with G/E Composite Case.

Functioning of SRM

The SRM is designed for three functional requirements:

- Mass flow rate
- Heat flux and
- Critical pressure

Considering the above inputs and functional requirements, the ballistic performance envelope (Pressure-time profile) for SRM is worked out with upper, nominal, and lower bounds. The variation in the specified operating temperature range (10-45 °C), propellant burn rate, density, characteristics velocity and throat diameter are considered, and upper, nominal (27° C), and lower bounds are predicted. Accordingly, motor case MEOP arrives.

4.2.2 Manufacturing Process

Glass roving, impregnated with an epoxy resin system, and wound over a mandrel using an FW machine. The composite case manufacturing is shown in Figure 4.4.

(a) F/W of G/E CRMC **(b)** Curing

Figure 4.4. G/E Composite Case Manufacturing.

- **Curing Cycle**

The case along with the mandrel is subjected to curing in a calibrated oven as per the specified cure cycle at an elevated temperature. The curing cycle is evolved by studying the resin cure characteristic by DSC and further experimental validation. The cure cycle is specified in Table 4.3.

Table 4.3 Curing Cycle – G/E Composite Case.

Sl. No	Temperature (°C)	Time (Min.)
1.	30°C - 130	90
2.	Hold at 130	60
3.	130°C - 150	30
4.	Hold at 150°C	240

- **Extraction**

The cured composite shell is parted into two parts, post parting, interface machining, NDT and dimensional inspection are carried out. The filament wound composite case is shown in Figure 4.5.

Figure 4.5. G/E Filament Wound CRMC.

4.2.3 Acceptance Testing

Test samples for density, resin content, Differential Scanning Calorimeter (DSC) test, V_f, and mechanical properties (ILSS, tensile properties) are drawn from control coupons and tested accordance with relevant ASTM standards. The Control coupons are manufactured and cured along with the composite case, control coupon density and resin content test results are shown below:

Table 4.4 Control Coupon Properties.

Test	Test Method	Test Data
Resin Content (%)	ASTM D3171/ D 2584	30 ± 5
Density (Kg/m^3)	ASTM D 792	2.0 ± 0.2

4.3 Summary

The key design, manufacturing process, and quality aspects of the FW composite case are discussed in this chapter. An insight into various material, process options and sub-systems of C/E and G/E CRMCs are identified and critical aspects are highlighted. In this chapter, the manufacturing process of C/E & G/E CRMC of ø1m X 4m (length) and ø132 mm X 410 mm (length) are discussed.

CHAPTER 5

STRUCTURAL INTEGRITY ASSESSMENT AND NATURAL AGEING STUDIES ON C/E CRMC

In this chapter, the acceptance test procedure of C/E CRMC is discussed. The CRMC once made is subjected to a hydro pressure test as an acceptance test procedure. The strain and dilations are measured during the pressure test. The dynamic behaviour of CRMC is observed through AE, strain, and dilation measurement. Post PPT, the structural integrity is assessed using UT & RT. The finding of UT and RT is correlated with the strain dilation and AE data acquired during the PPT.

The CRMC is stored and subjected to natural ageing at ambient conditions. The same article is re-tested again after 5 years. The results are then compared with the test result of virgin CRMC.

The Test results of the above two tests are compared with the rest result of a 10-year-old existing CRMC (manufactured using the same raw material system and established procedure). The findings are analysed and a structural integrity assessment of C/E CRMC is carried out for a service life of 10 years.

5.1 Test Article and Setup

The motor case of a booster stage, strap-on motors, and upper stage motors of strategic missile systems and LVs are being designed with high-performance composites, for weight advantage and superior performance vis-à-vis the metallic RMC. These structures are weight sensitive and designed with a margin of safety (MoS) of 1.25 on the MEOP (the minimum burst pressure shall be 1.25 times the MEOP. These casings are hydro pressure tested up to 1.1 times of MEOP as a part of process validation, quality conformance and product acceptance [7, 11]. Accordingly, during PPT, the CRMC experiences up to 88 % of the designed failure load. During PPT, resin-rich patches, if any may form de-laminations/ de-bonds and initiate resin and fibre failure. The achieved V_f, fibre ductility, degree of cure, resin-rich/lean areas etc. influences the damage prognosis during the pressurisation.

The casing is internally lined using EPDM rubber based TPS and pressure tested using water as a medium. During PPT, strains at various locations are measured using strain gauges and the dilations are monitored using Linear Variable Differential Transformers (LVDT). The strains and LVDT data are acquired through a data acquisition system with a sufficient no of channels. A standard test procedure is followed for PPT of the CRMC and the strain, LVDT and acoustic emissions are recorded through all the channels.

During PPT, the dynamic behaviour of the flaw is studied using AE. After PPT, the NDT i.e., UT and RT are carried out and a detailed structural integrity assessment of CRMC is made.

5.1.1 Test Article details

- Length: 4 m and Diameter: 1 m
- MEOP: 6.5 MPa
- Proof Pressure: 7.1 MPa
- Cylinder Shell thickness: 4 mm

The PPT is carried out in a vertical position and strain and dilations are measured at critical locations according to the instrumentation plan. The test setup, strain gauge and LVDT plan are shown in Figures 5.1 (a), 5.1 (b), 5.1 (c) and the test article along with the setup is shown in Figure 5.2, respectively. The CRMC is mounted vertically on a specially designed fixture, where the nozzle end opening is kept at the top side. Since the composite is hygroscopic in nature, it is internally insulation lined and then pressure tested. A hydraulic pump is used to pressurise water medium up to the required proof pressure level.

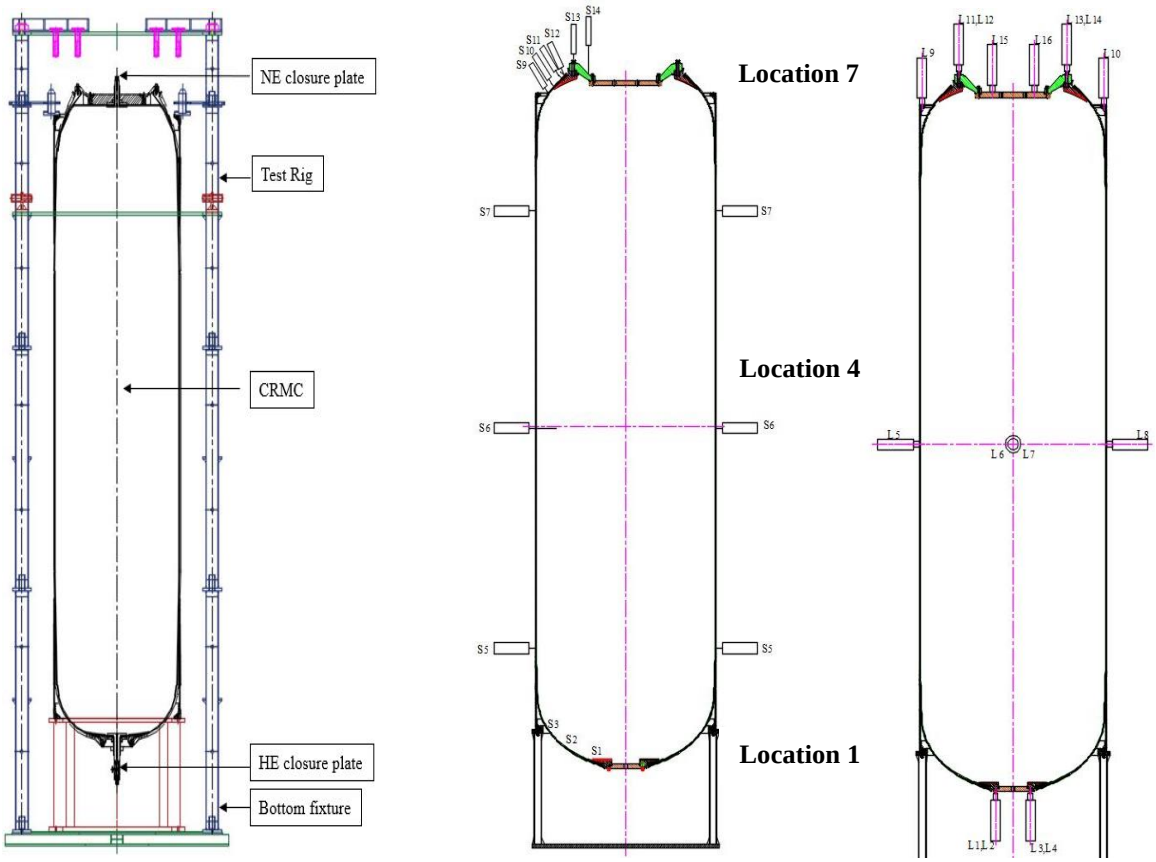

Figure 5.1. (a) PPT Set-up (b) Strain Gauge Plan (c) LVDT Set-up

Figure 5.2. Test Article (CRMC) with PPT Setup.

5.2 NDT

A detailed study is carried out at the sample level to study various NDT signatures of C/E composites (both with and without defects) and compared with product-level NDT signatures for decision-making [40, 41]. The specimen NDT signatures are instrumental to understand the behaviour of the full-scale product. The CRMC is subjected to detailed visual inspection followed by UT and RT before and after the PPT.

5.2.1 Ultrasonic Testing (UT)

- Technique: Dry scan through transmission without couplant
- Test equipment: Sonatest make and Type MS 410D
- Probe details: Frequency of 0.5 MHz and 10 mm diameter

The dry scan technique eliminates the couplant, geometric and porosity problems that arise with conventional ultrasonic. The ultrasonic energy is coupled between the probes and the material, and it relies on redirected sound energy. The NDT grid charts for parts, sub-assemblies and assembly are evolved based on experiences and manufacturing criticalities. It is divided into 7 zones and further, each zone is circumferentially divided into 8 sectors for UT grid points. The NDT scheme for UT and RT is shown in Figure 5.3.

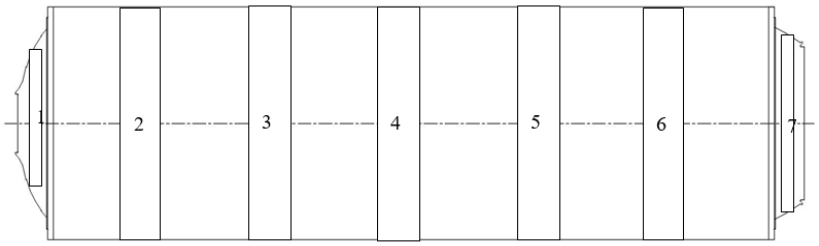

Figure 5.3. NDT Scheme - UT and RT.

The test dB point is determined by testing the component in through-transmission mode randomly at several points and noting the gain value among the values observed where the signal crosses 90% of signal height for the majority of zones. Based on wave velocity, attenuation studies and signatures of different defect types at the specimen level, the following grading is carried out in terms of the level of the test dB:

- Grade A: Nominal dB point
- Grade B: Nominal dB + 6 dB
- Grade C: Nominal dB + 12 dB
- Grade D: Nominal dB + more than 12 dB till total signal loss

The concerned zones with more than 6 dB addition, are mapped and studied thoroughly w.r.t AE response during PPT, strain values and post-PPT UT/RT observations, accordingly, a judgement is made on the overall health and structural integrity.

5.2.2 Radiography Testing (RT)

RT provides a means for the detection of internal defects like cracks, inclusions, delamination, and de-bond etc. The test is carried out using a high-energy flameproof radiography facility Linear Accelerator (LINAC) with a maximum of 4 mega electron volts and 180 Rads/ min capacity, the sensitivity is < 1%. The RT plan consists of tangential and normal RT shots with special emphasis on the cylindrical shell region, Y joint and dome regions. The RT test setup is shown in Figure 5.4.

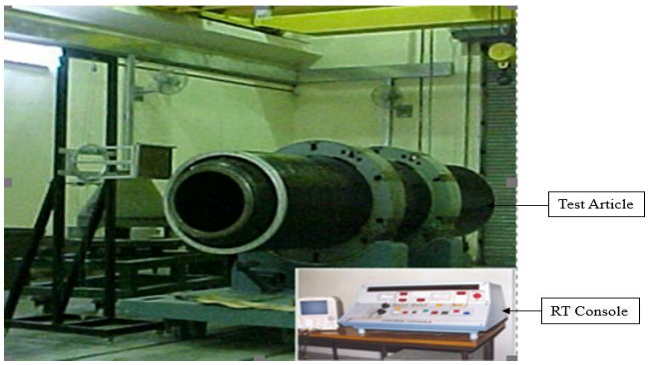

Figure 5.4. RT Test Setup.

The casing is divided into no of stations along the length, and at each station, it is further divided circumferentially, accordingly normal, and tangential shots are taken at every zone for defect mapping. Any identified suspicious zone based on UT and AET observation is subjected to RT to find the exact nature of discontinuity.

5.3 Acoustic Emission (AE) Testing–Online Structural Integrity Evaluation

Hydraulic PPT is used as a mandatory acceptance test for CRMCs. The conventional strain monitoring at certain locations and post-test NDT may not reveal the damages (if any) effectively. During PPT, AE testing is carried out to understand the dynamic behaviour of CRMC under the influence of pressure load. AE helps to understand the modes of failure and structural degradation. The application of AE testing during PPT enables effective monitoring of dynamic behaviour of micro and macro level flaws under proof load, therefore, structural integrity is assessed giving confidence for the subsequent use. The following are the steps to conduct a structural integrity assessment of a CRMC during PPT: determination of wave attenuation characteristics and velocity, sensor mounting scheme, pressurisation cycle, testing and analysis.

AE refers to the rapid emission of transient elastic waves from a localized source within a structure when stressed and its severity is recorded in terms of certain governing parameters such as amplitude, duration, hit rate, count rate and energy etc [38]. It plays an effective role in the quality assurance of CRMC by complementing other NDT techniques by effectively identifying zones of suspicion and intense activity. The typical AE waveform is displayed as a voltage versus time plot in Figure 5.5.

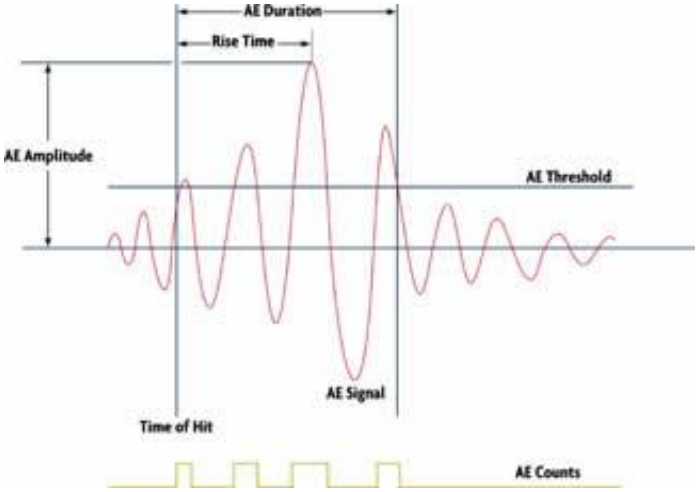

Figure 5.5. AE waveform.

5.3.1 Attenuation Studies

The AEs produced in the CRMC during PPT are highly attenuated as they travel in the material before being sensed by the piezoelectric sensors. The attenuation is more prominent for acoustic waves at higher frequencies. The composite material absorbs the energy of the wave and causes attenuation of the amplitude as the wave propagates. An attenuation study is conducted on the water filled CRMC in both circumferential and longitudinal directions. The energy loss can be expressed by an exponential dependence on the distance of wave propagation. The placement of AE sensors depends on the attenuation levels of the material. The attenuation plots are shown in Figure 5.6.

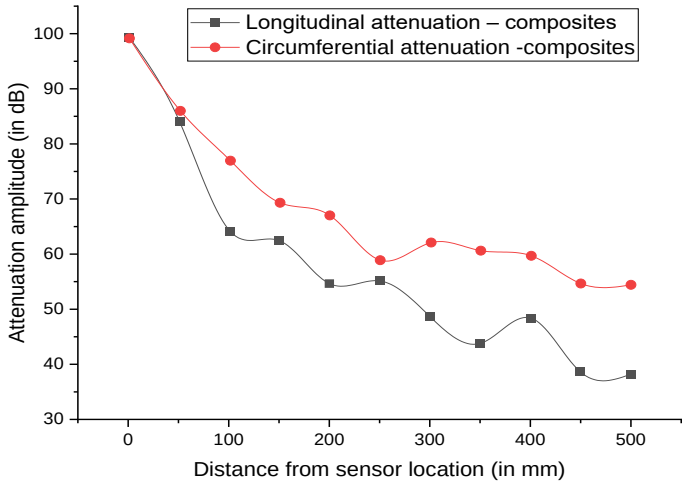

Figure 5.6. Amplitude vs Distance - Attenuation Studies.

5.3.2 Sensor Layout

The Figure 5.6 shows that the circumferential attenuation characteristics are better than the longitudinal ones and confirms that the inter-sensor distance can be maintained more in the circumferential direction vis-à-vis longitudinal direction. The inter-sensor distance is a function of attenuation characteristics of the material, an important parameter governing the accuracy of test results and helps in identifying the defect locations. The inter-sensor distance is calculated based on sensor response from a simulated pencil lead break test. Based on attenuation studies, availability of sensors, manufacturing criticalities and to cover the entire surface of the CRMC with diameter 'D', and length 'L', and to locate defects, a triangulation form of sensor arrangement is evolved. For a CRMC and minimum detectable amplitude AT (dB), the Circumferential distance between two sensors in a row, the longitudinal distance between two sensors, the distance between two rows, the no. of sensors per the and total no. of rows required are calculated. The mounting of AE sensors is carried out in accordance with ASTM guidelines, Figures 5.7, 5.8 and 5.9 show geometric triangulation, sensor location on the shell and distribution of sensors over a typical CRMC respectively.

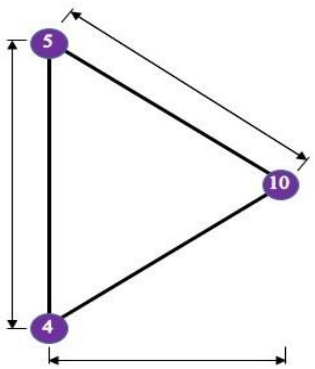

Figure 5.7. Geometric Triangulation.

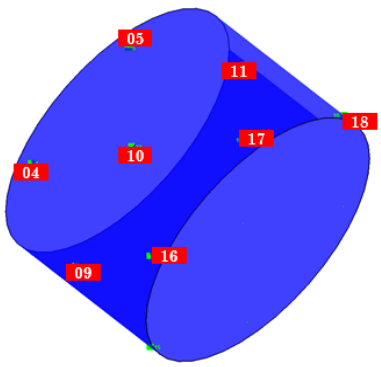

Figure 5.8. Sensor Location on the Shell.

Figure 5.9. Distribution of Sensors over a Typical Rocket Motor.

5.4 PPT

Sensor Type: Physical Acoustic Corporation makes, R15D differential type piezoelectric sensor with a preamplifier

- Bandwidth between 100 Kilo Hertz (KHz) and 500KHz
- Resonant frequency 150 KHz

An AE stress wave travels from the source through the structure and is detected by an AE sensor placed on the structure. The severity of the source is analysed by monitoring multiple events in the same area. A total of 24 No. of the calibrated sensor is used to acquire data. AE sensor serial no. 1, 2 and 3 are placed on the NE dome circumferentially 120° apart. The performance of each sensor is validated through an automatic sensor test by introducing a simulated signal at each sensor and recording the response [36, 39 & 42]. Further, secondary pencil lead break calibration is done at all channel locations by ASTM E 976 [91] and E 1106 [92] respectively to confirm the integrity of all sensors to record the expected level of amplitudes.

5.4.1 Pressure cycle

In the beginning, the CRMC is subjected to 3 cycles from 0 to 1 MPa pressure for stabilization of the instrument. Thereafter, it is pressurised in steps of 1 MPa with a pressurisation rate of 0.4 MPa/min (Figure.5.9). The rate of pressurisation is a vital factor for the quality of the data; accordingly, a suitable pressurisation rate is evolved as a faster pressurization rate which may give rise a lot of unwanted signals and whereas too slow pressurization may produce unnecessary stresses in the component due to long period.

For SHM during PPT, a re-pressurization cycle is introduced to monitor the felicity ratio. The Felicity Ratio (FR) is a qualitative indicator of structural health that the casing is structurally healthy up to MEOP. After MEOP, a re-pressurization cycle is introduced with AE monitoring to study the felicity effect which yields a good qualitative analysis of the rocket motor toward damage assessment [39, 42 & 43]. An average pressurization rate of 0.4 MPa/min is followed. The acceptance criteria specified by the standard test codes for the felicity ratio is 0.95 for composite pressure vessels. Therefore, for evaluating the felicity ratio

the reloading is introduced after reaching the MEOP before reaching proof pressure as shown in the pressure cycle for testing in Figure. 5.10.

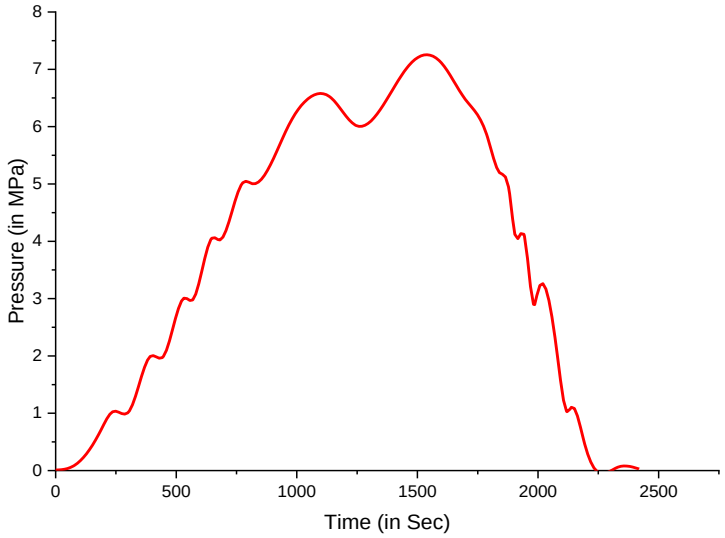

Figure 5.10. Pressure Cycle.

5.4.2 Online Monitoring of Structural Integrity

These AE parameters are established through extensive specimen-level characterization studies [42]. Acoustic emission activity roll-off is observed during hold periods. A Felicity Ratio (FR) of 0.962 is observed after re-pressurization, which is a ratio between the applied load at which acoustic emission reappears during the re-loading to the previous maximum applied load [43]. The Felicity plot based on the total energy content of all the channels for the tested rocket motor casing is shown in Figure 5.11 and FR is calculated and found to be 0.962 at MEOP where reloading is done.

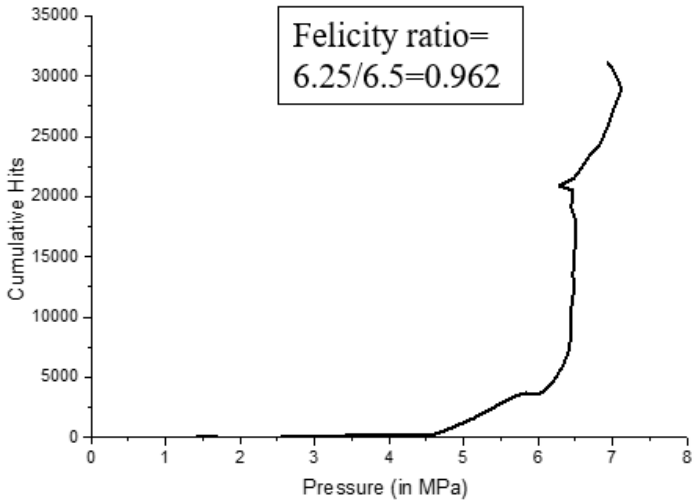

Figure 5.11. Felicity Ratio curve.

During PPT, AE activity on the location chart, amplitude, count, hit rate, count rate, cumulative hits, strain, and dilations are monitored and recorded for further analysis. The cumulative hit rate for all the sensors is given in Figure 5.12.

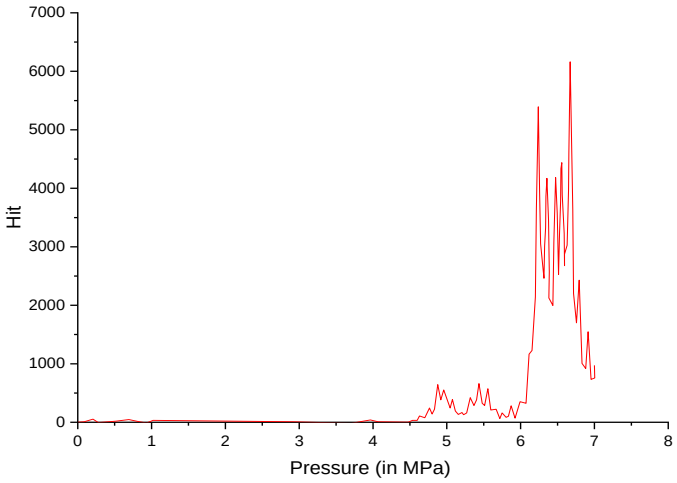

Figure 5.12. Cumulative Hit Rate for all the Sensors.

5.5 Test Result Analysis

5.5.1 AE – Test Results and Analysis

Hits registered during PPT are examined critically and it is seen that the high-amplitude and high-count hits are continuously encountered between 6 to 6.5 MPa, further at the 6.5 MPa hold period, AE activity remains silent. During the next re-pressurization up to 6.5 MPa, no significant hits are encountered. During pressurization from 6.5 MPa to 7.1 MPa, channels 2,4 and 17 recorded count rates of min. 3000 per sensor per second and a hit rate of min. 10 hits per sensor per second. The count rate and hit rate for channels no 2 (on NE dome), 4 and 17 (on the cylinder) are presented in Figure 5.13. and Figure 5.14, respectively. The AE test data for three selective channels covering the locations on the cylindrical and NE domes are shown in Table 5.1.

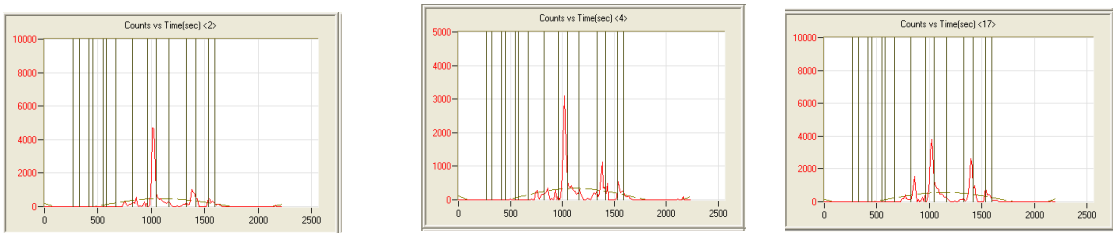

(a) **(b)** **(c)**

Figure 5.13. Count Rate for Channel no (a) 2 (b) 4 (c) 17.

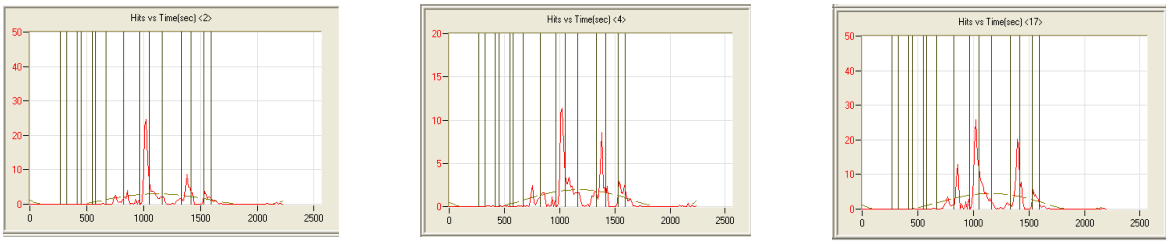

(a) **(b)** **(c)**

Figure 5.14. Hit Rate for Channel no (a) 2 (b) 4 (c) 17.

Table 5.1 AE Parameters During PPT (First Time).

Parameter	AE Channel No.		
	2	**4**	**17**
Total No. of Hits	21075	20070	22180
Amplitude range (dB)	60 - 96	60 - 91	60 - 98
Duration range (µs)	17-13497	16-13881	15-16389
Rise Time range (µs)	1-450	1-310	1-396

Based on AE test data and specimen studies, AE activities with less than 60 dB are not considered for analysis as a minimum threshold of 60 dB is used. All the zones with AE activity are critically examined and found to be free from any significant responses except a few isolated hits. The isolated AE activities are from local deformations such as matrix micro-cracking and lead to AE signatures around 6.5 MPa pressure. In the zone with significant AE activities and at those corresponding locations, the counts vs time plot is given in Figure 5.15 a) and b) respectively.

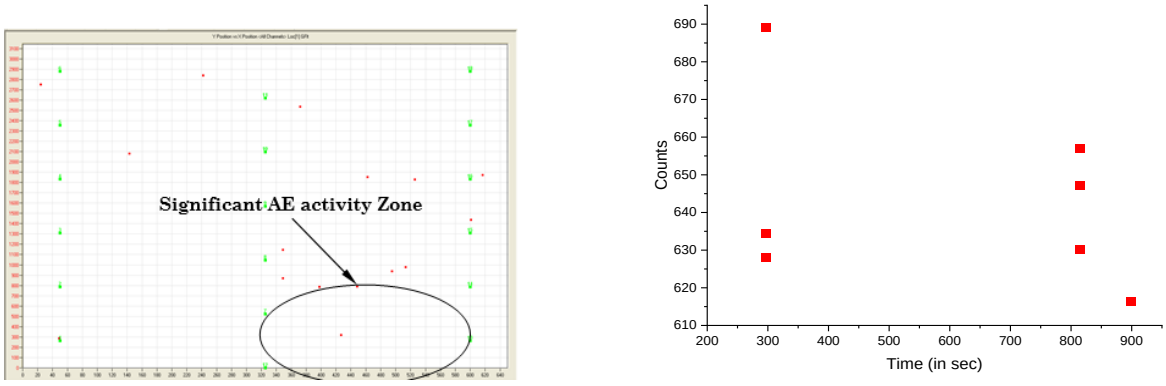

(a) **(b)**

Figure 5.15. (a) and (b) AE activities

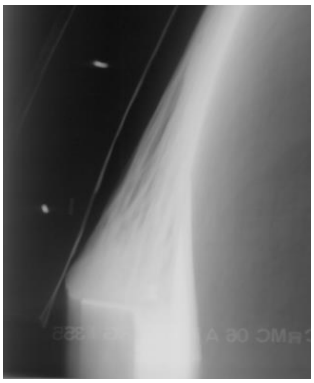

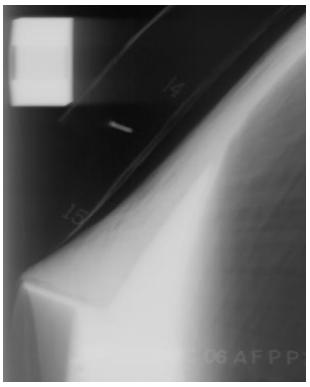

(a) **(b)**

Figure 5.16. (a) and (b) RT observation at Polar Boss Region

5.5.2 UT and RT Results

The UT observation recorded after post-PPT is shown in Table 5.2. Zone 7 recorded close to 10 dB loss which corresponds to a higher thickness region in the nozzle end dome. The same is comparable with pre-PPT results. The UT result does not indicate any major deterioration.

Table 5.2. Post PPT UT results.

Zone	Test (dB)	T	P1	R	Y1	B	P2	L	Y2
1	25			25		30	30	25	
2	25			25			30	25	
3	20				20				26
4	20	20	26			20			
5	20	20	26		20		32	20	
6	25			25		31		25	
7	35				35				

The identified zone according to AE activities is radiographed and corresponds to resin lean indication and matrix cracking near-polar boss regions with minor loss in input ultrasound dB levels compare to pre-PPT observation. The RT observations at polar boss regions are shown in Figure 5.16 (a) and (b) respectively.

5.5.3 Strain and Dilation Results

The strain and dilation are recorded at various locations as per the instrumentation plan and indicate the response of the composite structure against the pressure loads [35, 47]. The results are monitored during the pressure test and analysed offline after the pressure test. The

strain (observed at the cylinder, dome, and skirt region) and dilation observed on the cylinder are shown in Figure 5.16. The strains and dilations recorded at the IE dome, Cylinder and NE dome respectively are shown below:

- Location 1 – Correspond to IE cylinder near to pole opening
- Location 4 – Correspond to cylinder region
- Location 7 – Correspond to mid of the NE Cylinder dome

At each location, the casing is further divided circumferentially into 4 locations, 90 ° apart, i.e., Top (T), Bottom (B), Right (R) and Left (L). The strain recorded during PPT at locations 1, 4 and 7 (T & B) is shown in Figure 5.17 (a), (b) and (c) respectively. The dilation recorded at cylinders (T and B at location 4) is shown in Figure 5.17 (d).

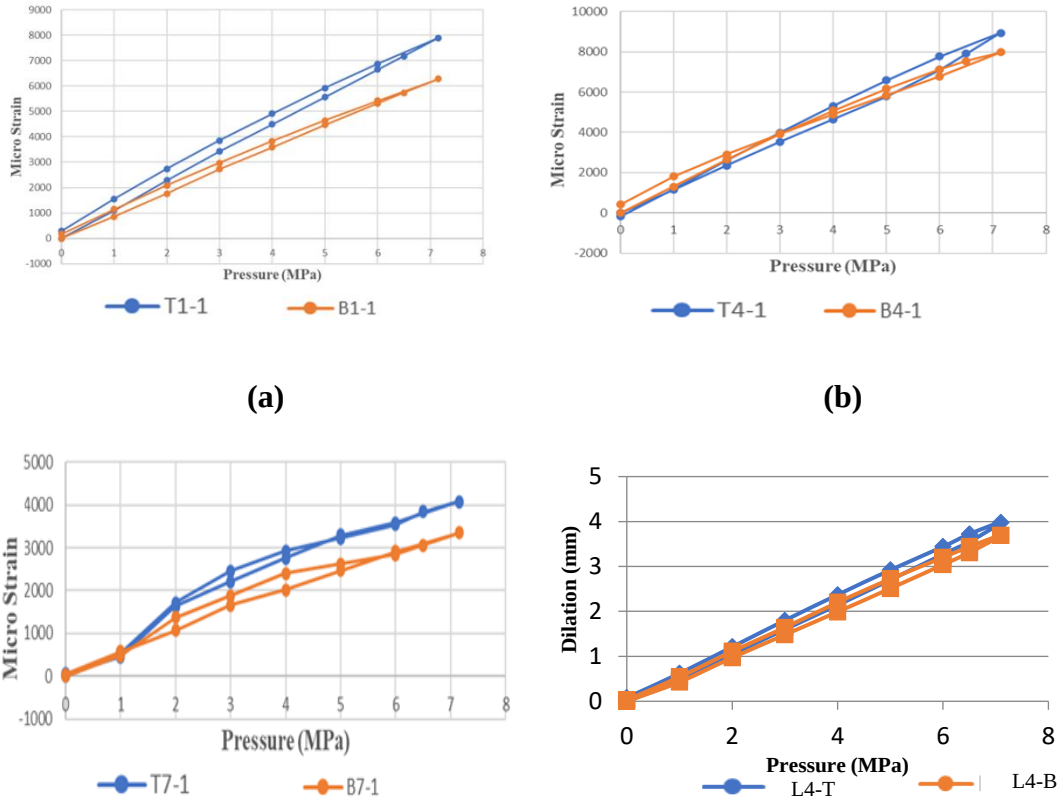

Figure 5.17. The Strains observed at the (a) IE dome (b) Cylinder (c) NE dome (d) Dilation observed on the Cylinder.

5.6 Natural Ageing Studies

These CRMCs are manufactured, acceptance tested and stored. Post-manufacturing, the propellant is cast and SRM is stored in an explosive magazine in a controlled atmosphere. From Table 5.3, it is evident that during most of the service life, CRMC is stored at ambient,

accordingly, to estimate the effect of storage and service environment, the CRMC after the first pressure test is left for natural ageing at ambient condition and re-tested after 5 years.

Table 5.3. Service Environment of C/E CRMC.

Activity	Working Environment	Duration (year)
Fabrication of casing from raw materials issued from stores	Any season Summer: 32–40 °C & 50-70% RH	0.5
Pressure test & post PPT activities	Rainy: 15- 25°C & 60-90% RH Winter:10–15 °C & 60-70% RH	0.25
Propellant filling and finishing		0.5
Storage and flight	Controlled environment Temperature: 25˚C & 70% RH	10

The PPT is repeated after 5 years to carry out a periodic health assessment for a service life of 5 years and the test results are tabulated below. The strain, dilation and NDT results are found to be comparable and do not show any significant change. The strain recorded at locations 1, 4 and 7 at the Top (T) location is shown in Table 5.4. The Strains at locations 1, 4 and 7 (T) are shown in Figure 5.18 and dilation at cylinder (location-4, T, B, R and L) is shown in Figure. 5.19.

Table 5.4 Strains at Location 1, 4 and 7 on CRMC after 5 years of Service Life.

Pressure (MPa)	T1-1 (T) (µs)	T4-1 (T) (µs)	T7-1 (T) (µs)
0	-27	-31	-31
1	622	847	788
2	1475	1908	1816
3	2343	2938	2823
4	3221	3952	3817
4	3661	4456	4313
5	4106	4964	4809
5.5	4559	5474	5295

6	5011	5983	5793
6.5	5660	6490	6288
7.1	6249	6905	6633
6	5041	6052	5864
5	4158	5062	4894
4	3282	4068	3923
3	2449	3107	2984
2	1674	2192	2092
1	730	1026	966
0	-145	-177	-166

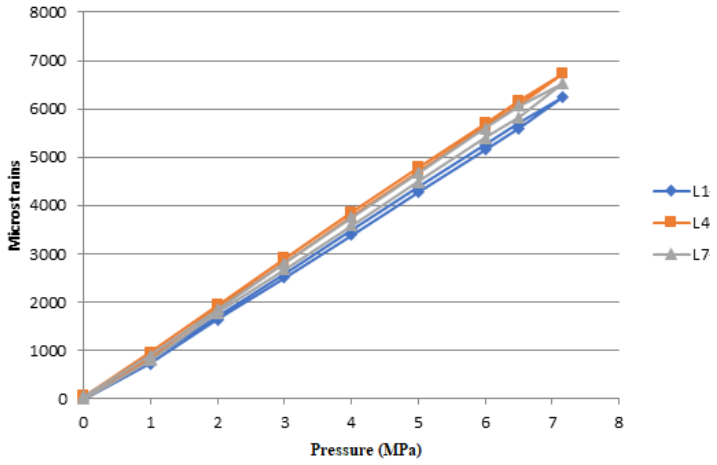

Figure. 5.18. Strains at Location 1 (T), 4 (T) and 7 (T) During Re-PPT (after 5 years of Service Life).

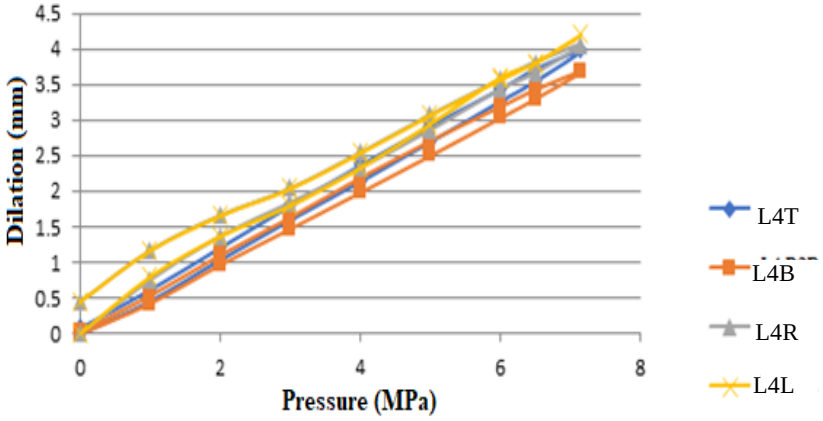

Figure. 5.19. Dilations at Cylinder during PPT after 5 years of Service Life.

The AE monitoring is carried out as per the plan and methodologies discussed in the earlier sections and the AE parameters for channel no 1,4 and 7 is shown in Table 5.5.

Table 5.5. AE Parameters during PPT after 5 years of Service Life.

Channel No.	**2**	**4**	**17**
Parameter			
Total No. of Hits	21861	21763	21256
Amplitude range (dB)	60 – 91	60 – 91	60 – 91
Duration range (µs)	1-15374	1 – 16203	1-18144
Rise Time range (µs)	1-270	1-324	1-377

Post, pressure test, UT and RT are carried out, The UT results are shown in Figure 5.6 and do not show any major change in UT signature and indicate sound health of the overall structure. The through transmission UT indicates a marginal increase in dB level near the dome region and Y joints at both ends. The casing is subjected to RT as per the plan and procedures discussed in an earlier section and the radiographs of the dome, skirt and cylinder region are shown in Figure 5.20, respectively. The radiograph observations are correlated with AE, UT, strain, and dilation observations. The dome regions show minor de-bonds and delamination accordingly, the same is also reflected in UT observations.

Table 5.6. UT Results after 5 years of Service Life.

Zone	**Test (dB)**	**T**	**P1**	**R**	**Y1**	**B**	**P2**	**L**	**Y2**
1	25			30		30	30	30	
2	25			25			30	25	
3	20				20				30
4	20	20	26			20			
5	20	20	26		20		32	32	
6	25			30		31		31	
7	35				35				

RT Results

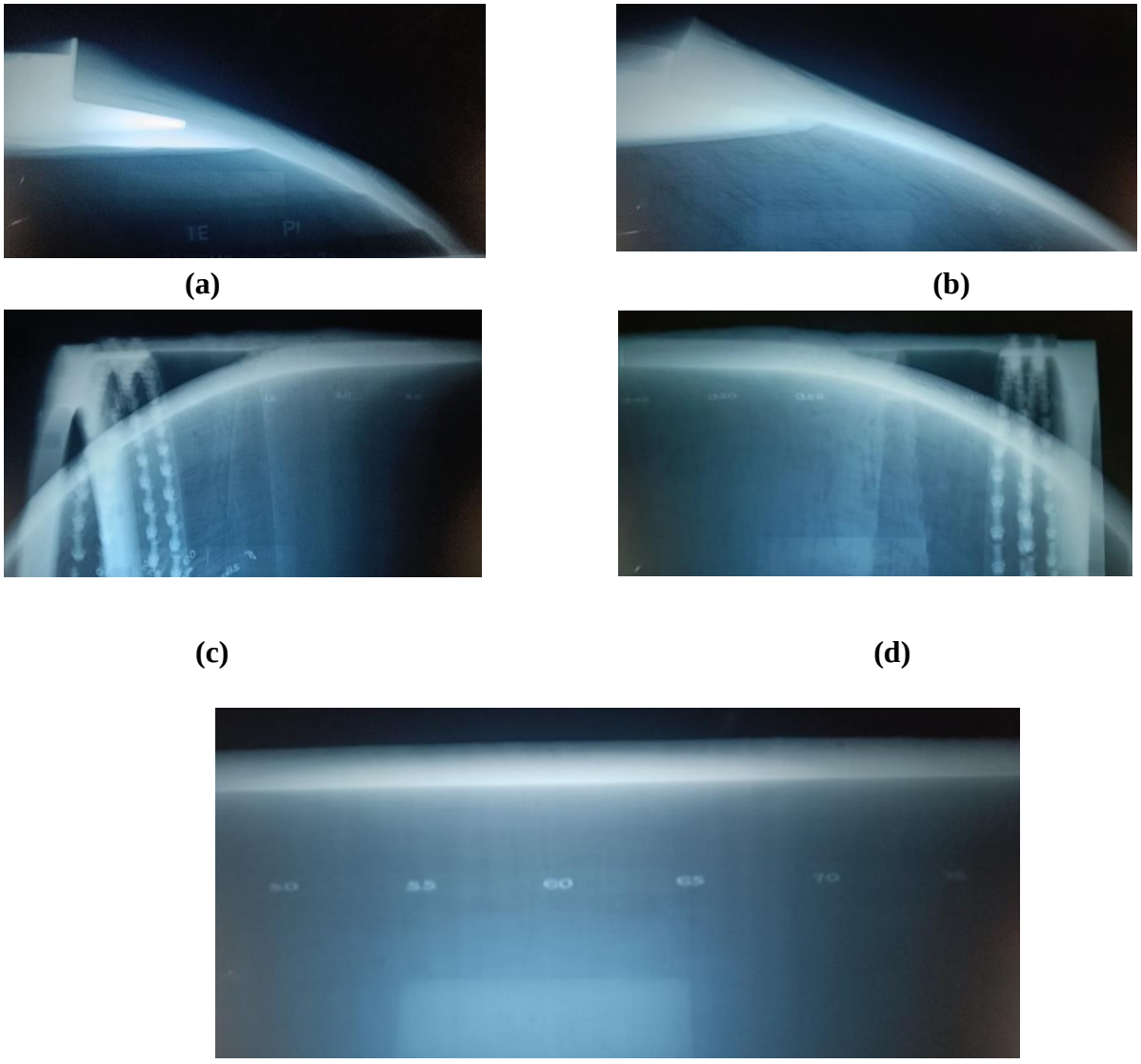

(a) **(b)**

(c) **(d)**

(e)

Figure. 5.20. RT Results of the casing after 5 years a) and b) Radiographs of dome region c) and d) Radiograph of skirt region e) Cylinder region

5.6.1 Comparative studies with CRMC of 10 years of service life

The CRMCs are expected to serve for a life period of 10 years, accordingly 10 years old CRMC is identified, and pressure tested. During the pressure test, strain, dilations, and AE is measured, and post-pressure test UT and RT are carried out. This casing is realised using the same material system and same approved manufacturing process as discussed in previous chapters. During PPT, the same test scheme is followed as discussed in Chapter 5. However, there is a slight variation in sensor location and grid markings as these locations and markings are redone. The Strain and dilation data are recorded and given in Table 5.7.

Table 5.7 Strains at Location 1, 4 and 7 on a CRMC with 10 years of Service Life.

Pressure (MPa)	R2T (T1) (µs)	R2T (T4) (µs)	R2T (T7) (µs)
0	-24	-9	-26
1	746	836	784
2	1692	1987	1779
3	2630	3219	2745
4	3572	4568	3703
5	4511	5885	4666
6	5456	7258	5630
6.5	5929	7901	6113
7.1	6550	8715	6742
6	5497	7629	5683
5	4564	6567	4741
4	3634	5490	3798
3	2743	4437	2888
2	1905	3411	2025
1	859	2101	932
0	-172	617	-169

The strain recorded at cylinder location (L4-R2T) is given in Figure. 5.21. and found to be around 8700 µs. The dilations at R2T and R2B locations at the Cylinder region (Location 4) are given in Figure 5. 22.

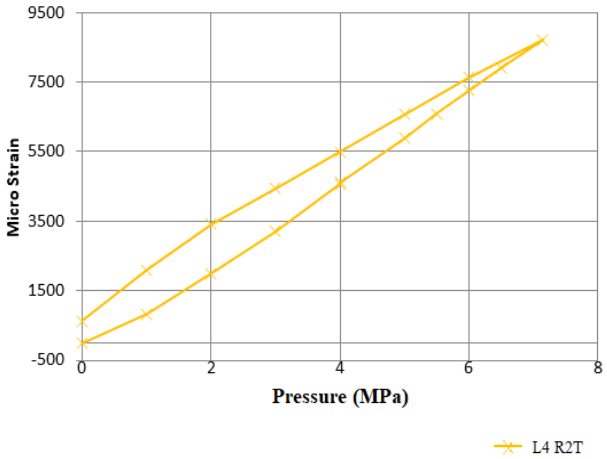

Figure. 5.21. Strain data at Cylinder (L4-R2T) on a CRMC with service life of 10 years.

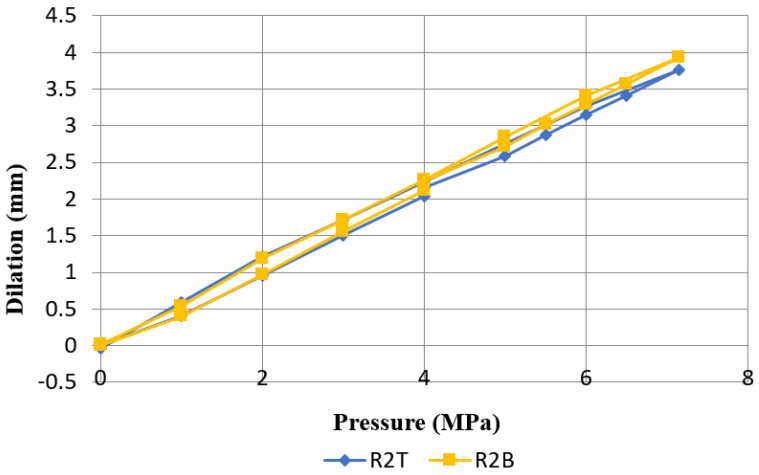

Figure. 5.22. Dilation on Cylinder Location During PPT on a CRMC with a service life of 10 years.

After, PPT, the casing is subjected to through-transmission UT and results are shown in Table No 5.8.

Table 5.8 UT Results on a CRMC with 10 years of Service Life.

Zone	Test (dB)	T	P1	R	Y1	B	P2	L	Y2
1	25			30		30	30	30	
2	25				25		30	25	
3	20					20			26
4	20	20	26				20		
5	20	20	26		30		32	26	
6	25			30		31		25	
7	35					35			

RT

RT results on CRMC with 10 years of service life are shown in Figure. 5.23.

(a)

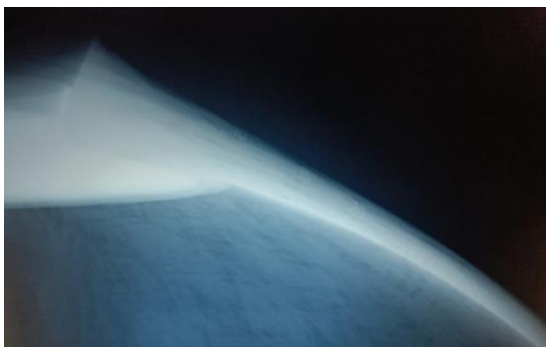

(b)

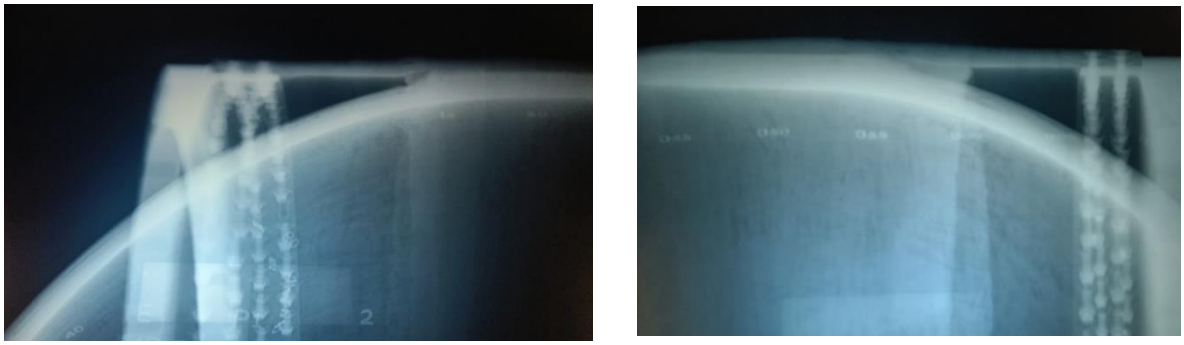

(c) **(d)**

Figure. 5.23. RT results on a CRMC with a service life of 10 years (a) Cylinder location (b) dome region (c) IE and (d) NE skirt region.

The AE parameters acquired during PPT from the casing (with 10 years of service life) are shown in Table No 5.9.

Table 5.9 AE Parameters during Re- PPT after 10 years of Life.

AE Parameters	**AE Channel No**		
	2	**4**	**17**
Total No. of Hits	19911	26672	32083
Amplitude range (dB)	60-92	60-93	60-93
Duration range (µs)	70 -5874	63-7933	41-6833
Rise Time range (µs)	1-378	1-385	1-425

5.7 Discussion

The strains and dilations for all three PPTs have been summarised in Table 5.10 and 5.11, respectively. The strains recorded at critical locations during all three PPTs are tabulated in Table 5.10, a close look indicates an increasing trend in strain. The long-term ageing affects the epoxy resin behaviour, fibre matrix interfaces and mechanical properties reducing the overall structural performance of composites. The test results are as expected, as with time, the strength is expected to degrade and strain within the structure increases. However, the increase is marginal w.r.t CRMCs with a service life of 5 and 10 years, respectively. The strains are well within the ultimate strain capability of the material with sufficient FoS.

At a few locations on the IE dome, cylinder and NE dome, the strains observed from 5 years old CRMC is showing minor reduction vis-à-vis PPT 01 and 03 results, which could be due to a mismatch in strain gauge location identification. The dilation (volumetric stretch) is within 4 mm at the cylinder location in all the three cases. The dilation at BH and polar boss locations are approximately 12 and 20 mm respectively in all three cases. The overall strain

and dilation results indicate the soundness of the structure and test data is linear in all cases and no sudden rise is observed, indicating absence of any critical failure mechanism initiations.

The AE parameters acquired during all three PPTs have been analysed. The AE activities started at around 20% of proof pressure and the corresponding amplitude is less than 80 dB up to 60% of pressure and beyond that, the amplitudes observed are as high as 98 dB. A dominant matrix cracking phenomenon is observed during the entire pressure cycle starting from 2 MPa onwards and found to be more stable during higher pressures close to MEOP. It is observed that the AE intensity is more in PPT-03 (CRMC with 10 years of service life) at the initial stage due to matrix cracking at the early stage compared to PPT-01 and 02. The amplitude pattern is uniform across all the channels for the entire pressure cycle during all three pressure tests. The hold periods indicate the absence of any major emissions. The time duration of all the AE hits in the entire pressure cycle is well within 2 x 10^4 µs, also at higher pressure no continuous high hit rate, high count rate, high amplitude and high energy emissions are observed. This indicates the absence of critical failure mechanisms like de-lamination and fibre breakage. The AE parameters for all three PPTs are comparable, and it is attributed to the uniform quality of cured properties of the resin which confirms the good process control during manufacturing.

Table 5.10 Comparison of Maximum Strains for the three PPTs

Location	**After realisation @PPT (µs)**	**Re-PPT (After 5 years of service life) @PPT (µs)**	**With a CRMC of 10 years of Service life @PPT (µs)**
IE Dome	5588	5966	5851
	7975	7334	7963
IE Skirt	3351	3427	3486
Cylinder	6742	6905	7579
	8695	7958	8715
	7904	7947	8228
NE Skirt	3064	3396	3481
NE	4077	3837	4994
Dome	4932	5657	5883

Table 5.11 Comparison of Dilations for the three PPTs.

Details	Cylinder (mm)	BH to BH (mm)	Boss to Boss (mm)
After realisation	3.15/3.93/3.34/3.05	11.69/13.25	20.94/20.47
With 5 years of life	3.43/4.14/3.40/4.10	11.71/12.22	19.86/18.20
With 10 years of life	3.77/3.98/3.16/3.13	11.96/11.50	19.19/18.62

5.8 Summary

PPT is carried out on a C/E CRMC, The AE activities along with strain/dilation measurements are monitored. Post-PPT, UT and RT are carried out and indicate sound structural health. The findings are summarised below:

- During first time PPT on a Virgin CRMC, the maximum strain and dilation (at the Cylinder location) is around 8700 µs and 4.1 mm, respectively. A re-loading cycle after (MEOP) is introduced for evaluating FR (AE activities) and indicating the soundness of the structure up to MEOP. UT and RT indicate minor delamination and resin rich areas in the polar boss region.
- The CRMC is re-pressure tested again after 5 years. The strains and dilations are comparable with first-time PPT. The UT, RT and AET results are comparable and do not indicate any major deterioration. The UT shows a minor increase in dB level at certain locations, those locations are analysed considering AE, strain, and RT. It corresponds to minor de-bond and outer layer delamination in HE and NE dome regions.
- A 10-year-old in service casing is pressure tested. The results are compared with the test results of the earlier two PPTs. The strain and dilations are in the same order, the maximum cylinder dilation is around 4 mm, and the maximum strains are below 9000 µs. The AE parameters are in a similar order in comparison to the earlier two PPTs. UT and RT also show minor degradation at a few isolated locations and indicate the absence of higher-order failure mechanisms like de-lamination and fibre failures.
- The PPT results of a virgin CRMC are compared with PPT test data after 5 years and also compared with the test data of a 10 years old in-service CRMC (manufactured using the same material system and manufacturing process). The results are tabulated in Table No. 5.10, it is evident that unidirectional fibre strains are increasing across the various zones of CRMC due to degradation in the mechanical strength of C/E composites. The strain data show an overall increasing pattern with time; however, the increase is not that significant. The performance after 10 years is satisfactory and strains, dilation indicates uniformity in properties across the structures and demonstrates overall soundness for the said MEOP.

CHAPTER 6

ENVIRONMENTAL STUDIES ON G/E CRMC

In this chapter, the effect of environmental conditions on the structural performance of G/E CRMC is carried out through static firing in an integrated and penultimate mode to assess overall health at the subsystem stage. The present study is formulated on a subsystem level resembling the actual flight hardware configuration and expected operational environment. The SRM (with composite case) is exposed to different environmental and operational conditions and subsequently, experimental performance evaluation is carried out through a ground qualification test, which is the closest possible alternative to that of an actual flight test.

6.1. Acceptance Testing

Proof Pressure Test (PPT)

The manufacturing process of G/E composite cases is discussed in Chapter 4. After manufacturing cases are subjected to PPT as a part of acceptance testing. The composite case along with a rubber bladder is hydro-pressure tested up to 11 MPa in a specially designed test fixture, to confirm the designed FoS. All the composite cases sustained the required proof pressure without any noticeable pressure loss. After PPT, again the filament wound cases are tested for geometrical attributes and accepted.

6.2. NDT

RT

The composite case is bonded with Nozzle End Insulation (NEI) and is subjected to RT before and after the PPT. The casing is divided into various zones and subjected to normal and tangential shots shown in Figure 6.1. The total no. of shots is worked out based on casing configurations. The defects such as fibre cut, de-lamination, de-bond, porosity, surface damage, cracks & inclusion etc. are given special emphasis and studied w.r.t its functional implications.

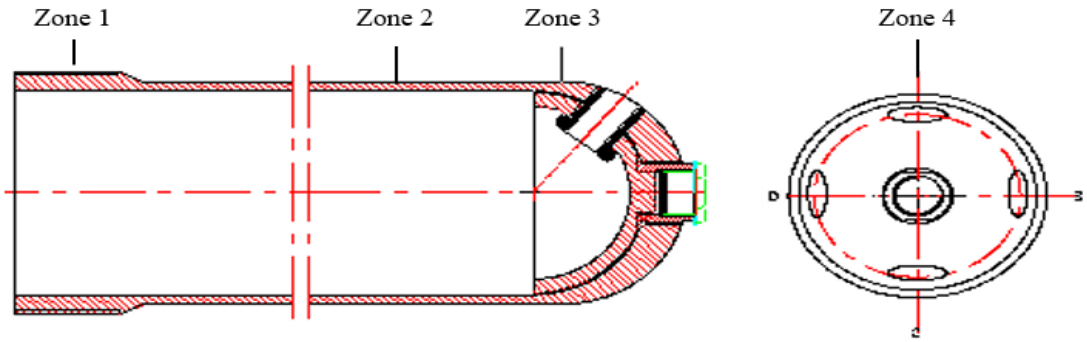

Figure 6.1. RT Plan - Composite casing.

RT is carried out on each casing before and after PPT and found to be free from defects. RT results are shown in Figure 6.2.

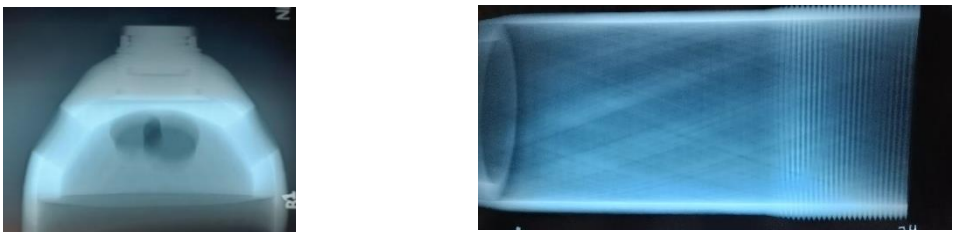

(a) **(b)**

Figure 6.2. Radiographs of: (a) NE Region (b) Cylinder with Threaded Region.

6.3 Burst Test

As a part of the one-time qualification and design validation, the composite case is subjected to a standalone hydraulic burst test and a min. burst pressure of 12.5 MPa is obtained which confirms and demonstrates the MoS.

6.4 Test Plan and Methodology

These SRMs with composite cases are single-shot devices and are generally assembled with flight articles only at the time of use. They are normally handled, shipped, and stored separately. Storage of the SRM is an important part of its life cycle as the environment in

which it is preserved, may have a large influence on the structural integrity and functionality during actual flight. The life cycle of SRM includes storage, deployment, and flight environments. A detailed program is designed to verify the operational capability for the range of expected service environments [27, 45 & 46]. The number of tests is derived envisaging the criticality, potential failure risk, load envelope, and availability of hardware. The overall performance evaluation test matrix is shown in Table 6.1.

Table 6.1 Performance Evaluation Test Matrix– SRM with G/E Composite Case.

Sl. No	Environment Test	Test Article No.								
1.	Stand-alone static firing at ambient	1-11								**Phase 1**
2.	HT Soak		2-11							**Phase 2**
3.	LT Soak			3-11						
4.	Vibration Test- Transportation Vibration (TV)				4-11					
5.	Vibration Test- Flight Vibration (FV)					5-11				**Phase 3**
6.	Acceleration Test						6-11			
7.	Shock Test							7-11		
8.	HT functional test								8-11	
9.	LT functional test									**Phase 4** 10-11
	Static Firing	1	2	3	4	5	6	7	8-9	10-11

A total of 11 numbers SRM's with the composite case are conditioned for different environmental factors and static fired for performance evaluation. In phase 1, one SRM is static fired (at ambient without any exposure) for stand-alone performance evaluation and comparison. In phase 2, the balance 10 numbers of SRMs are subjected to temperature environments and SRM Sl. no. 2 and 3 are static tested. In phase 3, balance SRMs are subjected to a dynamic environment comprised of acceleration, vibration, and shock. Post-exposure, SRM Sl. no. 4 to 7 are static fired after each exposure. During phase 1 to phase 3 evaluation, all the SRMs with the composite case were subjected to RT to assess the structural integrity, before and after static firing. In Phase 4 evaluation, SRM Sl. no. 8 to 11 are soaked at high and low temperatures and 2 numbers are fired (immediately after removal from the thermal chamber) to assess the performance at both respective temperature extremes.

6.5 Static Test and Results

6.5.1 Phase 1: Standalone Test

The propellant grain, SRBP tube and other subsystems are assembled with the composite case. The SRM is then assembled to a text fixture using the HE metallic flanges and static fired at ambient conditions (27°C). The calibrated pressure transducer is assembled to the flange adaptor for pressure measurement. The pressure-time curve obtained is in line with the prediction and taken as a reference for comparative studies with the rest of all other test condition results. The test setup and pressure versus time plot are shown in Figure 6.3. The pressure-time curve obtained is close to nominal (27°C) and the trend is as expected.

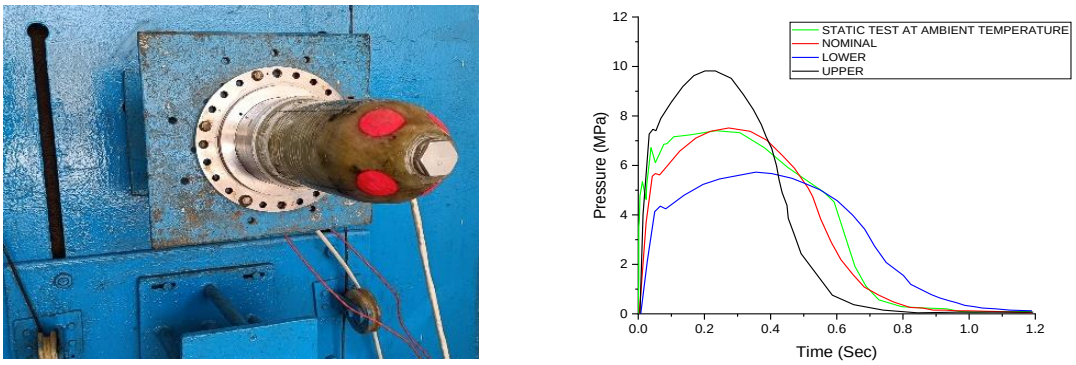

(a) b)

Figure 6.3. Stand-alone static test firing of an SRM with the composite case (a) Test Setup (b) Static Test result at ambient.

6.5.2 Phase 2: Temperature Environments

Two SRMs are subjected to HT and LT exposures to determine the operational performance against the expected temperature environments. Post exposures, both motors

are subjected to static firing. This test is carried out as per MIL-STD 810 G [93] guidelines. The temperature extremes are selected based on the design mission bound. To evaluate the effect of HT and LT on structural performance, the thermal conditioning is carried out at 10°C and 45°C, respectively. In the HT soak test, SRM is soaked at 45°, 55°, and 45°C for 6, 4, and 6 hours, respectively. For, the LT soak test, it is soaked at 10°, 0°, and 10°C for 6, 4, and 6 hours, respectively. Considering the propellant web thickness, the temperature is varied by 10°C, to ensure that the grain surface reaches the intended temperature extreme. The static test is carried out at ambient; the results shown in Figure 6.4 reveal that SRM performance is within the predicted performance bound and comparable with the static test result at ambient (27°C). The effect of HT and LT soaking is not significant and, in both cases, the peak pressure, burn duration and trend line obtained are almost comparable.

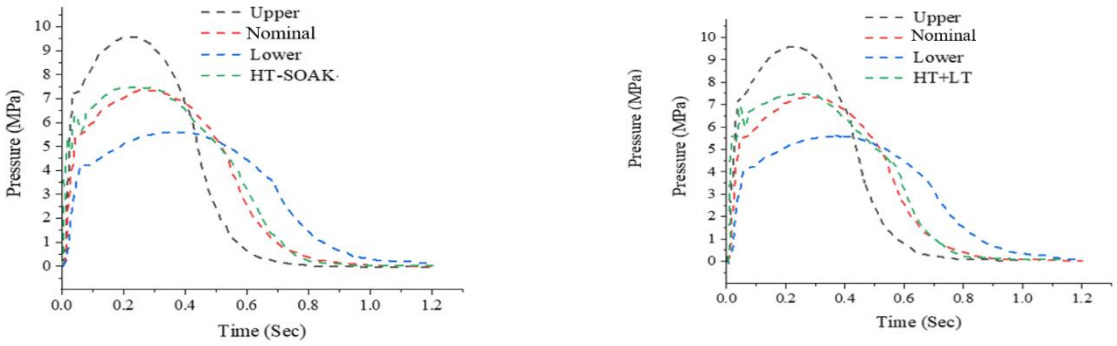

(a) **(b)**

Figure 6.4. Static Test Results after (a) HT (b) LT Soak Test.

6.5.3 Phase 3: Dynamic Environments

The SRM is exposed to various dynamic environments expected during service life and operational life concerning the vibration, acceleration, and shock environments.

6.5.3.1 Vibration Test

The vibration test is carried out to assess the operational capabilities against vibration severities expected during transportation and flight. The sources of vibration are propulsion and aerodynamic disturbances. Therefore, the test fixture is specially designed to simulate the case-to-missile interface and test setup. The test fixtures are stiffened suitably to be considered rigid for the expected test frequencies [10]. Experimental trials are carried out before the test to validate fixture design, and assembly procedure and to confirm testing requirements [10]. Test levels (Table 6.2) are chosen based on mission requirements and are arrived at using MIL-STD 1540 D guidelines [94]. Articles no. 4 – 11 (Table 6.1) were subjected to transport vibration conditions on a 2-ton dynamic shaker in both longitudinal and transverse directions

respectively followed by a static test of Sl. No 4. Further, articles Sl. no 5-11 were subjected to a flight vibration environment followed by a static test of Sl. No 5. The test setup for Random Vibration is given in Figure 6.5. The static test performance is satisfactory and comparable, and the result of both the transport and flight vibration test is given in Figure 6.6.

Table 6.2 Vibration Spectrum.

Sl. No	Type of test	Test specification	No of axes
1	Transport Vibration (TV)	• Frequency 5Hz-20 Hz, PSD 6 dB Octave • Frequency 20Hz-50Hz, PSD $0.02g^2$/Hz Rolling down to $0.001g^2$/Hz at 500 Hz • Total Duration – 2 Hrs	Two
2	Random Vibration (Flight)	• Frequency 20-2000 Hz, PSD $0.07g^2$/Hz, • Total Duration – 100 Seconds	Two

Figure 6.5. Test Set-up for Random Vibration.

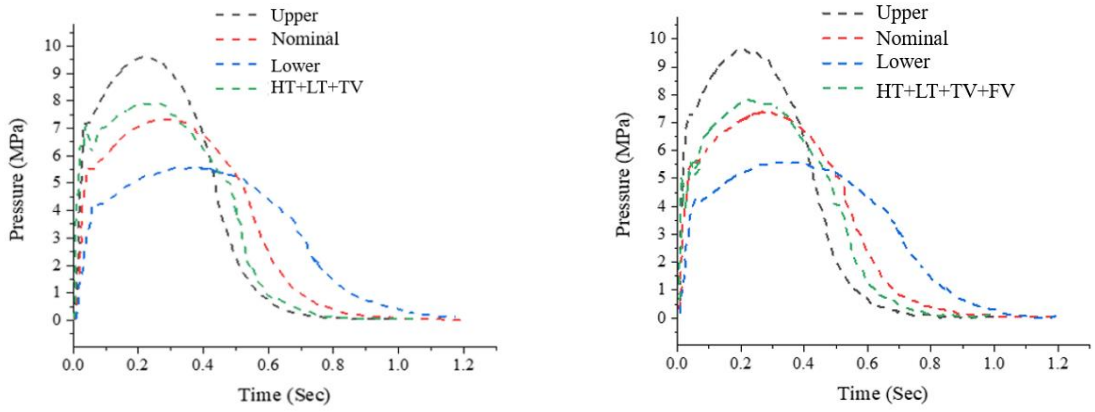

(a) (b)

Figure 6.6. Static Test Results after (a) Transport and (b) Flight Vibration Test.

6.5.3.2 Acceleration Test

This test is performed after subjecting SRMs to a steady acceleration environment of 17 g for 60 seconds according to mission specifications. The test setup is designed with a suitable fixture to facilitate the required level of acceleration in the desired direction simulating the flight interfaces. Articles Sl. no. 6-11 is subjected to an acceleration test followed by a static test of Sl. no 6. The test result is in line with the predicted performance bounds and comparable with the static test result at ambient. The Test setup and test results are given in Figure 6.7.

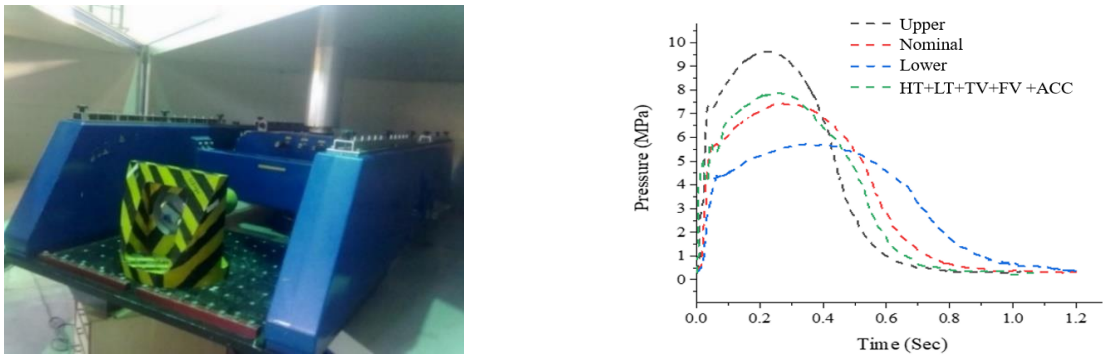

(a) **(b)**

Figure 6.7. (a) Test set-up - Acceleration Test and (b) Static Test Result after Acceleration Test.

6.5.3.3 Shock Test

The Shock test is carried out to verify the resistance of the SRM to mechanical shocks (expected in flight due to stage separation and explosive firing) by applying simple low duration reproducible impulsive acceleration. The test fixture is designed and qualified to simulate the flight interfaces and subjected to the required test levels in a suitable setup. Articles Sl. no 7-11 are subjected to a shock test as per the specifications given in Table 6.3.

Table 6.3 Shock Test Specification.

Sl.no	Type of test	Test specification	No of axes
1	Shock test	45g for 11 msec, half-sine wave	Two shocks in 2 longitudinal and 1 in radial axes

The RT (Figure 6.8) of SRM Sl. no. 7, conducted after completing all the dynamic environment exposures does not show any defects and demonstrates overall structural integrity.

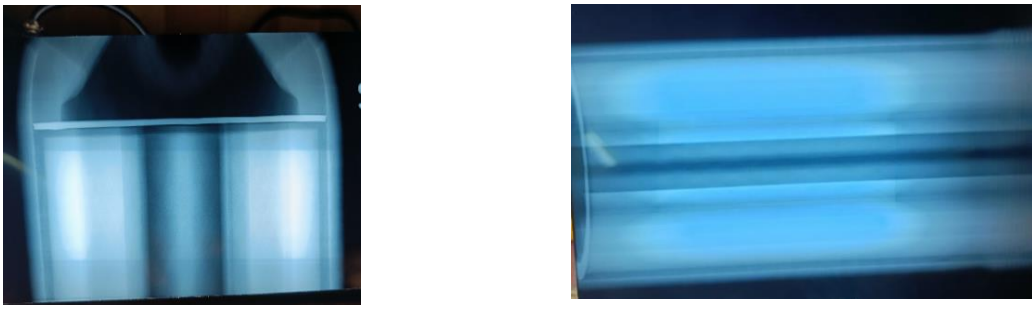

(a) **(b)**

Figure 6.8. RT after Shock test a) HE region b) Cylinder region.

Post RT, article Sl. no. 7 is test-fired. The static test performance is shown in Figure 6.9.

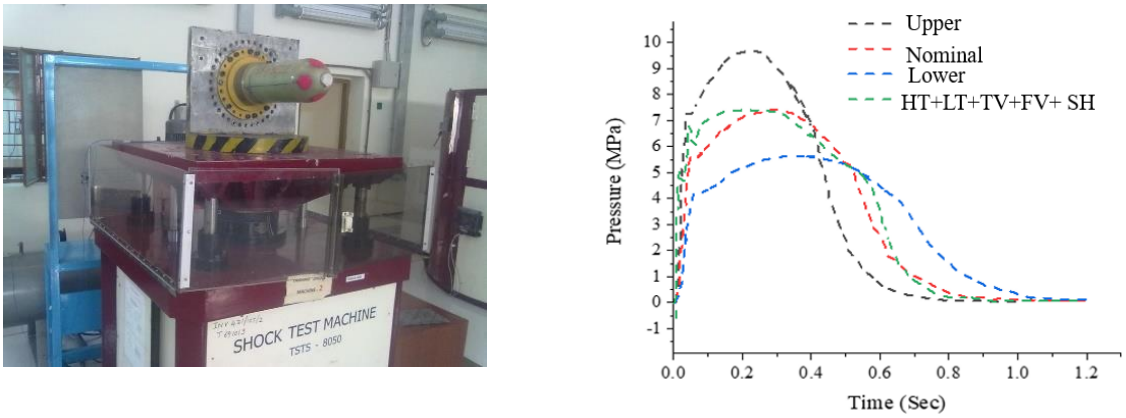

Figure 6.9. Static Test Result after Shock Test.

The pressure versus time plots of all the phase 3 dynamic tests reveal that vibration, acceleration and shock do not affect the ballistics and structural performance of SRM with the composite case. The pressure, burn duration and profile is following a similar trend in all cases.

6.5.4 Phase 4: High Temperature (HT) and Low Temperature (LT) Functional Test

To evaluate the performance of SRM for temperature extremes, both the high-temperature and low-temperature functional tests were carried out. Articles Sl. no. 8-11 is conditioned at high (55°C) for 12 hrs (10°C higher than the specified upper bound temperature) followed by a static test of articles Sl. no. 8 and 9.

Balance articles Sl. no. 10 and 11 were conditioned at 0°C for 12 hours (10°C lower than the lower bound temperature) and test fired. In both cases, the static test is carried out within 30 minutes of thermal conditioning to evaluate the effect of grain temperature on functional performance. As articles Sl.no. 8-11 underwent, the cumulative effect of all the environmental factors, for better comparison and repeatability, 2 no. of SRM were tested for each condition. The two functional tests are of utmost significance as it has undergone, the cumulative effect

of all the test conditions and are fired immediately after removing from the thermal chamber. The static test results are well within the bound and comparable with the standalone test. The results of the static tests are given in Figure 6.10.

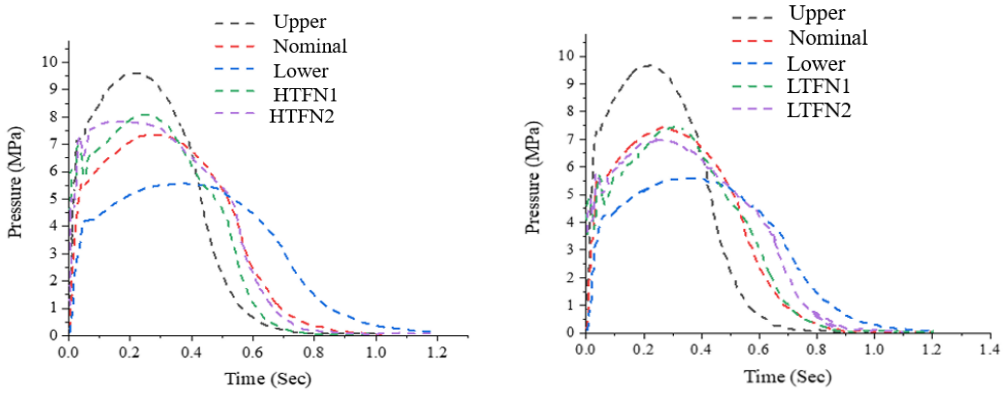

(a) **(b)**

Figure 6.10. Static Test Results (a) HT and (b) LT Functional Test.

6.6 Topical Exposure Testing

To evaluate the cumulative effect of temperature and humidity variation on the performance of composite cases, an SRM with the composite cases is subjected to tropical exposure conditioning as per JSS 55555-2012 guidelines [95]. It determines the ability of the composite cases to withstand the exposures and sustain the intended pressure when needed. The diurnal cycle (diel cycles) applies the temperature variation in a more realistic pattern, it represents a pattern that recurs every 24 hours considering earth rotation. These cycles do not consider the true environment within the missile and apply realistic temperature fluctuations. The tropical exposure test is significant in identifying potential design weaknesses in the system. The one tropical cycle is given below

- Raise the chamber temperature from 20°C to 45°C and 95% RH in 3 hrs
- Hold the chamber temperature for 12 hrs
- Decease the temperature from 45°C to 20°C in 3 hrs
- Hold the chamber temperature for 6 hrs at 20°C
- Total no of cycles – 14, and each cycle is of 24 hr duration

The SRM with the composite case is subjected to RT, the radiographs are shown in Figure 6.11.

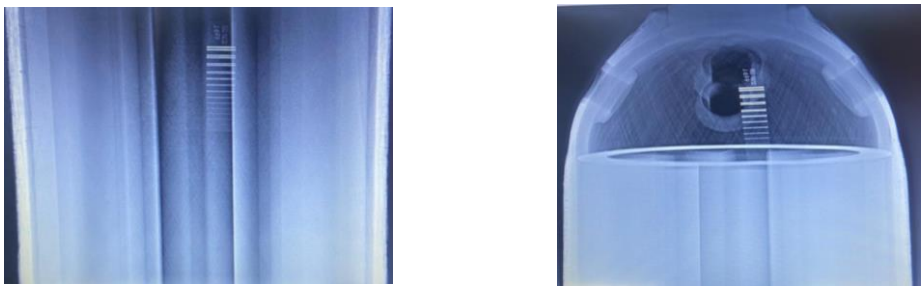

(a) **(b)**

Figure 6.11 Radiographs after topical exposures a) Cylinder region b) HE Dome.

The static test result after the exposure test is shown in Figure 6.12.

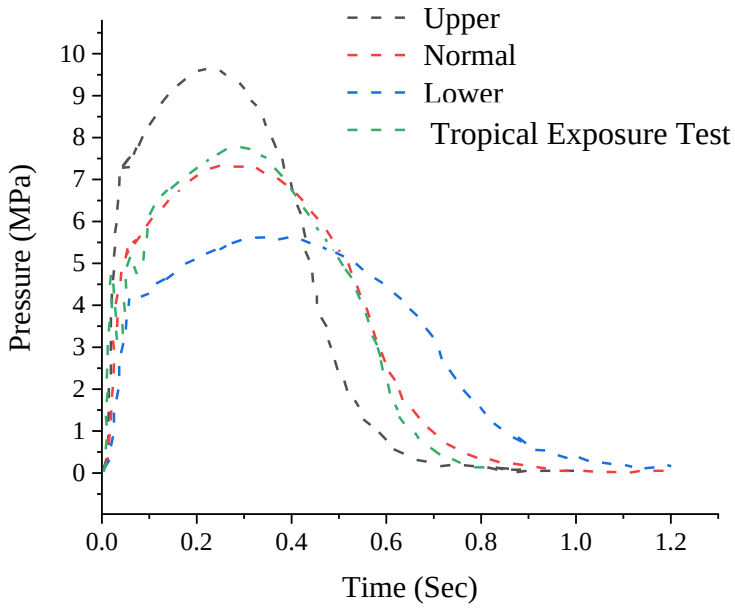

Figure 6.12. Static test results after tropical exposure.

The SRM with the composite case is subjected to the above cycle and then static fired. The Static test results after tropical exposure test results are compared with the virgin SRM and performance is comparable.

6.7 Discussions

To evaluate the effect of grain temperature on the ballistic performance of SRM, two test cases are identified. In the first test case, SRM is soaked at HT and LT respectively and then static tested. For the second test case, SRM is conditioned at HT and LT respectively for 12 hours and static tested within 30 minutes of removal from the thermal chamber. The pressure and burn time are tabulated in Table 6.4.

To evaluate the effect of the flight dynamic environment, a load envelope is evolved in accordance with MIL guidelines concerning the mission requirements. The SRM is subjected

to low-frequency transport vibration, worst-case flight vibration, acceleration, and shock test. The test setup and fixtures simulate the flight environment and the SRMs are subjected to those dynamic environments and static fired. The peak pressure and burn duration are tabulated in Table 6.4.

Table 6.4 Pressure and Burn Time from Static Test (after Environmental Conditioning).

Sl. No	Type of test	Max pressure (MPa)	Burn time (sec)
1	HT soak test	7.6	0.550
2	LT soak test	7.6	0.580
3	Transport Vibration (TV) test	8.1	0.490
4	Flight Vibration (FV) test	8	0.500
5	Acceleration (ACC) test	7.9	0.520
6	Shock (SH) test	7.7	0.580
7	HT functional test	8.3	0.480
8	HT functional test	8	0.530
9	LT functional test	7.6	0.580
10	LT functional test	7	0.600

All the SRMs are subjected to RT before and after the environmental exposures. The grain, composite case and all the interfaces were found to be intact and structurally integral. RT of article Sl. no. 7 (Fig.6.8), having undergone the cumulative effect of all four dynamic environments and before static firing, reveals no major effect on the overall structural integrity. The post-static test radiograph (post-static test radiograph after LT exposures) of the article is shown in Figure 6.13. The performance of SRM under the combined effects of all the environmental factors is as expected, repetitive and in line with prediction. The SRM with composite case withstood static firing during all the environmental conditioning.

(a) (b)

Figure 6.13. (a) SRM with Composite Case after Static Test (b) Radiograph after Static Test

6.8 Summary

The above study is focused to evaluate the effect of various environmental conditions (at the sub-system stage) on the performance of composite cases through static firing. This led to an overall structural integrity assessment of composite cases resembling actual flight configuration. The salient findings are summarised below:

- The G/E CRMCs are realized using the FW process described in Chapter 4. The casings are subjected to NDE followed by PPT. One out of ten casings are also subjected to a burst pressure test to demonstrate the design margin.
- The casings are assembled with other propulsion subsystems to realise SRM. These SRMs with composite cases are exposed to a rigorous performance evaluation program encompassing the entire product life cycle. The test program and specifications are designed to emulate various missile system service situations.
- The SRM is submitted to RT for structural integrity evaluation after every exposure. The static firing is carried out in a phased manner after every exposure. All the SRM with composite cases sustained all the environmental conditioning, including acceleration, shocks, vibration, and temperature extremes. All casings worked admirably and exhibited their capacity to endure pressure and temperature loads throughout the combustion process without compromising their structural integrity.
- The propellant burn rate is sensitive to temperature, as grain temperature increases (In case of the HT functional test), the propellant burn rate increases and propellant regresses faster and web consumes quickly reducing the burn duration. In the case of the LT functional test, due to low grain temperature, the propellant burn rate is on the lower side and accordingly peak pressure is closer to the lower bound and burn duration is maximum. The same effect is evident in pressure and burn duration data of HT and LT functional tests. In the case of HT exposure, the peak pressure is maximum, and the burn duration is shortest and in the case of LT exposure, the peak pressure is close to the lower bound and the burn duration is the longest among all the test cases.

CHAPTER 7
ACCELERATED AGEING STUDIES ON G/E CRMC

In this chapter, accelerated ageing studies are performed on SRM with G/E CRMCs. From, the literature survey it is evident that the storage environmental conditions are expected to alter the physical and mechanical properties of composites. Accordingly, subsystem level study is initiated and SRM with composite cases are subjected to an accelerated environment and then static fired resembling the flight operational conditions to establish long-term durability.

7.1 Introduction

The ageing of PMCs raises uncertainties about their long-term performance, durability, and service life. Polymer composites experience degradation during the service life, resulting in degradation in mechanical properties, thus affecting their performance and shortening their useful life [96, 97 & 98]. During service life, ageing leads to irreversible changes in properties and long-term degradation produces a substantial deviation in performance. With the ever-increasing use of these polymeric composites, the influence of environmental service conditions on their durability is an ongoing concern [96]. To evaluate the long-term effect of

the storage environment and to conduct life assessment studies on PMCs, accelerated test methods are being used [48, 63, 65, 68 & 69].

SRM with the composite case is designed to produce a specified mass flow rate, heat flux and pressure rise within a given time. The entire combustion is a series of events expected to take place in a controller and reproducible manner. The CRMC shall perform its required function under the specified storage and operational condition for the stipulated time intervals. Composite case being the critical element, it is essential to determine the periodic performance of composite cases for the intended service life. The lifetime of SRM depends on the life of the composite case, and thus in-service performance evaluation of the composite case is a key factor in determining the useful service life.

7.2 Ageing Studies

In the available literature, numerous investigations have been carried out to predict and evaluate the degradation in properties of the polymeric composite on specimens. The research work carried out by several researchers is studied in-depth and a background is established to draw a further road map on in-service performance assessment of filament wound composites to ensure safe life and specifically to evaluate their sustained performance. SRM are single-shot devices and to have high in-built reliability, a detailed qualification program is a necessity. This experimental study is aimed to evaluate the effect of long-term ageing on the structural performance of composite cases at the sub-systems level in an integrated manner through the Intensified Standard Alternating Trials (ISAT)-B exposures followed by a penultimate ground static test of SRMs at ambient, at HT and LT as deemed necessary.

As a part of risk assessment, design qualification, validation, and approval of products for defence applications, ISAT studies are carried out periodically for performance evaluation to mitigate any unprecedented risk, particularly in terms of detecting the environmental effects. ISAT plays a significant role in rocket component testing because moisture and long-duration temperature can have a potentially bad effect on structural integrity and interfaces. ISAT trials are based on the alternation between temperature, humidity, and ambient conditions (with condensation) and with a small element representing each week of dry heat to simulate tropical desert conditions. The combined moisture cycling, and thermal cycling environments are known to create damage, such as cracking near exposed surfaces and edges. The performance of the composite is prone to age due to moisture, elevated temperature, and cycling, therefore, the ISAT - B conditioning cycle is chosen herewith for life assessment studies based on Joint Service Guide (JSG) 0102:1984 [99].

7.3 ISAT-B Trials

ISAT-B environmental conditioning test cycle includes temperature and humidity variation. The duration of a single ISAT-B test is 1 week, and the cycle is given in Table 7.1. The ISAT B cycle limits the temperature to 40°C and 75°C with variable RH. The ISAT (B) cycle takes account of solar radiation by including a period of 8 hours of conditioning at 75°C, and 5 per cent RH.

An in-service surveillance program provides data on the serviceability of products after periods of real-time storage in the actual storage conditions existing in the particular or part of the conditions in which the missiles are deployed and stored. The performance is then assessed and compared with the results obtained from simulated real-life tests. The test results obtained from this surveillance program provide useful information about post-deployment service life.

Table 7.1 ISAT-B cycle.

Sl. No	Hours	Temperature (°C)	Relative Humidity RH (%)
1	48	46 ± 2	95 ± 2
2	24	60 ± 2	60 ± 2
3	24	Cooling	
4	8	75 ±2	dry (about 5%)
5	16	Cooling	
6	24	46 ±2	95 ± 2
7	24	Cooling	

7.4 Test Article

The G/E filament wound composite cases are realised as per the established process mentioned in Chapter 4.0. The cases are then acceptance tested and are assembled with other subsystems and SRMs are made ready. The approved manufacturing and QA procedures are followed for the realisation of these composite cases and SRMs.

7.5 Batch Acceptance Test

Considering the design inputs and mission requirements, a performance envelope is evolved. During the in-service surveillance program, all the performances are expected to be within the given design bounds. The same is verified and validated in the succeeding sections. All the SRMs are subjected to RT before the static test and are found to be free from any significant defects. As a part of batch acceptance tests, 3 nos. of SRMs are identified and

subjected to standalone ground test at ambient and for further comparison and validation with the test results of accelerated aged SRMs. The static firing results are shown in Figure 7.1.

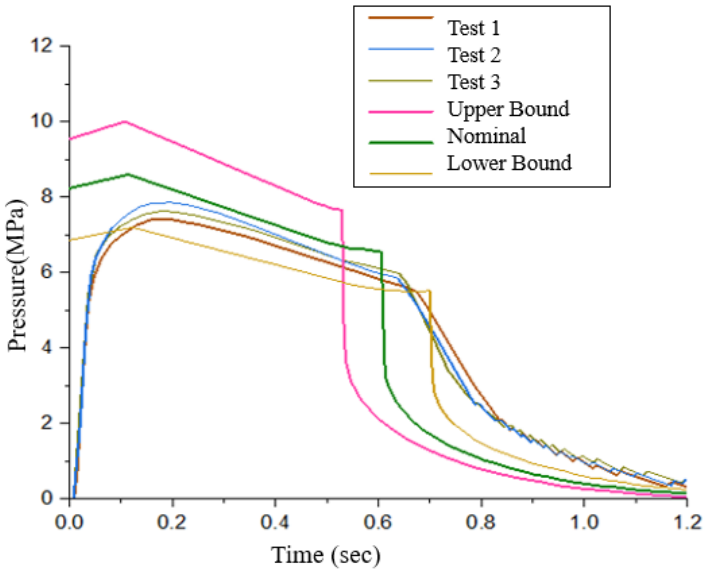

Figure 7.1. Static Test Result of SRM with Composite Case - Batch Acceptance Tests.

The key ballistic parameters are tabulated below (Table 7.2) and indicate repeatable and desired performance.

Table 7.2 Ballistic Parameters – from Batch Acceptance Static Test.

Ballistic parameters	Specs	Test-1	Test-2	Test-3
Ignition Delay, msec	<100 msec	12.8	15	16
Web burn time, msec	610 ± 100 msec	662	645	644
Action time, sec	<1.10	1.0382	1.05	1.041
Pmax, MPa	7.2 to 10.3	7.46	7.8	7.56

7.6 Test plan – Accelerated Ageing

After the batch acceptance tests, balance 10 no. of SRMS are subjected to ISAT exposures and static fired periodically to confirm the structural integrity. The metallic flanges (15CDV6) are coated with 2 coats of Rusted paint before subjecting to ISAT-B conditioning.

The SRMS are supported on the wooden saddles at either end of the conditioning chamber. The sample withdrawal plan is given in Table 7.3. Further, according to Ordnance Board (OB) proceedings 41102 [100], Climatic Environmental Testing of Land Service Guided Weapons, 1 cycle of ISAT-B trials is equivalent to 9 weeks in actual tropical storage. Accordingly, after every 12 ISAT (B) cycles, i.e., after 12, 24, 36,48 and 60 cycles, 2 no's of

SRMS are withdrawn and static fired corresponding to a service life of 2, 4, 6, 8 and 10 years respectively.

Table 7.3 ISAT – Test Sample Withdrawal Plan.

Withdrawal No.	**No. of ISAT-B cycle**	**SRMs Sr. No. 4-14 Undergoing test**				
1	12	4-13				
2	24		6-13			
3	36			8-13		
4	48				10-13	
5	60					12-13
Static Test	----------	4,5	6,7	8,9	10, 11	12, 13

7.7 Climatic Conditioning

The SRMs are kept in a suitable environmental conditioning chamber (Figure 7.2), based on the hazard classification code. The broad specifications of the environmental chamber are given below.

Chamber Dimension : 3m(L) X 2.5m (B) X 2.5m (H)

Temperature range : 0-100 ºC

Humidity : 20 to 98 % RH

Figure 7.2. Climatic Test Chamber.

7.8 Static Test Results

7.8.1 Static firing after first withdrawal (12 ISAT-B cycles)

2 SRMs are withdrawn after the completion of 12 ISAT-B cycles (Table 1). The pressure vs time graph is plotted and shown in Figure 7.3. The performance of both these SRMs is within the designed performance bounds. Thus, the total system comprises composite cases, other subsystems, and interfaces, passed the surveillance test and the service life is validated for 24 months after completion of 1st withdrawal.

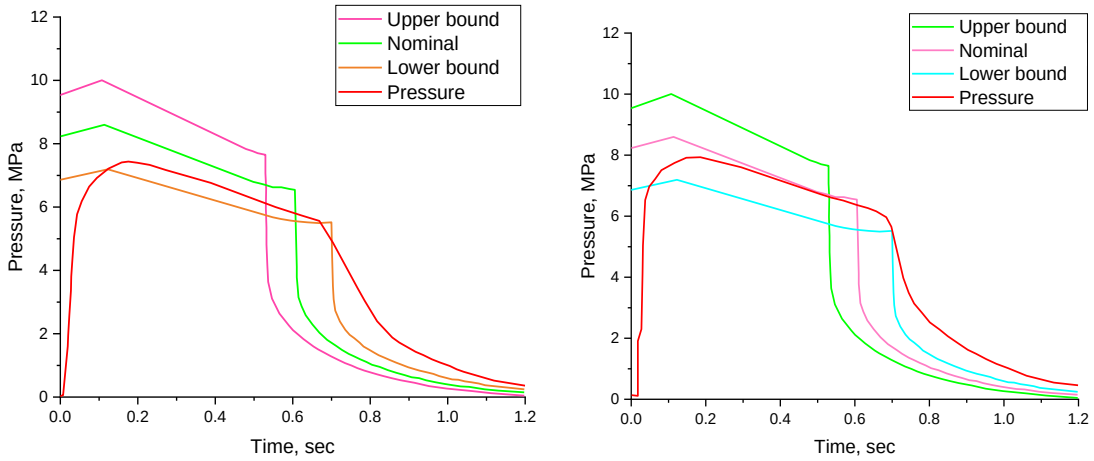

(a) Pressure vs time plot for Sl. no 04 **(b)** Pressure vs time plot for Sl.no 05

Figure 7.3. Pressure vs time plot after 12 ISAT-B cycles.

The ballistic parameters obtained from the test results are given in Table 7.4.

Table 7.4 Ballistic Parameters corresponding to 12 ISAT (B) cycles.

Ballistic parameters	Specs	Sl. No 4	Sl. No 5
Ignition Delay, msec	<100 msec	20	12.4
Web burn time, msec	610 ± 100 msec	609	662.6
Action time, sec	<1.10	1.028	1.042
Pmax, MPa	7.2 to 10.3	7.4	7.82

7.8.2 Static firing after second withdrawal (24 ISAT-B cycles)

After the withdrawal of 2 nos., the ISAT test is continued with the remaining 8 SRMs. Thereafter the completion of 24 ISAT-B cycles, 2 nos. are withdrawn and then static fired. The pressure vs time graph is plotted and shown in Figure 7.5.

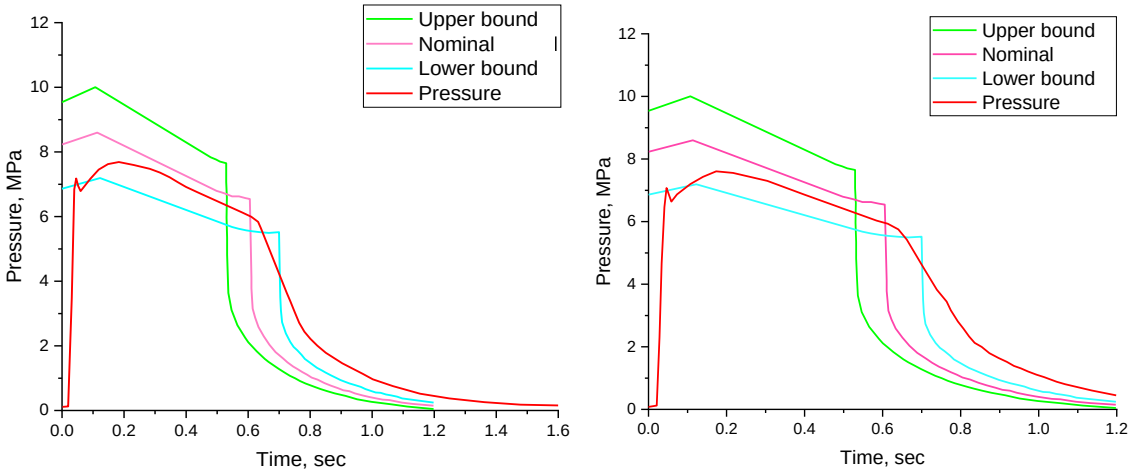

(a) Pressure vs time plot for Sl. no 06 **(b)** Pressure vs time plot for Sl.no 07

Figure 7.4. Pressure vs time for both SRM after 24 ISAT-B cycles.

The ballistic parameters obtained from the static test after 24 ISAT cycles are given in Table 7.5.

Table 7.5 Ballistic Parameters corresponding to 24 ISAT (B) cycles.

Ballistic parameters	Specs	Test-6	Test-7
Ignition Delay, msec	<100 msec	17.2	12.6
Web burn time, msec	610 ± 100 msec	598	647
Action time, sec	<1.10	0.991	1.034
Pmax, MPa	7.2 to 10.3	8.0	8.0

7.8.3 Static firing after third withdrawal (36 ISAT-B cycles)

2 no. SRMs are withdrawn after the completion of 36 ISAT-B cycles. The pressure vs time graph is shown in Figure 7.6.

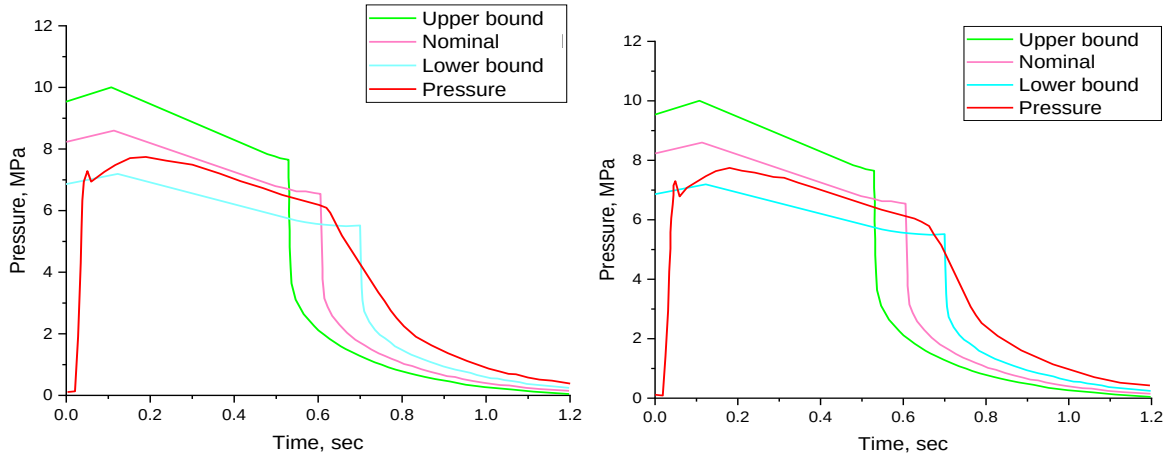

(a) Pressure vs time plot for Sl. no 08 **(b)** Pressure vs time plot for Sl.no 09

Figure 7.5. Pressure vs time for both SRM after 36 ISAT-B cycles.

The ballistic parameters obtained from the test are given in Table 7.6.

Table 7.6 Ballistic Parameters corresponding to 36 ISAT (B) cycles.

Ballistic parameters	Specs	Test-8	Test-9
Ignition Delay, msec	<100 msec	14.9	19.3
Web burn time, msec	610 ± 100 msec	636	685
Action time, sec	<1.10	1.039	1.037
Pmax, MPa	7.2 to 10.3	7.98	7.93

7.8.4 Static firing after fourth withdrawal (48 ISAT-B cycles)

Another 2 SRMs are withdrawn after the completion of 48 ISAT-B cycles. The pressure vs time graph is shown in Figure 7.7.

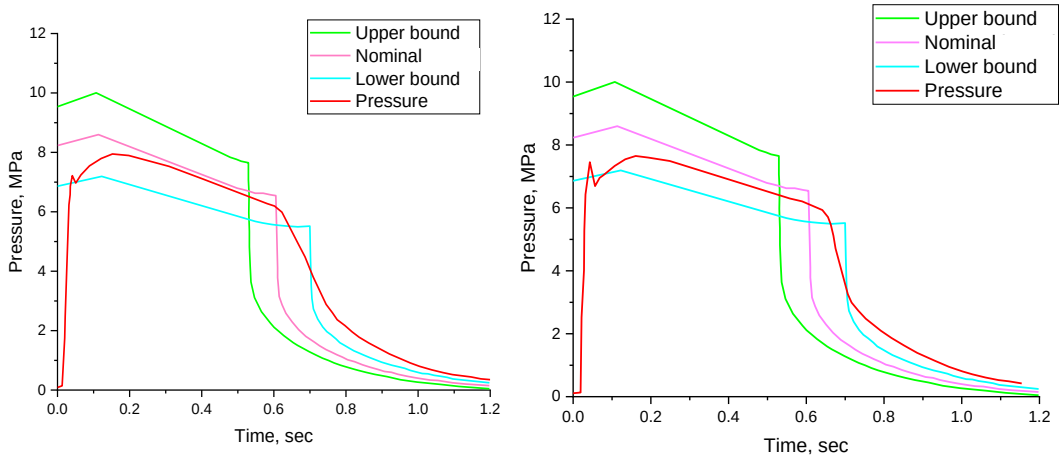

(a) Pressure vs time plot for Sl. no 10 **(b)** Pressure vs time plot for Sl.no 11

Figure 7.6. Pressure vs time for both SRM after 48 ISAT-B cycles.

The ballistic parameters obtained from the test results are given in Table 7.7

Table 7.7 Ballistic Parameters corresponding to 48 ISAT (B) cycles.

Ballistic parameters	Specs	Test-10	Test-11
Ignition Delay, msec	<100 msec	18.1	21.2
Web burn time, msec	610 ± 100 msec	612.4	642.4
Action time, sec	<1.10	1.081	1.105
Pmax, MPa	7.2 to 10.3	7.62	7.58

7.8.5 Static Firing after fifth withdrawal (60 ISAT-B cycles): -

Another 2 SRM s are withdrawn after the completion of 60 ISAT-B cycles. RT of SRM is shown in Figure 7.7. The pressure vs time graph is plotted for both SRMs as shown in Figure 7.8.

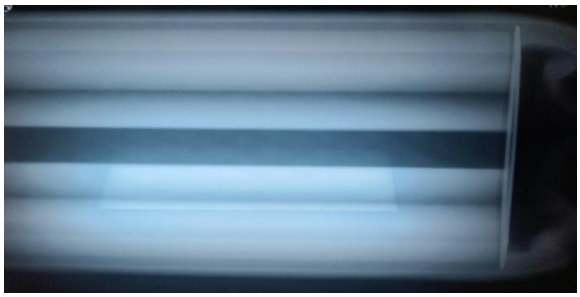

Figure 7.7. RT of SRM with Composite Case (after 60 ISAT B Cycles)

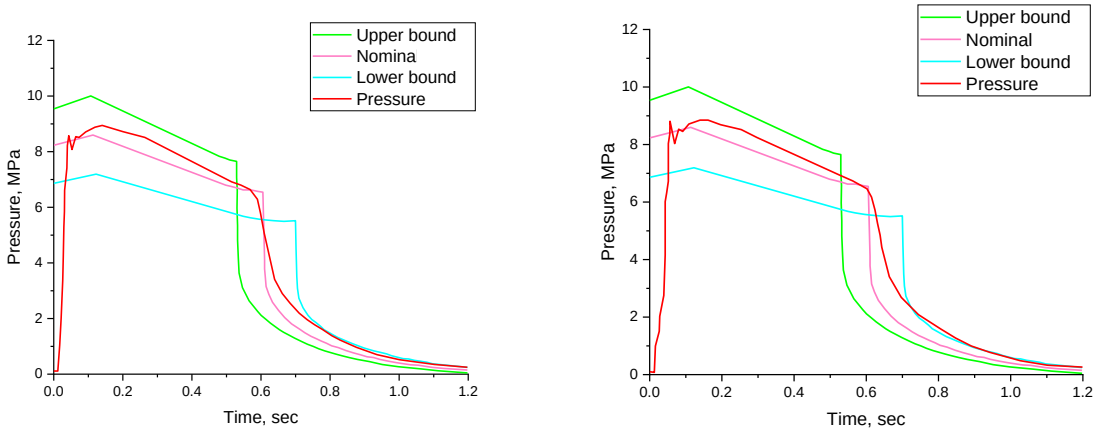

(a) Pressure vs time plot for Sl. no 12 **(b)** Pressure vs time plot for Sl.no 13

Figure 7.8. Pressure vs time for both SRM after 60 ISAT-B cycles

The ballistic parameters obtained from the test results are given in Table 7.8 Post static test, SRM is radiographed (Figure 7.9) and demonstrates complete structural integrity.

Table 7.8 Ballistic Parameters corresponding to 60 ISAT (B) cycles.

Ballistic parameters	Specs	Test-12	Test-13
Ignition Delay, msec	<100 msec	19.8	20.5
Web burn time, msec	610 ± 100 msec	635.8	612.3
Action time, sec	<1.10	1.098	1.098
Pmax, MPa	7.2 to 10.3	7.67	7.71

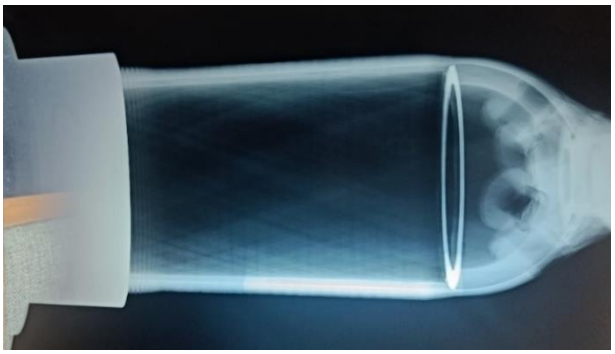

Figure 7.9. Post Static Test RT (after 60 ISAT-B cycles).

7.9 Effect of Natural Ageing

The results of acceleration tests are also validated with the results of a 10-year-old naturally aged SRM. The SRM is stored in a Magazine with air conditioning, limiting the ambient temperature to a maximum of 30˚C, as most of the total life of missile systems is under a controlled environment with temperatures not exceeding 30˚C. The silica gel bags are placed within the packing box for the absorption of moisture. The HE flange is protected with suitable painting for corrosion protection are inspected periodically for any possible corrosion. The radiographs of an SRM with a composite case with 10 years of life and the corresponding static test results are shown in Figures 7.10 and 7.11, respectively. The results are found to be comparable with the radiographs of SRMs after 60 ISAT-B trials and life up to a period of 10 years is validated.

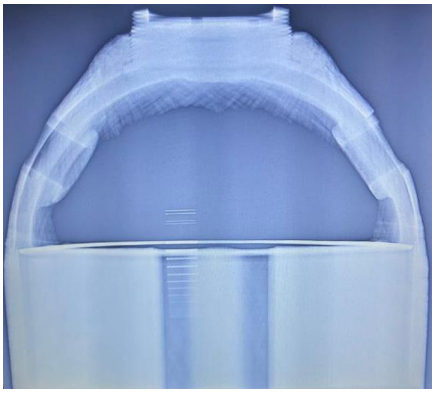

(a) (b)

Figure 7.10 Radiographs of an SRM with Composite Case with 10 years of Service Life a) at Cylinder Region and b) at HE Dome.

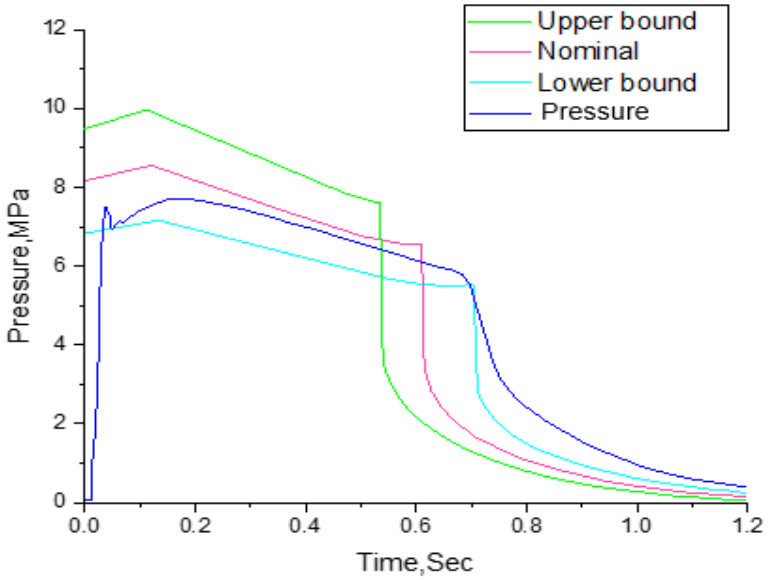

Figure 7.11. Pressure vs time plot of an SRM under Natural Ageing for 10 years.

7.10 Summary

Since no development program has a sufficient duration of time to test the product over the expected life period, a systematic test plan is evolved to validate the service life for a period of 10 years. This is essential to generate long-term data on storage life and life assessment. The salient findings are summarised below:

- The ISAT trials consist of both temperature and humidity variation and validate the performance for a cumulative period of 10 years. The tests are carried out after every 12 ISAT cycles simulating a life of about 2 years, and test is performed up to 60 no. of cycles corresponding to 10 years of service life.
- The SRMs after ISAT exposures of 24, 36, 48 and 60 ISAT cycles, reveal an initial kink in the pressure-time curve, however, the rise is within the design bounds and indicates a sudden rise in propellant burn surface area. The composite case sustains the required pressure and post-test RT indicates that all critical interfaces are structurally safe except for minor degradation at resin-bonded interfaces.
- The ISAT results are compared with the static test data of a 10-year-old naturally aged SRM with the composite case. The results are in line with the static test results (after 60 ISAT cycles).
- Accelerated ageing provides an early indication of the weakest link in the chain for the said period. The pressure versus time data is plotted and found to be comparable with the ballistic performance of a virgin SRM (without any ISAT exposures) and found to be well within the design bounds.

CHAPTER 8

SUMMARY AND CONCLUSIONS

The present research work is carried out to study the life of filament wound composites for aerospace applications. To complete this development, various studies are conceptualised, and the research objectives are formulated in three phases:

Phase 1

- Testing and evaluation of C/E and G/E composites
- Evaluation of drop in mechanical properties at maximum expected service temperature

Phase 2

- Study of dynamic behaviour and structural integrity assessment of a flight-worthy C/E CRMC through a pressure test
- Periodic Structural integrity assessment and performance evaluation of C/E CRMC for a service life of 5 and 10 years respectively under natural ageing

Phase 3 (an integrated study at the sub-system level)

- Environmental studies on an SRM with G/E composite case
- Accelerated ageing studies on SRM with G/E composite case

The salient outcomes of the phase-wise study have been presented below:

Phase 1

To conduct comprehensive experimental studies, C/E and G/E composite is synthesised using the FW process and tested to evaluate the characteristic and properties of starting raw materials. The characterisation studies are carried out for individual constituents i.e., for fibre and resin systems followed by an evaluation of physical properties and curing characteristics of cured composites. The cured composite specimen is tested for various major mechanical properties such as longitudinal and transverse modulus, In-plane shear modulus, poisons ratio, longitudinal tensile and compressive strength, transverse tensile and compressive strength, In-plane shear strength, ILSS and Flexural strength.

Two different C/E material systems are studied,

- T-700/ LY556 and HY5200 Epoxy Resin system
- T-700/ Epo1555 and FH5200 Epoxy Resin System

- T_g is tested using DSC and TMA methods and shows consistent and comparable results.
- The average longitudinal tensile strength obtained is 1585 and 2267 MPa for LY556/HY5200 and Epo1555/FH5200 epoxy resin systems, respectively. The filament winding (with 0° fibre orientation) on a flat surface or curved surface yields similar results.
- The average ILSS obtained is 50 and 60 MPa for LY556/HY5200 and Epo1555/FH5200 epoxy resin system, respectively. The average flexural strength obtained is 916 and 1307 MPa for LY556/HY5200 and Epo1555/FH5200 epoxy resin systems, respectively.
- The consolidated material properties are given in Table 3.29 and Table 3.30 for LY556/HY5200 and Epo1555/FH5200 epoxy resin systems, respectively. Both the resin system shows a similar trend in physical and mechanical properties. The properties are consistent and repetitive and in line with design properties. The results show a very small batch-to-batch variation.
- Epo1555 and FH 5200 epoxy resin system (with 4.2% elongation) demonstrates superior properties and shall yield a higher performance factor for composite casing application. This shows that matrix and interface characteristics dominate the final properties and yield higher results.
- C/E samples are exposed to maximum expected service temperature and drop in tensile, hoop tensile, ILSS and flexural properties are estimated.
- The maximum drop observed in longitudinal tensile strength at 125°C is 15.8% and 16% at for LY556/HY5200 and Epo1555/FH5200 epoxy resin system, respectively. The maximum

drop in hoop tensile strength at 125°C is 16.3% and 15.9% for LY556/HY5200 and Epo1555/FH5200 epoxy resin systems, respectively. The drop in property is following a similar trend in the case of both flat tensile and hoop tensile ring specimens.

- The maximum drop at 125°C in ILSS is 23.2% and 20.1% for LY556/HY5200 and Epo 1555/FH5200 epoxy resin system, respectively. The maximum drop at 125°C in Flexural strength is 24.8% and 28.8% for LY556/HY5200 and Epo1555/FH5200 epoxy resin system, respectively.
- The maximum drop in ILSS and Flexural properties are more sensitive at HTs (varying between 20-28 % at 125°C) vis-à-vis the tensile properties due to shear forces, bending and delamination.
- It is observed that near higher temp (close to T_g) the drop in mechanical properties is more sensitive and the drop increases with temperature and soaking time.

Phase 2

The product level studies (casing level) are performed on a C/E CRMC with Epo1555/FH 5200 resin system.

- The motor case is manufactured using the accepted and cleared batch of raw materials and with established procedures.
- FMEA studies are carried out to explore the probable and critical failure modes on a typical CRMC and it is observed that the main casing shell and polar boss failures are the most critical and frequently occurring failure modes.
- To assess the structural integrity and dynamic behaviours, the CRMC is pressure tested and AE, strain and dilation is monitored. The overall structural integrity of the CRMC is seen to be satisfied within the pressure range of 6.5 MPa (MEOP). A Felicity ratio of 0.962 is observed during AE monitoring indicating the overall soundness of the structures. The Re-pressurization cycle is also almost void of any significant emissions indicating the absence of any critical active defects The few isolated AE activities observed during hold periods and at higher pressure, are studied in-depth and it is noticed that activities are having amplitude close to 90 - 98dB, low duration, low energy, marginal hit and count rates.
- The maximum strain observed is 8695 μs at the cylinder region and the corresponding dilation is 3.9 mm.
- The zones with isolated AE activities are identified and referred to UT/RT indicating the presence of resin lean area, minor delamination, and matrix cracking near the polar boss

region. The UT results are within 6 dB gain across the entire structure except for a few isolated locations.

- The AE signatures, UT/RT and strain/dilation measurement indicate the soundness of the composite casing. The CRMC is found to be structurally integral for the said MEOP. The AET, NDT and strain dilation measurement enables a comprehensive structural integrity assessment of CRMC.
- To validate the performance of the CRMC under natural ageing, the casing is left for natural curing and re-tested after a period of 5 years. The AE monitoring shows the absence of any critical and significant activities, parameters such as total no. of hits, amplitude, duration and rise time are comparable with first-time test data. The maximum strain was 7958 µs and the results show an overall increasing trend across the structures except for a few locations. The maximum dilation reported is 4.10 mm at the cylinder location. The post-test RT indicates minor delamination in the polar boss region similar to first-time radiographs. The UT results show a marginal increase in dB level at a few locations and overall, the structural response was well within 6 dB gain except for 10 dB gain at one location (near NE Y joint region). The strain and dilations, AE and post-test NDT observations are compared with the test results of virgin CRMC and do not indicate any major deterioration with time and reflect the overall soundness of the structures.
- As the missile structure demands a service life of a minimum of 10 years, a CRMC of the same configuration (as above) is identified, manufactured 10 years ago using the same approved procedure and kept under natural ageing. The article is pressure tested, and AE, strain and dilation is measured. The AE parameters are comparable with the test results of virgin and 5 years old articles. The maximum strain recorded was 8715 µs and the dilation reported was 3.98 mm at the cylinder region. The RT indicates minor delamination at the polar boss region and is free from any major delamination, crack, or de-bond. UT results are within 12 dB across the structures. The results do not show any significant deterioration with time.
- From the three pressure test data, strain and dilation observed are comparable and demonstrate adequate FoS. The strain and dilation results indicate an overall increasing trend with time (as expected) however the increase is not that significant. The result shows overall sound structural health and validates the storage and service life of C/E CRMC for a period of 10 years.

Phase 3

SRMs with G/E composite cases are exposed to a rigorous performance evaluation program encompassing various missile system service situations. The SRM is subjected to RT for structural integrity evaluation after each exposure. The static firing is carried out in a phased manner after every exposure. The following are the salient findings and inferences from this research study:

- In HT and LT soak tests, SRM with the composite case is soaked at maximum and minimum expected service temperature and test fired. The article is also tested for low-frequency transport vibration and random vibration varying between 20-2000 Hz and static fired. The article is tested for a maximum of 17 g acceleration environment for about 60 sec and shock of 45 g. The results show that dynamic environments of vibration, acceleration and shock do not affect the structural integrity of grain, interfaces, and composite cases.
- The effect of HT and LT soak tests on ballistic performance is not that predominant, however, the effects of HT and LT functional tests are as predicted. The peak pressure obtained in HT functional test is 8.3 MPa and the burn duration is 0.48 sec. The peak pressure obtained in LT functional test is 7 MPa and the burn duration is 0.56 sec.
- The results show that the peak pressure is varying between 7 - 8.3 MPa and the burn duration is varying between 0.48 - 0.6 sec across all the tests.
- All the SRM with composite cases, sustained all the environmental and operational conditions, including acceleration, shocks, transport and flight vibration, temperature extremes and tropical exposures. All the composite cases worked admirably and exhibited their capacity to endure pressure and temperature loads throughout the combustion process. The results are within the predicted performance bounds and closely comparable with the results of virgin SRM (without any exposures). The low dispersion behaviour during all the static firing displayed the repeatability and reliability of the SRM performance along with the composite case. The above study demonstrates the safe life of SRM with G/E case for the said operational environments.
- SRM with G/E composite case is subjected to ISAT-B accelerated ageing test. The samples are withdrawn after 12, 24, 36, 48 and 60 cycles (corresponds to a life of 2, 4, 6, 8 and 10 years) and static fired. The burn duration is around 610 msec and the peak pressure obtained is between varying between 7 - 8 MPa. The RT results of SRM with composite case after 24, 36, 48 and 60 cycles show minor degradation in interface properties and minor de-bond is seen at the throat region.

- To further validate the results of artificial accelerated ageing studies with natural ageing, a 10-year-old and naturally aged in-service SRM with G/E composite case is static tested. The Radiographs indicate minor degradation at bonded interfaces; however, the static test performance was within the design bound and post firing the casing is structurally integrated as seen in the post-test radiographs Figure.7.10.
- The pressure vs time plots are repetitive and are within close bounds across all the tests. Based on the test results of static firing up to 60 ISAT cycles, a life of ten years is assessed for the SRM with G/E composite case.
- The above life validation program effectively combines the effect of time, temperature and humidity and the life of CRMC evaluated with this experimental methodology is suitable for aerospace application.

CHAPTER 9

FUTURE SCOPE OF WORK

The present research work can be extended for future scope of studies under the following broad framework:

- Suitable burst pressure prediction model along with necessary experimental validation for CRMC.
- NDT acceptance criteria for C/E and G/E filament wound composites.
- NDT characterisation for defect prognosis and generation of a suitable mathematical model.
- Continuation of ISAT trials to estimate the final service life of filament wound composites.
- Characterisation of carbon epoxy tow-preg (dry winding) and service life estimation at the product level.
- The design, process and defect aspects and their growth with time in composite dictate the failures. The design parameters are to be suitably validated with extensive specimen-level characterisation and with studies performed at subscale/prototypes. The filament winding process parameters are to be optimised for an optimal solution with experimental validation.

PUBLICATIONS

Technical papers

SCI

1. Srivastava, L., Krishnanand, L., Kishore Nath, N., & Laxman, D. (2022). Experimental Performance Evaluation of Small Solid Rocket Motor with Composite Case for Environmental Conditions. Defence Science Journal, 72(3), 485–494. https://doi.org/10.14429/dsj.72.17863

2. Srivastava, L., Krishnanand, L., Nath, N.K. et al. Effect of Blast Load on Dynamic Deflection Responses of Internally Damaged Carbon–Epoxy Laminated Composite Shallow Shell Panel using Experimental Properties. Trans Indian Inst Met (2022). https://doi.org/10.1007/s12666-022-02698-z

Scopus

3. Srivastava, L., Krishnanand, L., Kishore Nath, N., Hirwani, C. K., & Babu, M. R. M. (2022). Online structural integrity monitoring of high-performance composite rocket motor casing. Materials Today: Proceedings, 56, 1001–1009. https://doi.org/10.1016/j.matpr.2022.03.230

4. Srivastava, L., Krishnanand, L., Behera, S., & Kishore Nath, N. (2022). Failure mode effect analysis for a better functional composite rocket motor casing. Materials Today: Proceedings, 62, 4445–4454. https://doi.org/10.1016/j.matpr.2022.04.933

REFERENCES

1. Tajmar, M., & Bertolami, O. (2005). Hypothetical Gravity Control and Possible Influence on Space Propulsion. *Journal of Propulsion and Power*, *21*(4), 692–696. https://doi.org/10.2514/1.15240.
2. Sauvageau, D., & Allen, B. (1998, July 13). Launch vehicle historical reliability. *34th AIAA/ASME/SAE/ASEE Joint Propulsion Conference and Exhibit*. https://doi.org/10.2514/6.1998-3979.
3. Russell, D., Blacklock, K., & Langhenry, M. (1988, July 11). Failure mode and effects analysis (FMEA) for the Space Shuttle solid rocket motor. *24th Joint Propulsion Conference*. https://doi.org/10.2514/6.1988-3420.
4. Jenab, K., & Pineau, J. (2015). Failure mode and effect analysis on safety critical components of space travel. *Management Science Letters*, *5*(7), 669–678. https://doi.org/10.5267/j.msl.2015.5.006.
5. Peters, S T, Humphrey, W D, Foral, R F, Westinghouse Electric Corp., Marine Div., Sunnyvale, CA, & Brunswick Corp., Defence Div., Lincoln, NE).1991. *Filament winding - Composite structure fabrication. United States.*
6. Behera, S., Sahoo, S. K., Srivastava, L., & Srinivasa Gopal, A. S. (2019). Structural Integrity Assessment of Filament Wound Composite Pressure Vessel Using Through Transmission Technique. *Procedia Structural Integrity*, *14*, 112–118. https://doi.org/10.1016/j.prostr.2019.05.015.
7. Betti, F. (2007, July 8). Design and Development of Vega Solid Rocket Motors Composite Cases. *43rd AIAA/ASME/SAE/ASEE Joint Propulsion Conference & Exhibit*. https://doi.org/10.2514/6.2007-5810.
8. Sojourner, T., Richardson, D. E., Allen, B. D., Hyde, S., McHenry, S., Goldberg, B., Devries, D., & Ewing, M. (2015, July 27). Solid Rocket Motor Reliability and Historical Failure Modes Review. *51st AIAA/SAE/ASEE Joint Propulsion Conference*. https://doi.org/10.2514/6.2015-3873.
9. Suksila, T. (2018). Experimental investigation of solid rocket motors for small sounding rockets. *IOP Conference Series: Materials Science and Engineering*, *297*, 012009. https://doi.org/10.1088/1757-899X/297/1/012009.
10. Sutton, G.P. and Biblarz, O. (2001) *Rocket Propulsion Elements*. 7th Edition, John Wiley, Hoboken.

11. Biagi, M., Mauries, A., Perugini, P., & Pin, B. (2011, July 31). Structural Qualification of P80 Solid Rocket Motor Composite Case. *47th AIAA/ASME/SAE/ASEE Joint Propulsion Conference & Exhibit*. https://doi.org/10.2514/6.2011-5958
12. Allaer, K., de Baere, I., Lava, P., van Paepegem, W., & Degrieck, J. (2014). On the in-plane mechanical properties of stainless-steel fibre-reinforced ductile composites. *Composites Science and Technology*, https://doi.org/10.1016/j.compscitech.2014.05.009.
13. NASA/SP-8040, *Fracture Control of Metallic Pressure Vessels*, Nasa Space Vehicle Design Criteria (Structures) (May 1970).
14. NASA/SP-8025, *Guidelines and Practices for Design of Solid Rocket Motor Cases*. NASA Handbook (1970).
15. *Properties and Selection: Irons, Steels, and High-Performance Alloys*. (1990). ASM International. https://doi.org/10.31399/asm.hb.v01.9781627081610.
16. Kaw, A. K. (2005). *Mechanics of Composite Materials*. CRC Press. https://doi.org/10.1201/9781420058291.
17. Madhavi, M., Rao, K. V. J., & Rao, K. N. (2009). Design and Analysis of Filament Wound Composite Pressure Vessel with Integrated-end Domes. In *Defence Science Journal* (Vol. 59, Issue 1).
18. Azeem, M., Ya, H. H., Alam, M. A., Kumar, M., Stabla, P., Smolnicki, M., Gemi, L., Khan, R., Ahmed, T., Ma, Q., Sadique, M. R., Mokhtar, A. A., & Mustapha, M. (2022). Application of Filament Winding Technology in Composite Pressure Vessels and Challenges: A Review. *Journal of Energy Storage*, *49*, 103468. https://doi.org/10.1016/j.est.2021.103468.
19. Ramanjaneyulu, V., Balakrishna Murthy, V., Chandra Mohan, R., & Naga Raju, Ch. (2018). Analysis of Composite Rocket Motor Case using Finite Element Method. *Materials Today: Proceedings*, *5*(2), 4920–4929. https://doi.org/10.1016/j.matpr.2017.12.069.
20. Zu, L., Koussios, S., & Beukers, A. (2011). Integral Design for Filament-Wound Composite Pressure Vessels. *Polymers and Polymer Composites*, *19*(4–5), 413–420. https://doi.org/10.1177/0967391111019004-525.
21. Mertiny, P., & Ellyin, F. (2002). Influence of the filament winding tension on physical and mechanical properties of reinforced composites. *Composites Part A: Applied Science and Manufacturing*, *33*(12), 1615–1622. https://doi.org/10.1016/S1359-835X(02)00209-9.

22. Cohen, D. (1997). Influence of filament winding parameters on composite vessel quality and strength. *Composites Part A: Applied Science and Manufacturing*, *28*(12), 1035–1047. https://doi.org/10.1016/S1359-835X(97)00073-0.
23. Dash, A. P., Velmurugan, R., & Prasad, M. S. R. (2019). Effect of Helical Winding Angle on External Pressure based Buckling of Partially Filled Thin Composite Cylindrical Shells. *Defence Science Journal*, *69*(4), 313–319. https://doi.org/10.14429/dsj.69.12634.
24. Parhi, P. K., Bhattacharyya, S. K., & Sinha, p. K. (2001). Hygrothermal effects on the dynamic behaviour of multiple delaminated composite plates and shells. *Journal of Sound and Vibration*, *248*(2), 195–214. https://doi.org/10.1006/jsvi.2000.3506.
25. Hugh, L. McManus, Kessler, Seth., Raghavan, Ajay., Design, Metis., Hyer, Michael., Case, Scott., and Cain, Jason. (November 2009). *Service Life Assessment Methodology for Composites (SLAM-C): Models, implementation, and experimental calibration.* Fibre Reinforced Polymer (FRP) Composites for Infrastructure Applications Conference, San Francisco, CA.
26. Onder, A., Sayman, O., Dogan, T., & Tarakcioglu, N. (2009). Burst failure load of composite pressure vessels. *Composite Structures*, *89*(1), 159–166. https://doi.org/10.1016/j.compstruct.2008.06.021.
27. Hizli, H. (2019). Effects of environmental factors on performance of composite rocket motor cases. *AIAA Scitech 2019 Forum*. https://doi.org/10.2514/6.2019-0518.
28. T., S., & Lokavarapu, B. R. (2021). Strength degradation of glass epoxy composites under hygrothermal environment. *Materials Today: Proceedings*, *38*, 2845–2852. https://doi.org/10.1016/j.matpr.2020.08.778.
29. Idrisi, A. H., Ismail Mourad, A.-H., Abdel-Magid, B., Mozumder, M., & Afifi, Y. (2019, July 14). Impact of the Harsh Environment on E-Glass Epoxy Composite. *Volume 6A: Materials and Fabrication*. https://doi.org/10.1115/PVP2019-93858.
30. Idrisi, A. H., Mourad, A.-H. I., Abdel-Magid, B. M., & Shivamurty, B. (2021). Investigation on the Durability of E-Glass/Epoxy Composite Exposed to Seawater at Elevated Temperature. *Polymers*, *13*(13), 2182. https://doi.org/10.3390/polym13132182.
31. Bert, C. W., & Hyler, W. S. (1967). Design considerations in material selection for rocket-motor cases. *Journal of Spacecraft and Rockets*, *4*(6), 705–715. https://doi.org/10.2514/3.28940.

32. Alberto, M. (2013). Introduction of Fibre-Reinforced Polymers − Polymers and Composites: Concepts, Properties and Processes. In *Fibre Reinforced Polymers - The Technology Applied for Concrete Repair*. In Tech. https://doi.org/10.5772/54629.
33. Beaumont, P. W. R. (2017). Slow Cracking in Composite Materials: Catastrophic Fracture of Composite Structures. In *The Structural Integrity of Carbon Fibre Composites* (pp. 489–528). Springer International Publishing. https://doi.org/10.1007/978-3-319-46120-5_18.
34. Musthak, Md., Madar. Valli, P., Narayana Rao, S., & Madhavi, M. (2017). Prediction of Structural Behaviour of FRP Pressure Vessel by Using Shear Deformation Theories. *Materials Today: Proceedings*, *4*(2), 872–882. https://doi.org/10.1016/j.matpr.2017.01.098.
35. Park, J.-S., Kim, C.-U., Kang, H.-K., Hong, C.-S., & Kim, C.-G. (n.d.). *Structural Analysis and Strain Monitoring of the Filament Wound Motor Case*. https://doi.org/10.1106/002199802027870.
36. Bunsell, A. R., Barbier, F., Thionnet, A., Zejli, H., & Besanc¸on, B. (2010). Damage Accumulation and Lifetime Prediction of Carbon Fiber Composite Pressure Vessels. *ASME 2010 Pressure Vessels and Piping Conference: Volume 6, Parts A and B*, 303–310. https://doi.org/10.1115/PVP2010-25978.
37. Ibrahim, M. E. (2016). Non-destructive testing and structural health monitoring of marine composite structures. *Marine Applications of Advanced Fibre-Reinforced Composites*, 147–183. https://doi.org/10.1016/B978-1-78242-250-1.00007-7.
38. Huang, J. Q. (2013). Non-destructive evaluation (NDE) of composites: Acoustic emission (AE). *Non-Destructive Evaluation (NDE) of Polymer Matrix Composites: Techniques and Applications*, 12–32. https://doi.org/10.1533/9780857093554.1.12.
39. Waller, J. M., Andrade, E., Saulsberry, R. L., Thompson, D. O., & Chimenti, D. E. (2010). Use of Acoustic Emission to Monitor Progressive Damage Accumulation in Kevlar®49 Composites. *AIP Conference Proceedings 1211*, 1111-1118. https://doi.org/10.1063/1.3362168.
40. Chou, H. Y., Mouritz, A. P., Bannister, M. K., & Bunsell, A. R. (2015). Acoustic emission analysis of composite pressure vessels under constant and cyclic pressure. *Composites Part A: Applied Science and Manufacturing*, *70*, 111–120. https://doi.org/10.1016/j.compositesa.2014.11.027.
41. Chou, H.Y. (2011). *Damage Analysis of Composite Pressure Vessels Using Acoustic Emission Monitoring*. PhD. Thesis, School of Aerospace, Mechanical &

Manufacturing Engineering College of Science, Engineering and Health, RMIT University.

42. Mane, N., Mohanananthanarayanan, K., Jain, S., & Mishra, A. (2017). Acoustic emission monitoring during proof pressure testing of a solid rocket motor of high strength high alloy (HSHA) steel. *Indian National Seminar & Exhibition on Non-Destructive Evaluation NDE 2016*, Dec, Thiruvananthapuram. 22(6). https://www.ndt.net/?id=21195.
43. Weathers, D. E., Nichols, C. T., Waller, J. M., & Saulsberry, R. L. (2010). *Automated Determination of Felicity Ratio for Composite Overwrapped Pressure Vessels*. NASA Technical Report. https://doi.org/10.13140/RG.2.1.5150.1609.
44. Willemse, B., Angelone, M., Drevet, O., Serraglia, F., & Vita, G. (2007, July 8). An Overview of the Development of the VEGA Solid Rocket Motor Igniters. *43rd AIAA/ASME/SAE/ASEE Joint Propulsion Conference & Exhibit*. https://doi.org/10.2514/6.2007-5813.
45. Brauers, B., Angelone, M., Goorden, B., Gautronneau, E., & di Vita, G. (2009, August 2). Qualification and Production of the VEGA SRM Igniters. *45th AIAA/ASME/SAE/ASEE Joint Propulsion Conference & Exhibit*. https://doi.org/10.2514/6.2009-5322.
46. Tam, W. H.; Griffin, P. S. & Jackson, A. C. (2002). Design and manufacturing of a Composite Overwrapped Pressurant Tank Assembly, *38th AIAA/ASME/SAE/ASEE Joint Propulsion Conference & Exhibit, 2002*, 7-10 July, https:// doi.org/10/2514/6.2002-4349.
47. Siddani, Kumar Jush., Srinivas, C., Naik, L. Srinivas., & Chandra Sekar, T. (2018). Design and Experimental Validation of Composite Pressure Vessel. *International Journal of Engineering Science Invention*, Vol 7, Issue 4, PP 15-19, April www.ijesi.org||Volumewww.ijesi.org.
48. Maxwell, Antony & Broughton, W. & Dean, G & Sims, Graham. (2005). *Review of Accelerated Ageing Methods and Lifetime Prediction Techniques for Polymeric Materials*. National Physical Laboratory. Report number: NPL Report DEPC MPR 016.
49. Singh, S. B., Sivasubramanian, M. V. R., & Chawla, H. (Eds.). (2021). *Emerging Trends of Advanced Composite Materials in Structural Applications*. Springer Singapore. https://doi.org/10.1007/978-981-16-1688-4.

50. Schwartz, M M. (1997). *Composite materials. Volume 1: Properties, non-destructive testing, and repair*. United States.
51. Rao, R. M. V. G. K., Balasubramanian, N., & Chanda, M. (1984). Factors Affecting Moisture Absorption in Polymer Composites Part I: Influence of Internal Factors. *Journal of Reinforced Plastics and Composites*, 3(3), 232–245. https://doi.org/10.1177/073168448400300304.
52. Odegard, G. M., & Bandyopadhyay, A. (2011). Physical ageing of epoxy polymers and their composites. *Journal of Polymer Science Part B: Polymer Physics*, 49 (24), 1695–1716. https://doi.org/10.1002/polb.22384.
53. Chamis, C.C. and Sinclair, J. H. (1982). *Durability/Life of Fibre Composites in Hygro-thermo-mechanical Environments, Composite Materials, Testing and Design*, I. M. Daniel, I. M. (Ed). American Society for Testing and Materials, Philadelphia, PP. 498–512.
54. Davison, S. P. (2003). *Enviro-Mechanical Durability of Graphite/Epoxy Composite Materials. Blacksburg*, PhD Dissertation, Virginia Polytechnic Institute and State University, Virginia.
55. Shen, C.-H., & Springer, G. S. (1977). Effects of Moisture and Temperature on the Tensile Strength of Composite Materials. *Journal of Composite Materials*, *11*(1), 2–16. https://doi.org/10.1177/002199837701100102.
56. Asp, L. E. (1998). The effects of moisture and temperature on the interlaminar delamination toughness of a carbon/epoxy composite. *Composites Science and Technology*, *58*(6), 967–977. https://doi.org/10.1016/S0266-3538(97)00222-4.
57. Sethi, S. *Environmental Degradation Study of FRP Composites Through Evaluation of Mechanical Properties*. PhD Thesis. Department of Metallurgical and Materials Engineering, National Institute of Technology, Rourkela.
58. Singh, S. (2010). *Strength Degradation of Glass Fibre Reinforced Polymer Sandwich Composites Under Hygrothermal Loading Conditions*, Master's Thesis, Department of Mechanical Engineering Thapar University.
59. Li, M. (2000). *Temperature and moisture effects on composite materials for wind turbine blades*. PhD Thesis, Montana State University.
60. Patel, S. (2002). Durability of hygrothermally aged graphite/epoxy woven composite under combined hygrothermal conditions. *International Journal of Fatigue*, 24 (12), 1295–1301. https://doi.org/10.1016/S0142-1123(02)00044-0.

61. Porters, R. T., (1981). *Environmental effects on defect growth in composite materials*, NASA Technical Report.
62. Chawla, A. Sneha., (2009). *Characterization and Modelling of The Effect of Environmental Degradation on Flexural Strength of Carbon/Epoxy Composites*, MS Thesis, Department of Aerospace Engineering and Mechanics in the Graduate School of The University of Alabama.
63. Gates, T., & Grayson, M. (1999). On the use of accelerated ageing methods for screening high-temperature polymeric composite materials. *40th Structures, Structural Dynamics, and Materials Conference and Exhibit*. https://doi.org/10.2514/6.1999-1296.
64. Blikstad, M., Sjöblom, P. O. W., & Johannesson, T. R. (1984). Long-Term Moisture Absorption in Graphite/Epoxy Angle-Ply Laminates. *Journal of Composite Materials*, 18(1), 32–46. https://doi.org/10.1177/002199838401800103.
65. Reilly, S. P., Faull, K. and Thomason, J. L. (2012). The effect of ageing on the mechanical properties of carbon fibre reinforced epoxy. *ECCM15 – 15th European Conference on Composite Materials*, Venice, Italy.
66. Angrizani, C. C., Freitas, B., Oliveira, D. E., & Amico, S. C. (2015). Evaluation of the Durability Performance of Glass-Fibre Reinforcement Epoxy Composites Exposed to Accelerated Hygrothermal Ageing. *Journal of Materials Science and Engineering with Advanced Technology* (Vol. 11, Issue 2).
67. Karbhari, V. M., & Padmavathi, S. (2006). *Hygrothermal Effects on Durability and Moisture Kinetics of Fibre-reinforced Polymer Composites*. Structural Systems Research Project Report No. SSRP-06/15. Department of Structural Engineering University of California, San Diego, California.
68. Jang, J. H., Hong, S. bin, Kim, J. G., Goo, N. S., & Yu, W. R. (2021). Accelerated testing method for predicting long-term properties of carbon fibre-reinforced shape memory polymer composites in a low earth orbit environment. *Polymers*, 13(10). https://doi.org/10.3390/polym13101628.
69. Gates, Thomas. (2003). *On the Use of Accelerated Test Methods for Characterization of Advanced Composite Materials*. NASA Technical Report NASA/TP-2003-212407.
70. Sutter, J. K., Salem, J. L., Thesken, J. C., Russell, R. W., Littell, J., Ruggeri, C., & Leifeste, M. R. (2008). *Kevlar ® 49/Epoxy COPV Ageing Evaluation*. Ageing Aircraft 2008, Conference Paper, National Aeronautics and space administration.

71. D, ASTM 792. *Standard Test Methods for Density and Specific Gravity (Relative Density) of Plastics by Displacement*. American Society for Testing and Materials. 6. https://doi.org/10.1520/D0792-08.2.
72. D, ASTM 4018. *Standard Test Methods for Properties of Continuous Filament Carbon and Graphite Fiber Tows*. American Society for Testing and Materials. https://doi.org/10.1520/D4018-11.
73. D, ASTM 2290. *Standard Test Method for Apparent Hoop Tensile Strength of Plastic or Reinforced Plastic Pipe*. American Society for Testing and Materials. https://doi.org/10.1520/D2290-19A.
74. D, ASTM 2344. *Standard Test Method for Short Beam Strength of Polymer Matrix Composite Materials and Their Laminate*. American Society for Testing and Materials. https://doi.org/10.1520/D2344_D2344M-22.
75. D, ASTM 2393. *Standard Test Method for Viscosity of Epoxy Resins and Related Components.* American Society for Testing and Materials.
76. D, ASTM 891, *Standard Test Method for specific gravity, apparent of liquid industrial chemicals.* American Society for Testing and Materials. https://doi.org/10.1520/D0891-18.
77. D, ASTM 1652, *Standard Test Method for Epoxy Content of Epoxy Resins*. American Society for Testing and Materials. https://doi.org/10.1520/D1652-11R19.
78. D, ASTM 2471, *Standard Test Method for Gel Time and Peak Exothermic Temperature of Reacting Thermosetting Resins*. American Society for Testing and Materials.
79. E, ASTM 1356, *Standard Test Method for Assignment of the Glass Transition Temperatures by Differential Scanning Calorimetry*. American Society for Testing and Materials. https://doi.org/10.1520/E1356-08R14.
80. D, ASTM 638, *Standard Test Method for Tensile Properties of Plastics.* American Society for Testing and Materials. https://doi.org/10.1520/D0638-14.
81. D, ASTM 3171, *Standard Test Method for Constituent content of composite materials*. American Society for Testing and Materials. https://doi.org/10.1520/D3171-22.
82. E, ASTM 1545, *Standard Test Method for Assignment of the Glass Transition Temperatures by Thermomechanical Analysis*. American Society for Testing and Materials. https://doi.org/10.1520/E1545-22.

83. D, ASTM 3039, *Standard Test Method for Tensile Properties of Polymer Matrix Composite Materials.* American Society for Testing and Materials, https://doi.org/10.1520/D3039_D3039M-08.
84. D, ASTM 3410, *Standard Test Method for Compressive Properties of Polymer Matrix Composite Materials with Unsupported Gage Section by Shear Loading*. American Society for Testing and Materials, https://doi.org/10.1520/D3410_D3410M-16E01.
85. D, ASTM 3518, *Standard Test Method for In-Plane Shear Response of Polymer Matrix Composite Materials by Tensile Test of a ±° Laminate*. American Society for Testing and Materials. https://doi.org/10.1520/D3518_D3518M-18.
86. D, ASTM 790, *Standard Test Method for Flexural Properties of Unreinforced and Reinforced Plastics and Electrical Insulating Materials*. American Society for Testing and Materials. https://doi.org/10.1520/D0790-17.
87. Rudenko, S., Berladir, K., Trojanowska, J., Varenyk, S., Shvetsov, D., & Kravets, V. (2021). Application of FMEA for Assessment of the Polymer Composite Materials Quality. *Journal of Engineering Sciences*, *8*(2). https://doi.org/10.21272/jes.2021.8(2).b3.
88. Mo, J. P., & Suparayan, B. (2019). Failure mode–driven quality analysis of operational risks for composite fibre-reinforced plastic assembly. *Proceedings of the Institution of Mechanical Engineers, Part B: Journal of Engineering Manufacture*, *233*(1), 267–277. https://doi.org/10.1177/0954405417711733.
89. A, MIL HDBK 1629. (1980). *Military Handbook: Procedures for Performing a Failure Mode Effects and Criticality Analysis*.
90. Seo, H., Jang, H., & Lee, I. (2017). Experimental investigation of salt fog effect on the CFRP laminates. *Advanced Composite Materials*, *26*(4), 321–334. https://doi.org/10.1080/09243046.2016.1187822.
91. E, ASTM 976, *Standard Guide for Determining the Reproducibility of AE Sensor Response*. American Society for Testing and Materials. https://doi.org/10.1520/E0976-15R21.
92. E, ASTM 1106, *Standard Test Method for Primary Calibration of Acoustic Emission sensors*. American Society for Testing and Materials. https://doi.org/10.1520/E1106-12R21.
93. G, MIL STD 810. (2008). *Department of Defence Test Method Standard: Environmental Engineering Considerations and Laboratory Tests.*

94. D, MIL STD 1540. (1999). *Department of Defence Standard Practise: Product Verification Requirements for, Launch, Upper Stage and Space Vehicles.*
95. JSS 55555, *Joint Service Specification on Environmental Test Methods*.
96. Cysne Barbosa, A. P., P. Fulco, A. P., S.S. Guerra, E., K. Arakaki, F., Tosatto, M., B. Costa, M. C., & D. Melo, J. D. (2017). Accelerated ageing effects on carbon fibre/epoxy composites. *Composites Part B: Engineering*, 110, 298–306. https://doi.org/10.1016/j.compositesb.2016.11.004.
97. Miyano, Y., Nakada, M., & Sekine, N. (2005). Accelerated Testing for Long-term Durability of FRP Laminates for Marine Use. *Journal of Composite Materials*, 39(1), 5–20. https://doi.org/10.1177/0021998305046430.
98. Vijaykumar, M. S., & Saravanan, R. (2017). *Analysis of Epoxy Nano Clay Composites Compressive Strength during Tropical Exposure Test*. International Journal of Mechanical Engineering and Technology, 8(5), 1101–1104.
99. JSG 0102. (1984). *Joint Service Guide on Environmental Testing of Armament Store*.
100. OB 41102, *Ordnance Board Proceedings on Climatic Environmental Testing of Land Service Guided Weapons*.

Annexure-I

Nomenclature	Function	Failure modes and causes	Failure effects			Failure detection method	Compensating provisions	Severity class
			Local effects	Next higher level	End effects			
Composite main casing	Sustain pressure	Mid-cylinder breaks due to the less helical thickness End dome rupture	Cylinder initiating breaking either circumferentially or axially	Casing burst/motor pressure drop	Failure of the rocket motor/mission	AT (PPT, NDT) Qualification Testing (QT) Burst Test Structural load test	-Raw material batch evaluation -Design adequacy check -Process control -NDT	Catastrophic
Composite skirt	Stage intersection joint and transmit thrust	Compressive strength failure Buckling	-Local breakage of the fibre -Instability	Unable to transmit load	Mission failure	QT & NDT (UT & RT)	-Design adequacy check -Process control -NDT (UT & RT)	Critical
Polar Boss Joint	Structural integrity to attach Nozzle and Igniter	Boss Blow out due to bad adhesive bonding	De-bond between rubber and metal	Rupture of dome	Failure of rocket motor (mission failure)	Structural analysis NDT (UT and RT)	-Raw material batch qualification -Adhesive qualification	Catastrophic
Y-joint	Join casing to skirt	Strength failure due to debonding between casing and skirt	Bond failure	Unable to transmit load	Mission failure	Structural analysis Structural load test	-Raw material batch qualification -Adhesive qualification	Critical
Bulkhead Joint	Casing to the metallic bulkhead	-De-bond (adhesive failure) -Rivet failure	Disclose of Bulkhead	Unable to transmit load	Mission failure	QT Structural load test	-Raw material qualification -Rivet qualification	Critical

Annexure-II

Nomenclature	Function	Potential Failure Mode	Potential Effects of Failure	Severity (S)	Potential Causes of failure	Occurrence (O)	Current Process Control	Detection (D)	RPN	Criticality Rank
Composite main casing	Sustain pressure	- Mid-cylinder break - End dome rupture	-Cylinder initiating breaking either circumferentially or axially - Casing burst/motor pressure drops - Failure of the rocket motor/mission	10	less helical thickness	7	AT (PPT, NDT) QT Burst Test Structural load test	8	560	80
Composite skirt	Stage intersection joint and transmit thrust	- Compressive strength failure - Buckling	-Local breakage of the fibre -Instability - Unable to transmit load - Mission failure	7		6	QT & NDT (UT & RT)	7	294	42
Polar Boss Joint	Structural integrity to attach Nozzle and Igniter	Boss Blow out	-De-bond between rubber and metal - Rupture of the dome - Failure of rocket motor (mission failure)	10	bad adhesive bonding	8	Structural analysis NDT (UT and RT)	9	720	80
Y-joint	Join casing to skirt	Strength failure	-Bond failure - Unable to transmit load	8	debonding between casing and skirt	6	Structural analysis Structural load test	5	240	48

			- Mission failure							
Bulkhead Joint	Casing to the metallic bulkhead	-de-bond -Rivet failure	-Disclose of Bulkhead - Unable to transmit load - Mission failure	8	adhesive failure	3	QT Structural load test	9	216	24